Soleil SAXS and WAXS reveal the structure of fat crystals formed upon storage of breast milk at 4°c

Christelle Lopez, Javier Perez

INRA SOLEIL 10 years

CONTENTS

- SOLEIL EDITORIAL 4
- INRA EDITORIAL 5
- SOLEIL SYNCHROTRON 6
- INRA AT SOLEIL 10
- FOOD SCIENCE, NUTRITION, HEALTH 16
  - Thermal denaturation of meat and "foie gras" proteins studied by synchrotron FT-IR and DUV micro-spectroscopies 18
  - High-resolution imaging of mechanical properties using mid-Infrared Synchrotron radiation 20
  - *Escherichia coli* facing silver nanoparticles: when synchrotron FTIR microspectroscopy helps preventing biofilm formation 22
  - Lipid digestion in emulsion: timeresolved monitoring of coexisting nanostructures using synchrotron SAXS 24
  - SOLEIL SAXS and WAXS reveal the structure of fat crystals formed upon storage of breast milk at 4°C 26
  - Delivery of vitamins: impact of nanostructures in food emulsions 28
  - Synchrotron Infrared and Deep UV fluorescent microspectroscopy study of PB1-F2 β-aggregated structures in Influenza A virus-infected cells 30
  - SMIS beamline, a powerful tool to detect chemical changes occurring in spinal cord and to assess gene therapy efficacy in an animal model of Pompe disease 32
  - SOLEIL light reveals common allergenic structures involved in wheat allergies 34
  - Short ragweed pollen allergy in the light of SOLEIL beamlines 36
- PLANT SCIENCE UNDER CLIMATE CHANGE 38
  - Ascorbate is the key to unlocking Fe transport in seeds 40
  - *In vivo* monitoring of hydraulic failures in trees 42
  - Orientation under stress of cell wall polymers of the wheat aleurone cells: coupling mechanical test and infrared microspectroscopy 44
- TOWARDS BIOECONOMY 46
  - Biomass hydrolysis: a time-lapse localization of enzymes and modifications of maize stem cell walls by autofluorescence imaging and IR microspectroscopy 48
  - Depict the mode of action of amylolytic enzymes on starch granules 50

- Time resolved study of starch reorganization in starch based biomaterials: effect of immersion in physiological media 52
- New development on the SMIS beamline for a non invasive analysis of single bacterial cells 54
- Biochemical composition of microorganisms at the single-cell level by synchrotron FTIR microspectroscopy 56
- Lipid cell structure imaging and membrane fluidity measurement in single living microorganisms 58

DECIPHERING THE STRUCTURE OF COMPLEX ASSEMBLIES 60

- A low resolution study of the *Bacillus subtilis* Ku protein: deciphering the DNA double strand break repair by the bacterial NHEJ pathway 62
- Full of SOLEIL on a plant exudate structure: acacia gum 64
- Synchrotron radiation as a way to reveal the structural complexity of carbohydrates using mass spectrometry 66
- Astringency and the interactions between a human salivary proline-rich protein and tannins 68
- Autofluorescence varies with the muscle fiber type and postmortem time 70
- SOLEIL sheds the light on lipid bodies protein structure 72
- Polysaccharide skeleton under X-rays 74

FOCUS ON THE BEAMLINES AND SETUPS PRIMARILY USED BY INRA SCIENTISTS 76

- The DISCO beamline: a multipurpose beamline dedicated to biology and chemistry 78
- DUV Imaging branch at DISCO beamline: DUV autofluorescence microscopy for cell biology and tissue 80
- Hierarchical length-scale scanning imaging at the Nanoscopium beamline to study simultaneously the elemental and morphological variation of the sample 82
- SWING beamline: Characterize biological and soft matter at nanometer scale 84
- Development of new autosampler for direct injection of inhomogeneous sample through cell measurement 86

PROSPECTS 88

SOLEIL editorial

This document follows an earlier edition, published in 2012, to mark the first five years of partnership between INRA and SOLEIL. I am pleased to sign today the editorial of this “10 year version”, which confirms the success of the strong collaboration between our teams and brings new examples of research with increasingly varied themes. Nearly 140 scientific publications already report the results obtained, and original and "isolated" subjects five years ago have since resulted in beautiful scientific stories, arising from work on several of our beamlines, using multiple complementary approaches and analytical techniques.

Since 2012, SOLEIL’s experimental stations were equipped with new devices in order to keep taking into account the evolution of the users’ expectations. From the beginning of the INRA-SOLEIL collaboration, the three INRA engineers working, on secondment, on our beamlines are a link between the synchrotron and INRA. Their mission is triple: prospection and information of the INRA laboratories that are not yet aware of the possibilities of SOLEIL as a Very Large-Scale Research Facility, as well as offering specific advice and assistance to get some "beam time". Thanks to this tailor-made support, experimental time attributed to INRA teams, since the partnership began, has more than doubled. The same trend is also found in the growing number of beamlines hosting INRA experiences: there are now 12, and new projects are underway on other beamlines. This reflects the diversity of techniques used by the user teams in imaging, in all energy ranges (IR, UV or X-ray) and also in diffraction, small angle scattering, circular dichroism...

The INRA-SOLEIL association definitely is a win-win partnership, which I am delighted to promote. I thank all its creators and actors, and I look forward to the third edition of this document with confidence.

Jean Daillant
Director General of SOLEIL

INRA editorial

Ten years full of remarkable results have already gone by since the two first engineers from INRA came to work on SOLEIL's beamlines, DISCO and SMIS, followed in 2009 by a third engineer on the beamline SWING.

Back in 2006, this innovative partnership was truly unique. Its objective was to tackle the challenges of investigating complex systems—a major element in all of INRA's research areas—in both their structural and dynamic aspects, through multi-scale and multi-spectral approaches and coupling of real-time methods.

This opened up an endless range of possibilities, only limited by our own imagination!
This booklet presents a few results from this original partnership, which started with one INRA department and was gradually extended to nearly all the departments covering the major themes explored at INRA: Plant and Animal Science, Food Quality and Safety, Nutrition, and Bioeconomy. Beyond the scientific questions were also some technical challenges that the researchers and engineers had to take up. In this report, you will also find details on our current work organization, which has been renewed and strengthened through the recruitment of engineers and the arrival of scientists working in association with SOLEIL. I would like to offer them all my sincere thanks for their motivation and commitment. May this adventure continue and grow as the new beamlines are being developed, in close collaboration with the management team of SOLEIL, whom I would also like to thank for their ever-renewed interest for our partnership.

Many thanks to all of our colleagues who have contributed to the success of our collaboration through their work and commitment. Good luck to all and may you continue to inspire others!

Monique Axelos
INRA – Adviser for European affairs on Food,
Nutrition and Bioeconomy

WHAT IS SOLEIL?

SOLEIL produces an extremely bright light which extends from the far-infrared to hard X-ray, and which can be used to explore matter.
This light comes from very high energy electrons circulating in a ring with a perimeter of 354 meters, at a speed close to the speed of light. This ring is equipped with magnetic devices - bending magnets (also called "dipoles"), undulators and wigglers - which force the electrons to follow curved or wavy trajectories. Each time they go through these magnetic devices in which their trajectory is altered, the electrons lose energy in the form of electromagnetic radiation: synchrotron light. This radiation exhibits unique polarization and tunability characteristics over a wide range of photon energies, brilliance, a high degree of collimation emitted from a very small radiation source, as well as a temporal structure. These unique properties are used to advantage in the study of ultra-thin matter or the monitoring of processes at the scale of a few hundredths of a nanosecond, or to obtain data at high spatial resolutions (a few tens of nanometers). Experiments using synchrotron radiation are conducted in the various beamlines built around the ring (fig. 1).

TAILORED BEAMLINES

Each beamline is a laboratory designed for the use of a given range of wavelengths (fig. 2) and instrumented to prepare and analyse any kind of matter sample. The emitted photons are focused on the sample and, thanks to very specific techniques, enable the study of its structure and geometry in surface or volume, or its chemical, electronic or magnetic properties...
The experimental program includes the provision of 29 beamlines. In 2016, 26 of these 29 beamlines are open to scientists, hosting around 2,400 users each year, according to a 24-hour operating system, 6 days/a week and 250 days a year.

In addition to the SOLEIL beamlines, sample preparation and instrumentation laboratories are available for users: chemistry, biology, high pressure, ancient materials and surfaces.

A RANGE OF CUTTING-EDGE SCIENTIFIC EQUIPMENT

The use of synchrotron radiation involves a wide range of activities both in fundamental research as well as in applied research:

SOLEIL SYNCHROTRON

To produce an extremely bright light source, whose brilliance and wavelength can penetrate the innermost secrets of matter: this is the mission of a synchrotron radiation facility like SOLEIL. Serving scientists and industrialists, this very high-tech facility provides investigative means indispensable to researchers.

A RESEARCH CENTRE AND HIGH-LEVEL SCIENTIFIC RESOURCE AT THE SERVICE OF SCIENTISTS

physics, chemistry, material sciences, electronics, life sciences, medicine, Earth and atmospheric sciences, environment, food processing, cosmetics, pharmaceuticals... The research conducted at SOLEIL is as varied as the fields it covers.
Complementary to other matter scanning devices, SOLEIL offers a very wide range of specific techniques. These techniques may be classified into four families:

- X-ray diffraction/scattering techniques: structural information
- IR, UV, and X-ray spectroscopy: chemical information
- Photoemission, circular dichroism: electronic and magnetic information
- Imaging and radiography/tomography: morphological information

The use of techniques that complement one another makes it possible to analyse, simultaneously or sequentially, the same sample by several complementary techniques. Such an approach is encouraged by an extended spectral range, from far infrared to hard X-rays encourages.

In addition, the use of synchrotron radiation often yields decisive advantages for material analysis because it makes it possible to gain orders of magnitude in the quality of measurements compared to the use of traditional light sources.

▸ ALMOST 400 PEOPLE IN THE SERVICE OF SCIENCE

At SOLEIL, almost 400 people work each day to ensure that users of beamlines have access to optimal research conditions. The primary mission of SOLEIL is to be a service tool for the entire scientific and industrial community. But SOLEIL is also a laboratory that develops its own research themes within very advanced scientific teams.

Specifically, the SOLEIL teams:

- Design and develop the beamlines to constantly meet the highest level of requirements of their users
- Ensure the best welcome possible to external users and offer them assistance tailored to their needs
- Conduct their own research of excellence, mainly obtained using SOLEIL facilities.

▸ WHO FINANCES THE SOLEIL PROJECT?

SOLEIL was launched with the support of five partners. The two largest French research bodies - the CNRS and the CEA - respectively own 72% and 28% of shares in the French public company Synchrotron SOLEIL. The Région Ile de France and the Conseil Départemental de l'Essonne have contributed financially to its construction and today ensure close monitoring of its development. Finally, the Centre-Val de Loire Region is involved in developing three of the 29 SOLEIL beamlines: DIFFABS, DISCO and SWING.

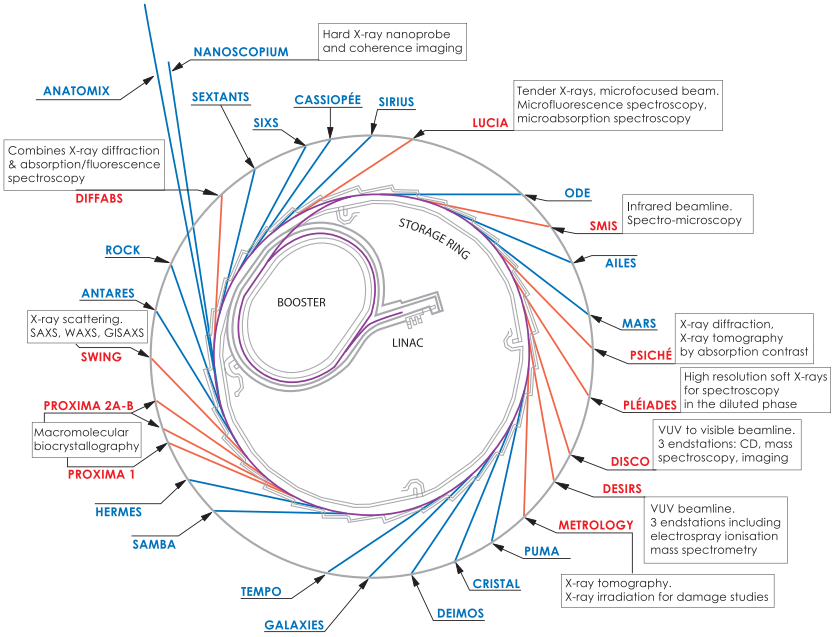

▶ *Figure 1: The 29 SOLEIL beamlines. In red, the beamlines that have already hosted INRA user projects.*

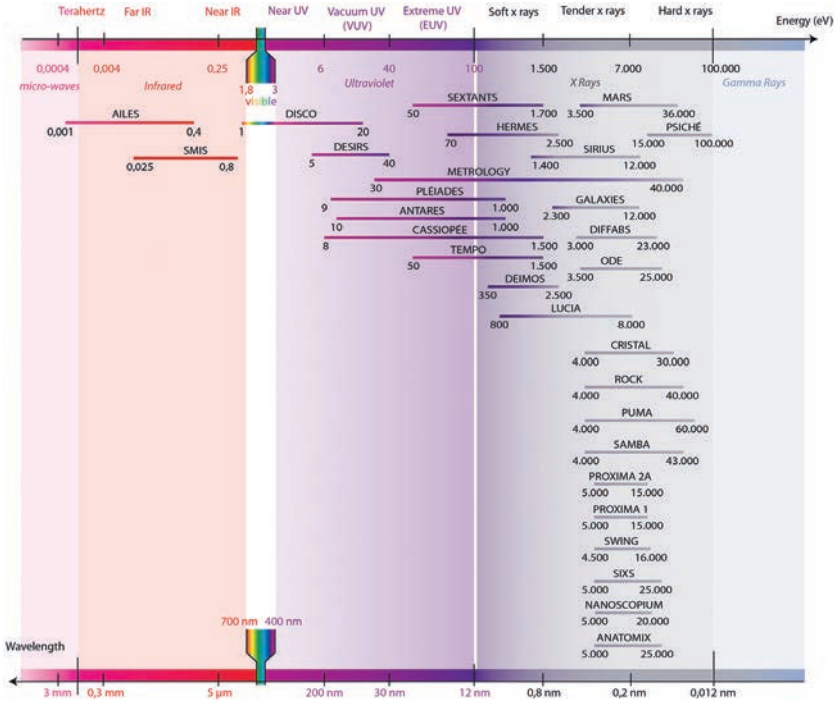

▶ *Figure 2: The classification of SOLEIL beamlines according to the range of wavelengths/ energy they cover.*

HOW TO ACCESS TO SOLEIL

SOLEIL synchrotron is both a research centre and a scientific resource, dedicated to the study of matter through its interaction with light used as an exciter. SOLEIL carries out two main missions: on the one hand to lead research projects of scientific excellence and, on the other hand, to support research and innovation carried out by teams from public research laboratories, companies, hospitals, museums...

SOLEIL offers to its users four complementary access modes to the beamlines: free access after selection by the Peer Review Committee (PRC), service analysis, joint research activities and rapid access.

▶ THE SCIENTIFIC PROJECTS SELECTED BY THE PEER REVIEW COMMITTEE

SOLEIL has established a peer evaluation system, the "Peer Review Committee" (PRC) for beamtime allocation, in the framework of two annual calls for proposals (the deadlines are mid-February and mid-September). The scientific projects submitted to SOLEIL are evaluated and classified within a competitive framework by the PRC, based on their scientific quality and relevance of synchrotron radiation use. The result

of these evaluations is submitted to the SOLEIL Scientific Direction for validation.

The PRC covers the following scientific disciplines:
1. Diluted matter
2. Electronic and magnetic properties of matter - Surfaces and Interfaces
3. Properties of matter and materials: Structure, Organisation, Characterisation, Development
4. Chemistry and Chemical Physics- Reactivity in situ - Soft Matter
5. Biology - Health
6. Ancient materials - Earth and Environment

In this context, two types of projects are proposed in order to cover the needs and expectations of users:

• Standard proposals
The beamtime is allocated to users in a 6 month period consecutive to the PRC decision.
• Block Allocation Group (BAG)
BAG proposals involve Macromolecular crystallography experiments and Small Angle X-ray Scattering in the field of biology. A scientist is in charge of the BAG and coordinates applications from several teams. The BAG beam time allocation period covers one year.

The main features of this access mode are:
- Access volume representing at least 65% of the total available beam time for experiments.
- Free access to beamlines. Accommodation and travel expenses may also be covered by SOLEIL. Maximum of 3 users carrying out an experiment, for which available beam time was allocated by the PRC, and which belong to a French research home institute (regardless of region) can benefit from a subsidy for:

- Guest house accommodation.
- Meals in the canteen.
- Transport subsidy only applies to users whose institute or laboratory is located outside the Ile de France region

Specific funding programs (Trans-National Access) are available to researchers in a home institute located in a member state or associated with the European Union outside France.

- Availability of one or more beamlines (maximum 3); the collection of experimental data is carried out directly by the applicant, with support from the beamline staff
- Waiting period for access to the beamline: after the communication of results to users (which takes place three months after the proposals submission) and a period of a month and a half to schedule and organise the reception of the first projects. Experiments are staggered over a 6 month period
- Current selection rate: on average on all beamlines, 1 proposal out of 2 is accepted
- Obligation to submit an experiment result report and publish the results, mentioning the use of the SOLEIL beamline on which the data were collected

▸ INVOICED SERVICES

When synchrotron studies require fast access and/or confidentiality, external users may resort to invoiced services.

The main characteristics of this mode of access are the following:
- "A la carte" service based on the specific user requirement for each of their project needs, from simple provision of a beamline to a complete service (sample preparation, collection, analysis and interpretation of experimental data, preparation of analysis report)
- Invoicing based on access time to beamlines and the time spent by the SOLEIL staff in carrying out the service
- Continuous access (during periods of operation) with no prior selection
- Volume access up to 10% of the total beam time allocated for experiments
- Reduced access delay (a few weeks on average)
- Guarantee of the confidentiality requested by the user.

▸ RESEARCH PARTNERSHIPS

In the framework of the scientific research and instrument development activity conducted by SOLEIL beamline teams, representing 20% of the total beamtime available for beam experiments, joint research activities are carried out with external, public and/or private teams. Based on the common use of means and governed by agreements: pooling of resources (intellectual, human, technical and financial) by the partners, definition of rules for property sharing and use of the research results.

▸ RAPID ACCESS

A limited number of proposals can be accepted by the scientific direction in the framework of rapid access for urgent work, up to 5% of the total beamtime available for experiments.

INRA at SOLEIL

At SOLEIL, research projects are selected twice a year by program review committees (see page 9) on the basis of their scientific interest. Paul Colonna (Deputy Scientific Director Food, Nutrition and Bioeconomy) and Alain Buléon (research Director at INRA) were asked by the General Direction of INRA to set up a specific organization to help INRA scientists accessing SOLEIL so that their experiments can be performed under optimal conditions. From 2014 they were assisted in this by Thierry Chardot (research Director at INRA).

This organization relies on several INRA engineers, specialized in synchrotron techniques and working full time at SOLEIL. In 2006, Alexandre Giuliani and Frédéric Jamme (up to 2012), then Pierre Roblin in 2009 (up to 2016) and Camille Rivard in 2015, respectively joined the DISCO, SMIS, SWING and NANOSCOPIUM/LUCIA beamlines. They are tasked with preparing projects in cooperation with INRA scientists, supporting the scientists during their experiments on site, and when necessary designing and assembling new sample environments. In addition to their commitment as beamline scientists, INRA engineers visit laboratories and INRA centers to introduce the SOLEIL facility. Their work notably results in the development of collaborations between SOLEIL teams and INRA researchers, who become associated scientists (such as Fernanda Fonseca and Marie-Françoise Devaux). This tight collaboration has also been reinforced by the setting up of the co-supervision of Julie Meneghel, PhD student, by SOLEIL and INRA researchers. INRA scientists are also involved in SOLEIL PRCs (Marie-Hélène Ropers, PRC4 up to 2016, Thierry Chardot PRC5).

Furthermore, an INRA scientific committee comprised of 12 members meets twice a year, prior to SOLEIL calls for proposals. This committee helps INRA scientists improve their proposals before submission to the program committees. Altogether, the INRA organization increases the success rate of carefully prepared high quality projects presented to the PRCs.

▶ TO CONTACT US:
inra-soleil@synchrotron-soleil.fr

Alain Buleon

Research Director at the "Biopolymers, Interactions, Assemblies" laboratory from INRA in Nantes, Alain Buleon was asked in 2003 by the management of INRA to set up links and organization allowing INRA to have access to SOLEIL matching its scientific ambitions. Main topics concerned the complex assemblies present in living organisms, the related bioinspired/ mimetic systems and soft matter. During the construction of the facilities, it was decided to add an INRA research engineer to the staff of 3 different SOLEIL beamlines, in order to help INRA researchers to optimize their proposals and to train them for experimental work and data processing once the proposal accepted.

A. Buleon recruited those 3 engineers in 2006 and 2009, organized a scientific committee of INRA users of SOLEIL and met scientists of many INRA research units to try to set up some preliminary trials or new proposals. This organization was extended to different INRA Departments and a large extent of topics, as biotechnology, environment, biorefinery, animal health or plant physiology. A. Buleon coordinated this organization up to July 2014 and is now replaced by Thierry Chardot. He was also the chairman of the PRC "Life Science and Health" at SOLEIL from 2006-2011 and a member of the scientific advisory committee (SAC) of SOLEIL (2007-2013).

Thierry Chardot

In 2014, Thierry Chardot took over coordination of INRA scientific activities at SOLEIL from Alain Buléon.
Thierry Chardot, Ph.D, is a research Director at INRA, specialist in plant biochemistry. He studies various aspects of lipid metabolism related to the specific organelles called lipid bodies and their associated proteins. He is a user of several SOLEIL beamlines (DISCO, SMIS, SWING, METROLOGY) and belongs to one of the 6 Program Committees (Life Science and Health) since 2011. Together with the three INRA scientists working at SOLEIL, his goal is to provide INRA users with scientific opportunities at SOLEIL, and ensure them a high rate of success in SOLEIL project calls.

Alexandre Giuliani

In 2003, Alexandre obtained a PhD at the Université de Liège (Belgium) in molecular spectroscopy. After a 2 year post-doctoral fellowship at the Institut de Chimie des Substances Naturelles (Gif-sur-Yvette, France) where he learnt analytical mass spectrometry, he joined INRA in 2006, to work at the SOLEIL facility on the DISCO beamline, where he is currently on secondment. His main interests are atmospheric pressure photoionization, activation and spectroscopy of trapped ions.

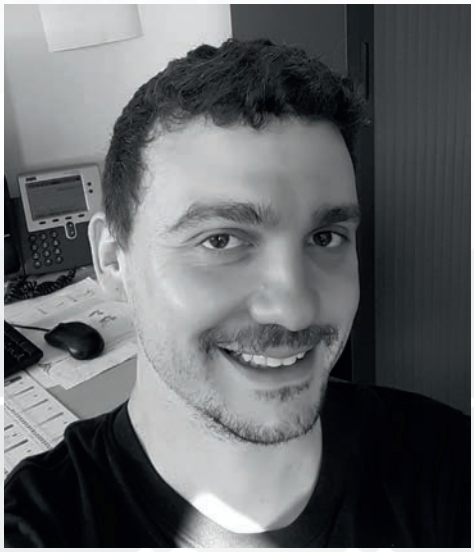

Pierre Roblin

Holding an engineering degree from INSA in biochemical engineering and a PhD in Structural Biophysics, Pierre Roblin specialized during his thesis and postdoctoral training in Small Angles X-ray Scattering (SAXS) applied to the study of in solution macromolecules. He joined the SWING beamline team in 2009, where he continued to develop HPLC sample environment dedicated to biology and designed a variety of automated systems for the transfer of liquid sample (automated sample holder), and for the characterization by SAXS of reaction kinetics of synthesis or degradation of biomolecules (micro-reactor). He now works at the "Laboratoire de génie chimique de Toulouse".

Camille Rivard

Engineer from the National School of Geology with a specialization in Environmental sciences, Camille Rivard completed her training with a PhD in Geosciences (LIEC, Vandœuvre-lès-Nancy). During her PhD, she discovered the “synchrotron world” by conducting several X-ray fluorescence and X-ray absorption spectroscopy experiments at SOLEIL (LUCIA beamline) and at the Canadian Light Source.
She moved thereafter to the ESRF (European Synchrotron Radiation Facility in Grenoble) for a post-doctoral position on ID21 beamline. Her activities of users “local contact” and instrumental development allow her to deepen her knowledges in X-ray fluorescence, punctual and full-field X-ray absorption micro-spectroscopy and X-ray diffraction. Through her collaborations with different organisms, Camille developed knowledge on characterization in soils and sediments by synchrotron techniques. She also acquired competences in cryogenic sample preparations and analyses of biologic tissues. Camille is now works on the NANOSCOPIUM and LUCIA beamlines, and is involved, more broadly, in X-ray imaging projects.

Frédéric Jamme

Frédéric learnt analysis techniques using infrared synchrotron radiation (SRS synchrotron, Daresbury, UK) during his PhD thesis in Surface Physics, carried out in Nottingham University. After a postdoc at the Central Laser Facility (Rutherford Appleton Laboratory, Didcot, UK) he continued in this path at SOLEIL, with a post-doctoral position at the SMIS beamline, specialized in imaging. Then, for seven years, Frédéric was one of the INRA engineers working as a beamline scientist - his attachment both to SMIS and DISCO beamlines was a unique situation at SOLEIL. He now works as a SOLEIL beamline scientist at DISCO beamline, where he keeps broadening his skills sets in molecular imaging.

Fernanda Fonseca

Fernanda Fonseca is a senior scientist at the Joint Research Unit of Microbiological and Food Process Engineering (UMR GMPA, INRA-AgroParisTech), Versailles-Grignon Centre. In 2011, she initiated a tight collaboration and partnership with two synchrotron beamlines at SOLEIL: SMIS and DISCO.

Her main research interest is on biotechnology and process engineering, with particular emphasis on fermentation, formulation and stabilization of micro-organisms by freezing and drying. Her work particularly focuses on the thermophysical and chemical changes of biomaterials following production processes, in order to relate them to their biological and functional responses.

The brilliance and large wavelength range of the synchrotron radiation make possible meeting the challenging study of individual micro-organisms for identifying and quantifying the mechanisms governing their degradation and/or preservation during their manufacturing processes.

This fruitful partnership with SMIS and DISCO beamlines, respectively for IR and deep UV cell studies, has led to joint development of innovative approaches and specific devices for studying in situ and in real time such isolated cells, and to a PhD project (J. Meneghel) co-supervised by INRA (F. Fonseca) and beamline scientists (F. Jamme and P. Dumas).

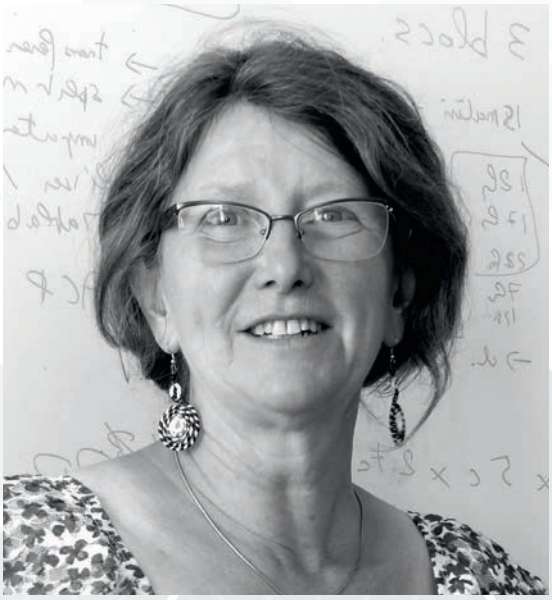

Marie-Françoise is engineer in the research unit Biopolymers, Interaction, Assemblies, in the PVPP team (Plant cell wall and their polysaccharides). She develops image analysis tools at different scales for the quantification of plant tissue morphology and of the spatial distribution of biochemical constituents. Morphology and histology are obtained from visible images and spectral imaging is a powerful means to get chemical information without any labelling of the sample.
In 2009, Marie-Françoise started a collaboration with Frederic Jamme (scientist at the SMIS and DISCO beamlines, at that time), by co-supervising a PhD student, F Allouche. Since 2013, Marie-Françoise is a SOLEIL associate research scientist, she devotes a quarter of her time to the DISCO beamline in order to complete the chemometric multibloc analysis of multimodal hyperspectral images with different spatial resolution. This collaboration contributes to connect the different information scales obtained through INRA equipment and the synchrotron facility.

Marie-Françoise Devaux

PhD student (2013-2016) at the joint research unit for Microbiology and Food Process Engineering (GMPA) at INRA Grignon, Julie Meneghel's thesis is also co-supervised by two SOLEIL scientists: Paul Dumas, former head of the SMIS beamline, and Frédéric Jamme, scientist on DISCO beamline. This privileged partnership enables her to investigate the lactic acid bacteria (LAB)'s responses to environmental stresses of industrial relevance (suffering of cells during production, preservation for their final use) by Fourier Transform IR spectroscopy and Deep UV imaging.

Julie Meneghel

Food science, nutrition, health

Contribute through research to the global challenge of delivering healthy food with high standards in quality and safety is a priority of INRA. SOLEIL permits the imaging of protein matrixes, of mechanical properties of food matrixes, and allow exploring changes at the subcellular level induced by nanoparticles.
Infrared (IR) spectro-microscopy on the SMIS beamline highlighted the importance of the supramolecular state of the protein matrix in determining the fat loss of 'foie gras' (Astruc *et al.*).
Touffet *et al.* extended former work on oil diffusion in fries and on the migration of small molecules, from packaging to food (DISCO beamline), to the imaging of mechanical properties using mid-IR synchrotron radiation (SMIS beamline).
Silver nanoparticles have antibacterial properties and they are widely used by the industry. Mercier-Bonin *et al.* used synchrotron FTIR micro-spectroscopy (SMIS) with high spatial resolution to monitor subtle cellular changes at the single-cell level induced by silver nanoparticles.

Similarly, studies of the structure and mobilization of nutriments are important for the conception of healthy foods. Understanding the fate of oil in water emulsions undergoing external changes, such as temperature changes or enzymatic action is highly challenging.
Marze *et al.* successfully recorded time-resolved SAXS profiles of polydisperse emulsions undergoing intestinal digestion (SWING). This information is of primary importance as these assemblies are responsible for the transport of lipids, lipophilic vitamins and other lipophilic bioactive molecules towards their absorption sites.
Milk fat globules thermal behavior, and the structure of artificial nano-emulsions designed for delivery of nutriments to humans, were finely characterized using the SWING beamline (Lopez *et al.*, Relkin *et al.*).

Human and animal health scientists clearly benefit from SOLEIL and from the possibility of submitting projects using complementary beamlines.
Chevalier *et al.* combined multimodal Fourier Transform (FT)-IR and deep Ultraviolet (DUV) micro-spectroscopy on SMIS and DISCO, to discover and study amyloid proteins in the Influenza virus.
The high brilliance of the SMIS IR beamline allowed glycogen mapping at the subcellular level and therefore the evaluation of gene therapy efficiency on mice with Pompe disease, a genetic disease characterized by glycogen accumulation in cells (Dubreil *et al.*).
Food and environmental allergens represent major concerns for populations. DISCO participated in the determination of the structures of allergens from cereal seeds that probably play an important role in disease initiation or the triggering of symptoms (Denery-Papini *et al.*).
Short ragweed pollen is a major atmospheric strong allergen. Multi-beamline experiments (PROXIMA-2A, SWING and DISCO) permitted determination of the 3D structure of the allergen contained in this pollen (Groeme *et al.*).

Thermal denaturation of meat and "foie gras" proteins studied by synchrotron FT-IR and DUV micro-spectroscopies

SCIENTISTS INVOLVED

T. Astruc[1], A. Vénien[1], L. Théron[1,2], X. Fernandez[2], F. Jamme[3], P. Dumas[3], M. Réfrégiers[3]

[1] QuaPA, INRA, 63122 Saint-Genès-Champanelle, France

[2] GenPhySE, INRA, 31326 Castanet-Tolosan, France

[3] Synchrotron SOLEIL, 91190 Gif-sur-Yvette, France

CORRESPONDENCE

Thierry Astruc
thierry.astruc@inra.fr

REFERENCES

[1] T. Astruc et al (2012) Food Chem. 134, 1044-1051.

[2] L. Théron et al. (2014) J. Agric. Food Chem., 62, 5954–5962.

KEYWORDS

Skeletal muscle fibers; fatty liver, protein thermal denaturation, DUV microspectroscopy; infrared microspectroscopy, histology.

Cooking improves palatability, preservation and protection against microorganisms but causes tissue shrinkage, increasing shear forces thus releasing juice and fat outside the food. In meat, the water loss that can reach 40% of initial weight of raw meat is usually accompanied by an increase in toughness. In foie gras, cooking causes a fat loss (3-40% of the original weight) which variability affects the organoleptic qualities of foie gras.

Many studies have been conducted to understand the mechanisms underlying the changes in meat products and foie gras during heating, the ultimate goal being to limit the variability of quality. At molecular level, heating breaks the weak bonds between aminoacids, leading to a loss of three-dimensional protein conformation. The changes in the tissue structure and at a lower scale, in the molecular structure of proteins, affect the water holding capacity and the lipid retention of meat products and foie gras respectively.

Infrared or fluorescence microspectroscopy approaches allow to directly characterizing the molecular structure of a compound identified by microscopy on a histological section free of any chemicals. The use of synchrotron radiation allows higher spatial resolution than internal sources.

SCIENTIFIC QUESTIONS

The scientific question was: what are the effects of heating on the muscle and liver proteins structure in order to understand the mechanisms involved in the variability of cooked meat and foie gras quality.

Muscle is composed of 4 types of muscle cells (I, IIA, IIB and IIX) whose intracellular proteins composition is different, and of a collagen rich complex extracellular matrix containing small content of elastin. One objective was to highlight the thermal denaturation kinetics of muscle proteins during its cooking and whether it was variable depending on the type of fiber and extracellular protein. On foie gras, differences in the molecular structure of the protein matrix were suspected to affect its mechanical resistance during cooking and thereby modulate lipid retention. So, the molecular structure changes of foie gras proteins during heating was a prerequisite to understand the molecular mechanism involved in fat loss variability.

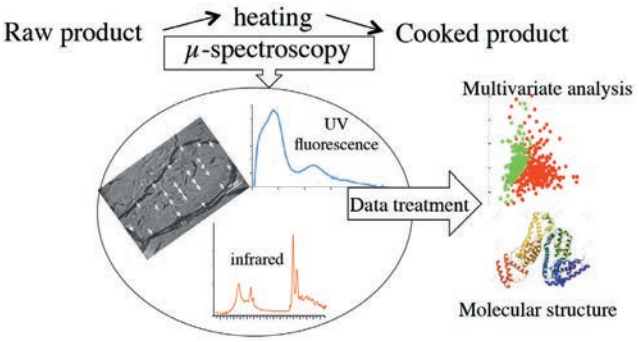

Figure 1: In situ characterization of macromolecular changes along heating.

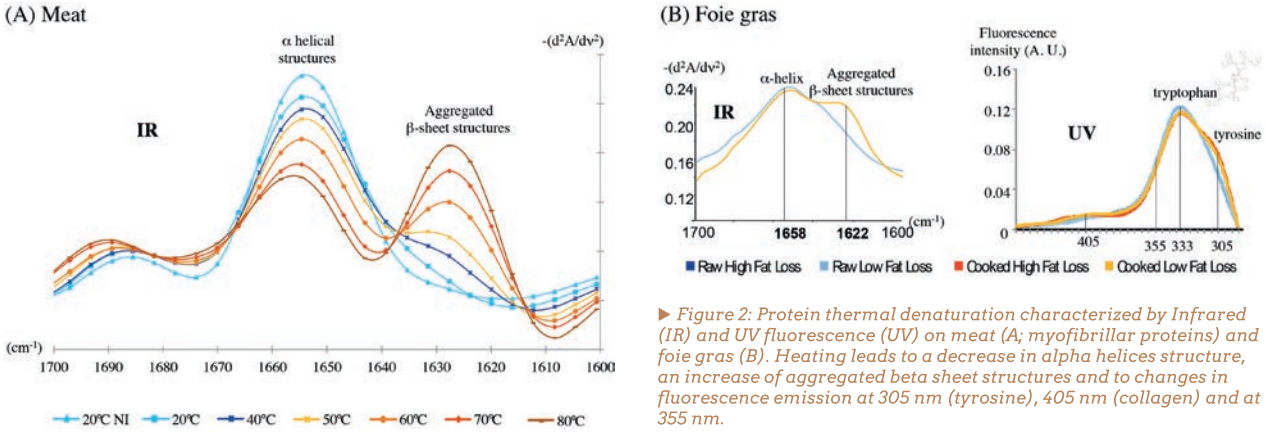

▶ *Figure 2: Protein thermal denaturation characterized by Infrared (IR) and UV fluorescence (UV) on meat (A; myofibrillar proteins) and foie gras (B). Heating leads to a decrease in alpha helices structure, an increase of aggregated beta sheet structures and to changes in fluorescence emission at 305 nm (tyrosine), 405 nm (collagen) and at 355 nm.*

To answer these scientific questions, we studied the effect of increasing temperature on protein structure changes from different muscle fiber types (I, IIA, IIX and IIB muscle fibers types) and on different compartments of muscle tissue (muscle fibers, extracellular matrix) to characterize the sequence of in situ muscle protein denaturation subjected to heating [1].
In another experiment, the protein structure changes of foie gras before and after cooking were assessed and correlated the data with fat loss after cooking [2].

Histochemistry, FT-IR and fluorescence microspectrocopy were identified as the best approaches to characterize the in situ protein denaturation (fig. 1). FT-IR microspectroscopy is hampered by the fact that laboratory sources limit spatial resolution to 20 square microns. However, the synchrotron SMIS beamline which have a confocal geometry microscope used with a bright-source synchrotron radiation makes possible the *in situ* spectral acquisition of biological tissues at subcellular scale. So, this specific equipment enables the acquisition of high-quality spectra of size-limited extracellular matrix excluding the surrounding muscle cells, thus improving measurement accuracy.

Synchrotron deep ultraviolet (DUV) fluorescence spectra provide knowledge of chemical composition with a spatial resolution that may reach 300 nm. The simultaneous approaches of located microspectroscopy and histochemistry are therefore well-suited to characterize cellular morphology and molecular structures of targeted areas on the same tissue section.

▶ MAIN RESULTS AND PERSPECTIVES

Whatever the organ studied (muscle or liver) and excepted for elastin protein, increasing temperature resulted in a decrease in alpha-helix secondary structure and an increase in aggregated beta-sheet structure of proteins (fig. 2) [1-2].

In skeletal muscle, this phenomenon was more pronounced for intracellular muscle proteins than for connective tissue. Although hybrid fibers were generally somewhat less sensitive to unfolding than the pure types, the amplitude of the thermal denaturation of intracellular muscle proteins was practically independent of fiber type.

In foie gras, results revealed a higher level of thermal protein denaturation in high fat loss than in low fat loss foie gras. In addition, the fluorescence and infrared responses of the raw tissue revealed differences according to the level of fat losses after cooking. These findings highlight the importance of the molecular state of the protein matrix in determining fat loss of foie gras.

The next steps are to characterize the molecular structure changes in proteins according to different time / temperature combinations. Concurrently, instrumental qualities measurements would allow connecting the molecular structure to sensory, technological and nutritional qualities of food.

▶ CONCLUSION

This study highlights the usefulness of infrared and UV fluorescence localized microspectroscopy on histological sections. Indeed, these techniques prevent the aggressive extraction steps generally carried out to analyze macromolecules by biochemistry. Moreover, molecular interactions specific to the organization of the tissue which often stabilize the structures are then taken into account in the characterization of changes due to technological process.

High-resolution imaging of mechanical properties using mid-Infrared Synchrotron radiation

▶ SCIENTISTS INVOLVED

M. Touffet[1], A. Patsioura[1], J.M. Vauvre[1], M. Da Silva[2], M. Nguyen[1], X. Fang[1], F. Jamme[3], P. Dumas[3], O. Vitrac[1]

[1] UMR 1145 GENIAL "Food Processing and Engineering", INRA, Agroparistech, Université Paris-Saclay, 91300 Massy, France

[2] McCain Food Ltd., 28 Havers Hill, Scarborough, YO113BS, United Kingdom

[3] Synchrotron SOLEIL, 91190 Gif-sur-Yvette, France

▶ CORRESPONDENCE

Olivier Vitrac
olivier.vitrac@agroparistech.fr

▶ REFERENCES

[1] J.-M. Vauvre et al. (2015) AIChE Journal, 61, 2329–2353.
[2] A. Patsioura et al. (2015) AIChE Journal, 61, 1427–1446.
[3] J.-M. Vauvre et al. (2014) Eur. J. Lipid. Sci. Tech., 116, 741-755.

▶ KEYWORDS

Food, health, FTIR, mechanical properties, cell walls, frying, drying, cellulose, pectins.

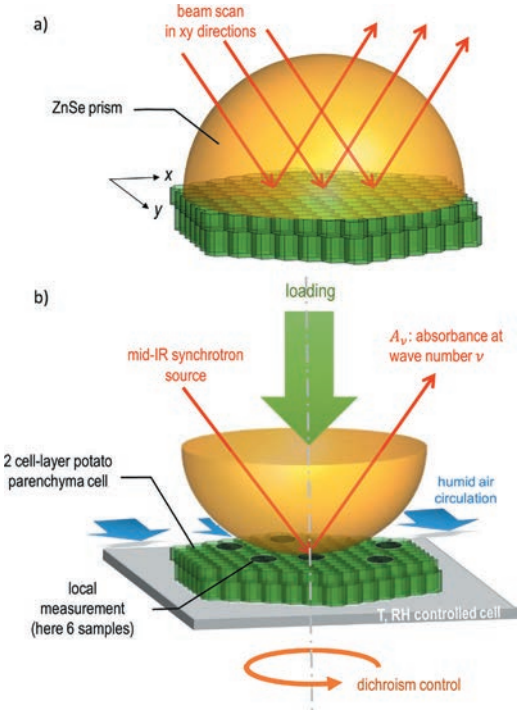

▶ *Figure 1: Experimental setup to image the vibrational properties of primary cell walls: a) principles of measurement in attenuated total reflection mode (ATR, ZnSe prism); b) configuration with fixed beam used to correlate vibrational spectra with mechanical properties using 2D spectroscopy (coupled with temperature T or relative humidity RH, scans).*

▶ SCIENTIFIC QUESTIONS ADDRESSED

The measurement of microscopic mechanical properties in food or in related materials with biological origin is of general interest for studying the impact of hydrothermal treatments such as drying, frying, freezing... To develop a generic technique to map mechanical properties, we proposed to correlate mid-infrared (mIR) vibrational spectra of isolated parenchyma cell walls without significant loading with their mechanical behaviors (rubber or glassy ones) in the hygroscopic domain. The technique should be able to image the possible variations of glass transition temperature in samples with cellular structures subjected to strong water content gradients. The methodology was first developed and tested for parenchyma cells equilibrated in superheated steam at different temperatures to mimic the state of crust of a French-fry (see results and methodology in [1-3]) as shown in **Fig. 1**. On the SMIS beamline, the brilliance of the IR synchrotron radiation combined with a small beam enabled to decrease the diffraction limit down to the size of parenchyma cell junctions (2 to 6 µm) and enabled the measurement of vibrational spectra of polymers constituting isolated cell walls. The principles of this kind of measurements were validated by comparing the dependence of the spectra with temperature (T) and with water content (X). Increasing water content plasticizes cell walls and decreases the glass transition temperature (Tg). According to the free-volume theory, shifting T *or* $-Tg(X)$ should displace similarly the absorption spectra.

▸ MAIN RESULTS AND FURTHER DEVELOPMENTS OR PERSPECTIVES

The variations of optical properties with temperature affected significantly baselines above 2500 cm^{-1} and only the regions between 1800 cm^{-1} and 800 cm^{-1} were sufficiently reproducible and exploitable to identify the effects of temperature (T) or water content (X). Increasing T and X (in original samples or by increasing locally the relative humidity) led to similar effects on normalized spectra ($\hat{A}_\nu^*$) as shown in **Fig. 2**. The band at 1230-1270 cm^{-1} associated to pectins was chosen as reference to normalize all spectra because it was insensitive to dichroism (pectins are amorphous). The variations of the intensities of the major peaks are plotted in **Fig. 3**. Critical temperatures and critical water contents (denoted T_{cr} and X_{cr}) were detected by abrupt changes of the slopes of absorbance with X and with T, respectively.

Critical temperatures (or equivalently critical water contents) were identified with T_g of cellulose and pectins. In particular, the variations of T_g with X modified spectra in a same extent as an opposite variation of T. As predicted by theoretical T_g values of pectins and cellulose, the two T_{cr} values were separated by 40°C in samples with $X = 0.13$ kg kg^{-1} solid basis. In practice, the shift of the stretching band of CH_2 at 1319 cm^{-1} was particular efficient to detect T_g of pectins whereas the bending band of CH_2 at 1375 cm^{-1} was more specific to detect T_g of cellulose.

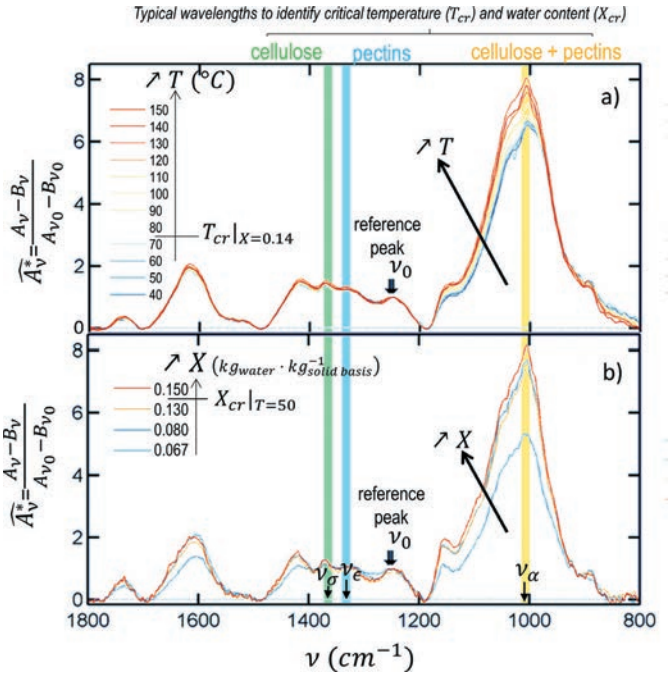

▸ *Figure 2: Variations of spectra with a) temperature (T) and b) water content (X). A_ν and B_ν are the raw spectra, as measured, and the baseline estimate, respectively.*

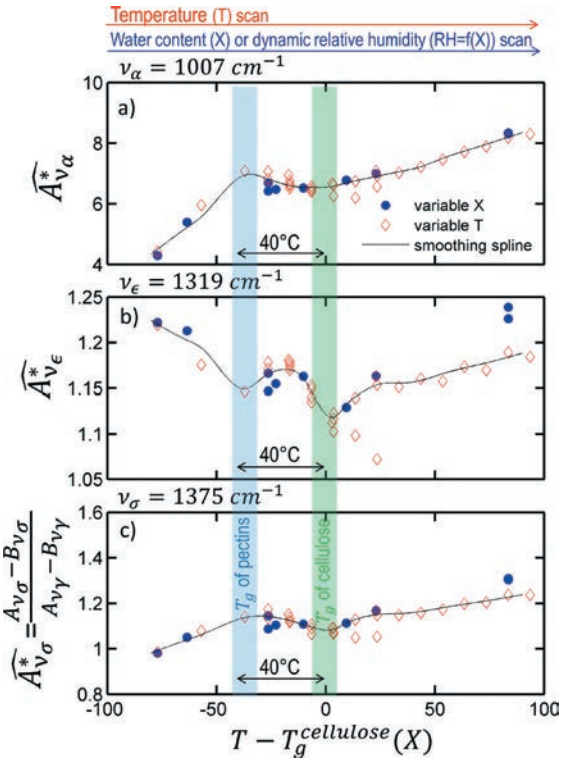

▸ *Figure 3: a, b, c) variations of normalized absorption bands with T-T_g during a scan of temperature or water content. All results are compared by choosing the glass transition temperature of cellulose as reference.*

▸ CONCLUSION

A methodology formulation to image the distance *T-T_{cr} (X)* or equivalently *T-T_g (X)* from mid-infrared vibrational spectra in the fingerprint region has been tested and validated. Based on the configuration depicted in fig. 1a, a simple scan of temperature enables to map rubber and glassy regions, mechanical properties. The whole methodology is currently applied to understand propagation of ruptures in the crust of parfried frozen products.

Escherichia coli facing silver nanoparticles: when synchrotron FTIR microspectroscopy helps preventing biofilm formation

▶ SCIENTISTS INVOLVED

M. Mercier-Bonin[1], C. Saulou-Bérion[2], R. Briandet[3], M. Cocaign-Bousquet[4], L. Girbal[4], C. Maranges[4], P. Dumas[5], F. Jamme[5]

[1] Toxalim INRA, INPT, UPS 31300 Toulouse, France

[2] GMPA, INRA, AgroParisTech, 78850 Thiverval-Grignon, France

[3] Micalis, INRA, AgroParisTech, 78350 Jouy-en-Josas, France

[4] LISBP, INRA, INSA, UOS, INP, 31400 Toulouse, France

[5] Synchrotron SOLEIL, 91190 Gif-sur-Yvette, France

▶ CORRESPONDENCE

Muriel Mercier-Bonin
muriel.mercier-bonin@inra.fr

▶ REFERENCES

[1] C. Saulou et al. (2013) Anal. Bioanal. Chem., 405, 2685-2697.
[2] A. Allion-Maurer et al. (2015) Surf. Coat. Technol., 281, 1-10.
[3] C. Saulou-Bérion et al. (2015) PLoS One, 10, e0145748.

▶ KEYWORDS

Silver nanoparticles, Escherichia coli, biofilm, anti-biofilm plasma-deposited coating, biochemical composition, sFTIR microspectroscopy, ageing.

Biofilms can be defined as a complex and dynamic ecosystem, constituted by a community of microorganisms adhering to a substrate and often embedded within a self-produced extracellular polymeric matrix. Biofilm formation can lead to harmful effects, including medical device-related infections, food spoilage, spread of foodborne diseases, biofouling of materials and environmental concerns. Surface engineering for preventing microbial adhesion and biofilm formation is thus a challenging question, which has fuelled an explosion of research in surface science for the development of antimicrobial and/or anti-adhesive materials by physical or chemical modifications. Much attention has been directed toward silver-based coatings, due to the broad-spectrum biocide activity of silver towards many bacterial, fungal and viral agents at low concentrations. In particular, plasma-assisted silver nanoparticles (nanosilver) technology was shown to achieve the desired structural and functional film properties for limiting adhesion of bacteria, like *Escherichia coli*. However, the antimicrobial activity of the plasma-deposited nanosilver-coating on *E. coli* biofilm and the evolution of the coating structural properties with time remained to date unknown. Likewise, the biochemical response of *E. coli* facing silver stress was still largely ignored.

In this framework, the antimicrobial activity of the coating vs. bare stainless steel was evaluated on *E. coli* biofilm-forming bacterial cells by combining fluorescent bacteria labelling and confocal laser scanning microscopy. To support the temporal evolution of its anti-fouling properties, a thorough characterization of the coating was performed before and after ageing by combining a set of analytical tech-

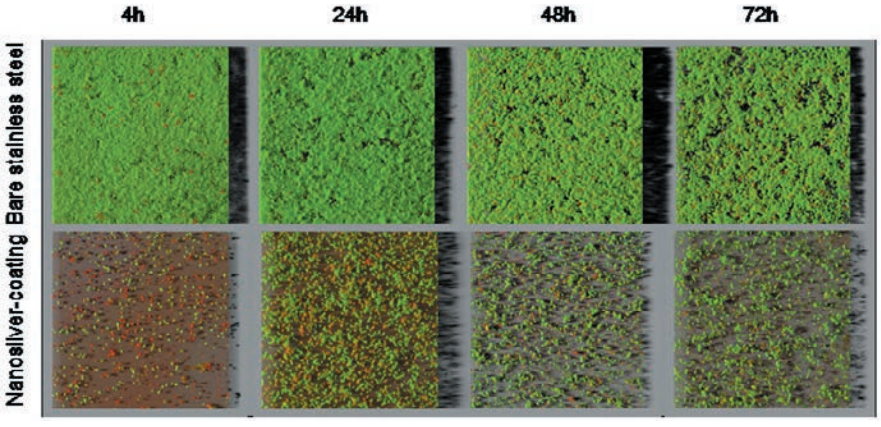

▶ *Figure 1: Representative confocal laser scanning microscopy images over time of E. coli biofilm growing on bare stainless steel (top) or plasma-deposited nanosilver-coating (bottom). Bacterial cells are labelled with the Live/Dead® BacLight™ kit: viable bacteria are labelled in green by SYTO® 9 while dead ones are coloured in red by propidium iodide.*

niques, notably electron microscopy. Then, using synchrotron FTIR (sFTIR) microspectroscopy, the biochemical composition of *E. coli* was unraveled after exposure to silver in its ionic form, due to its major role in nanosilver-induced bacterial changes.

▸ SCIENTIFIC QUESTION

For the first time with bacteria, sFTIR microspectroscopy performed with a high spatial resolution, thanks to a zinc-selenide (ZnSe) ATR hemisphere, was demonstrated to be an outstanding method for monitoring at single-cell scale cellular changes, even subtle, induced by silver [1]. Indeed, due to the small size of studied bacteria (length ~ 2 µm), a very good signal to noise ratio and a high spatial resolution are required. The use of the synchrotron source allowed optimizing the signal detection. In addition, with the ZnSe hemisphere and the high refractive index of the crystal, the spatial resolution was improved by roughly a factor of 2.4 (thus reaching the micrometre order).

▸ MAIN RESULTS

The antimicrobial property of the native nanosilver-coating towards an *E. coli* biofilm was determined. For short contact times, bacteriostatic (i.e. inhibition of biofilm growth) and bactericidal properties were associated [2]. The bacteriostatic effect was maintained over the 72-h exposure period tested. However, beyond 48 h, a loss in bactericidal activity was observed (Fig. 1). Such results could be related to the kinetics of silver release, the sequestration of released silver by some organic components of the biofilm matrix and/or the increase with time in tolerance of *E. coli* bacterial cells within the biofilm towards silver. To support these findings, the morphology of the coating before and after ageing was visualized by electron microscopy [2]. For the native film, a granite-like aspect was observed, with a uniform distribution of spherical and nano-sized silver particles within the bulk matrix (Fig. 2). However, after ageing, the film morphology was substantially altered and a gradient in silver content was detected, with a quasi-absence of nanoparticles nearby the surface (Fig. 2). Based on these results, the biochemical response of *E. coli* after ionic silver exposure was characterized using sFTIR microspectroscopy. We considered bacterial cells grown in presence of ionic silver at a lethal (100 µM $AgNO_3$) vs. sub-lethal (5.0, 6.5, 8.5 µM $AgNO_3$) concentrations [1]. The raw single-cell spectra are shown in Fig. 3. To improve the detection of shifts in the characteristic absorption bands, a sensitive and powerful method for analysis was developed [1]. We demonstrated that, for lethal ionic silver concentration, both fatty acids (i.e. shortening of the aliphatic chains of bacterial lipids) and proteins (i.e. alteration of the protein secondary structure) were affected. Under sub-lethal conditions, similar changes in biochemical composition occurred, albeit at a different extent. A 5-µM $AgNO_3$ concentration altered fatty acids, this impact being not significantly accentuated at higher tested concentrations. However, the effects on protein conformation were observed for 6.5 and 8.5 µM but not noticed for the lowest $AgNO_3$ concentration. Then, variations in the biochemical composition of *E. coli* cells were highlighted even for very subtle differences in conditions of silver exposure [1].

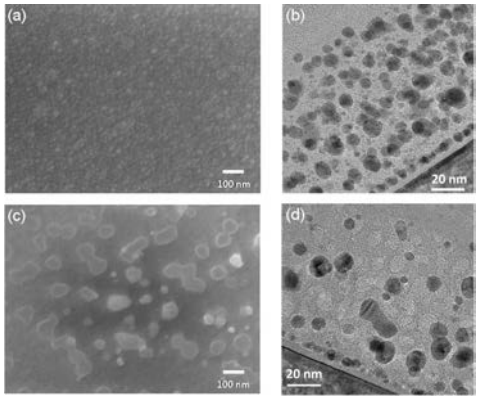

▸ *Figure 2: SEM planar views (a,c) and TEM micrographs (b,d) of the plasma-deposited nanosilver-coating; (a,b) before ageing; (c,d) after ageing in saline solution (NaCl 150 mM).*

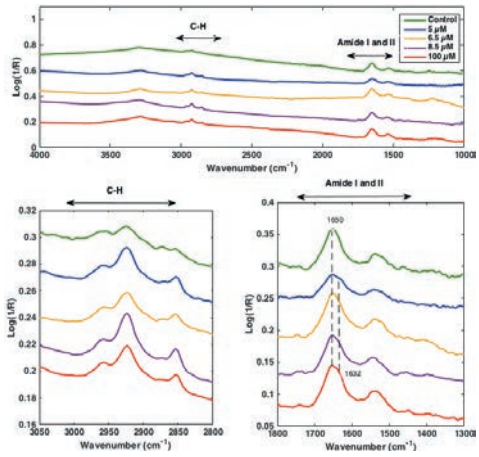

▸ *Figure 3: (Top) sFTIR raw spectra in the 4,000–1000 cm^{-1} region recorded at a single-cell scale on E. coli grown without (control) or in the presence of ionic silver at lethal (100 µM $AgNO_3$) or sub-lethal (5.0, 6.5, 8.5 µM $AgNO_3$) concentrations. The regions of interest are identified by horizontal arrows in the figure; (Bottom left) Focus on the fatty acid region (3,050–2,800 cm^{-1}); (Bottom right) Focus on the region (1,800–1,300 cm^{-1}), including amide I and amide II bands, which are characteristics of the peptidic bonds of peptides and proteins. The downshift in the amide I band (α-helix, 1650 cm^{-1}) between control E. coli cells (in green) and 100-µM $AgNO_3$ treated cells (in red) is also indicated as an example.*

▸ CONCLUSION

Bacteriostatic and bactericidal effects of the plasma-deposited nanosilver-coating were combined for limiting *E. coli* biofilm growth, by targeting cell fatty acids and proteins, at an extent depending on the silver exposure conditions. These biochemical changes were recently related to the physiological and transcriptional responses of *E. coli* [3]. From a process point of view, characterization of the film properties after ageing revealed that a silver reservoir was still present and potentially active in the deep layers of the coating. These findings may now offer new issues for tailoring plasma-deposited nanosilver-coatings to requirements for specific technological or environmental applications.

Lipid digestion in emulsion: time-resolved monitoring of coexisting nanostructures using synchrotron SAXS

SCIENTISTS INVOLVED

S. Marze[1], C. Gaillard[1], P. Roblin[2,3]

[1] BIA, INRA, 44000 Nantes, France

[2] Synchrotron SOLEIL, 91190 Gif-sur-Yvette, France

[3] CEPIA, INRA, 44300 Nantes, France

CORRESPONDENCE

Sébastien Marze
sebastien.Marze@inra.fr

REFERENCES

S. Marze et al. (2015) Soft Matter, 11, 5365-5373.

KEYWORDS

Lipid, digestion, emulsion, micelle, vesicle, triglyceride, model.

The absorption of lipids is only possible after a number of physicochemical processes within the gastrointestinal tract. One of the most important is the formation of assemblies enabling their transport. Lipids are emulsified in the stomach, so that droplets can be transformed into micelles and vesicles in the small intestine. The scientific goal of this study was to characterize these structural changes during intestinal lipid digestion. The main challenge was to measure the size of various nanostructures coexisting during digestion with a high resolution in time. This could only be achieved by small angle X-ray scattering (SAXS) using a synchrotron source.

The *in vitro* intestinal digestion of various emulsions diluted to 5 v% lipid was studied, differing only in the triglyceride (tricaprylin TC, or triolein TO) and emulsifier (β-lactoglobulin BLG, or sodium oleate NaO) used. These parameters were supposed to influence the digestion kinetics, thus the structural transitions. SAXS profiles in the range 0.009 $Å^{-1} < q < 0.8 Å^{-1}$ were obtained in intervals of 20 seconds for at least one hour and up to about three hours of digestion depending on the emulsion. A special sampling device was designed to continuously flow sample through the measurement capillary, from an emulsion that was constantly stirred and regulated to 37°C (fig. 1). As their initial droplet diameter was much smaller than 1 µm, the emulsions were stable against creaming throughout the experiment.

Transition times as characterized by intensity changes in the SAXS profiles were found to be mainly dependent on the triglyceride type, much faster for tricaprylin than for triolein (fig. 2). The first transition we were able to monitor started after 3 to 5 minutes of digestion. Then other transitions occurred within 15-30 minutes. After this period, the final state was reached for the tricaprylin systems, whereas more than 2 hours were needed for the triolein systems. The log-log slopes of the SAXS profiles indicated transitions between large spherical, lamellar, and small spherical organizations (fig. 3).

To go further in the interpretation, shape-independent and shape-dependent models were derived to fit the SAXS profiles. The first model allowed the evaluation of the smallest characteristic sizes in the systems, being the oil-water interface thickness, the long spacing of the molten lipid arrangement, and the micelle size. The second model captured the two latter, plus the larger vesicle size. Moreover, it enabled the calculation of the number density (number of objects per unit volume) for micelles and vesicles. This showed that these assemblies coexist after only 100 seconds of digestion, with a much higher number of micelles than of vesicles. Plotting these parameters as a function of digestion time revealed a growth of these assemblies by coalescence, much more marked for the triolein than for the tricaprylin systems. Moreover, the assemblies made from triolein digestion products took much more time to reach their final size than the ones made from tricaprylin digestion products, confirming the initial qualitative observations.

This study brings more questions about lipid digestion kinetics, in particular the earliest formation of assemblies from digested emulsion droplets. Stopped flow measurements with very high time resolution would enable the monitoring of this transition. Such a fast recording is only possible using X-ray from a synchrotron source, so this will be the focus of our next proposal to SOLEIL.

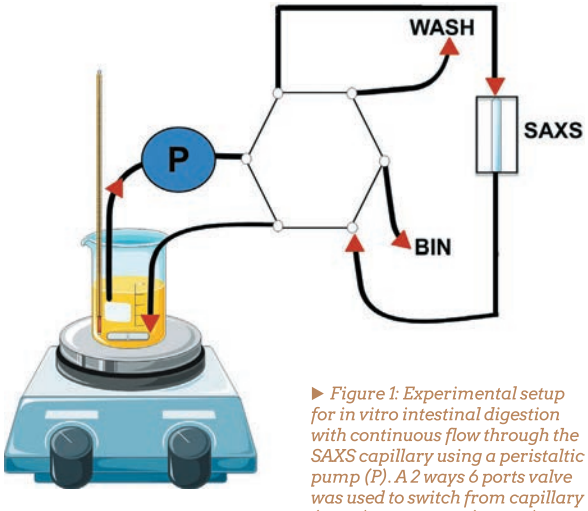

▶ *Figure 1: Experimental setup for in vitro intestinal digestion with continuous flow through the SAXS capillary using a peristaltic pump (P). A 2 ways 6 ports valve was used to switch from capillary (SAXS) to cleaning (WASH) or disposal (BIN).*

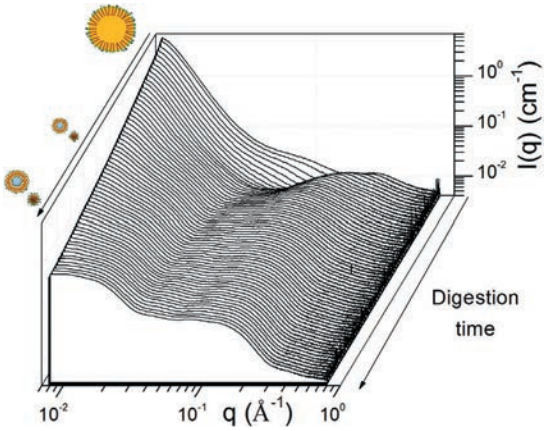

▶ *Figure 3: SAXS profiles for triolein emulsion stabilized by sodium oleate as a function of intestinal digestion time. Illustrations show the structural transitions from droplets to micelles and vesicles.*

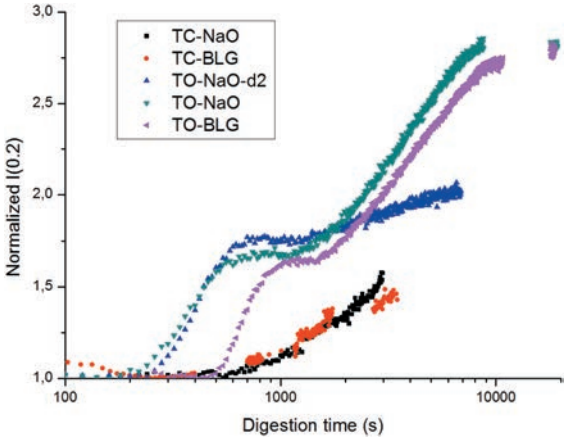

▶ *Figure 2: Normalized scattering intensity at 0.2 $Å^{-1}$ as a function of intestinal digestion time, highlighting some transitions (d2 corresponds to an additional 2-fold dilution of the emulsion).*

▶ CONCLUSION

The measurement of time-resolved SAXS profiles of emulsion undergoing intestinal digestion at the SWING beamline was a success. Their interpretation allowed the calculation of various parameters related to transition times and characteristic sizes. The results revealed that the kinetics and sizes are mainly dependent on the triglyceride type, and that both micelles and vesicles coexist throughout the digestion. This constitutes important information as these assemblies are responsible for the transport of lipids, lipophilic vitamins and other lipophilic bioactives towards their absorption site. A good understanding of their formation kinetics will thus certainly help optimizing their absorption efficiency.

SOLEIL SAXS and WAXS reveal the structure of fat crystals formed upon storage of breast milk at 4°C

▶ SCIENTISTS INVOLVED

C. Lopez[1], J. Perez[2]

[1] STLO, INRA-Agrocampus Ouest, 35000 Rennes, France

[2] Synchrotron SOLEIL, 91190 Gif-sur-Yvette, France

▶ CORRESPONDENCE

Christelle Lopez & Javier Perez
christelle.Lopez@inra.fr
javier.perez@synchrotron-soleil.fr

▶ REFERENCES

[1] C. Lopez (2011) Current Curr. Opin. Colloid Interface Sci., 16, 391-404.
[2] C. Lopez et al. (2013) Food Res. Int., 54, 1541-1552.
[3] S. Bugeat et al. (2011) Food Res. Int., 44, 1314-1330.
[4] S. Bugeat et al. (2015) Food Res. Int., 67, 91-101.

▶ KEYWORDS

Lipids, crystals, polymorph, X-ray diffraction, differential scanning calorimetry.

Breast milk contains 3 to 5% lipids contributing about 55% of the total energy intake and providing bioactive molecules to infants. Lipids are secreted in the form of lipid droplets called the breast milk fat globules (mean diameter 5 μm; [1]). The core of milk fat globules is composed by hydrophobic lipids, the triacylglycerols (TAG), containing 48 to 57% of saturated fatty acids. The fatty acid composition and the internal structure of TAG are important parameters governing their physical properties, in particular their crystallization properties. Little attention has been paid to the physical properties of TAG within human milk fat globules despite their importance in the mechanism of TAG digestion and nutritional consequences in infants. The mothers that cannot directly breast feed their infant can express their milk by pumping and store the human milk in the fridge (4 – 7°C). The objective of this work was to address the following scientific question: What is the effect of cooling breast milk from 37°C down to 4°C in the fridge on the crystallization properties of TAG within fat globules? [2]

▶ SOLEIL TAKES UP THE CHALLENGE

The challenge was to investigate the organization of TAG in the solid state, at a molecular level, *in situ* in breast milk containing low fat content dispersed within emulsion droplets and with a very small solid fat amount.

Moreover, identification of the melting behavior of TAG crystals as a function of temperature required the recording of short-time X-ray diffraction (XRD) patterns in combination with differential scanning calorimetry (DSC). The use of synchrotron radiation XRD recorded at both small (SAXS) and wide (WAXS) angles was therefore necessary to determine the longitudinal organization of TAG molecules in lamellar structures and to identify the polymorphic form of TAG crystals, respectively. Such methodological approach has been already experienced by our group on the Swing Beamline of SOLEIL synchrotron to study the crystallization properties of milk TAG within emulsion droplets of various sizes and fatty acid compositions [3], and in their anhydrous state [4].

▶ MAIN RESULT AND IMPACT

Storage of breast milk in the fridge alters the physical state of TAG dispersed within fat globules with the liquid to solid phase transition of at least part of milk fat. Microscopy experiments performed at 4°C revealed the non-spherical distorted shape of breast milk fat globules (fig. 1A), due to the presence of TAG crystals that have been formed in the core of fat globules during storage for 48 hours in the fridge. High-flux synchrotron XRD experiments performed at 4°C showed that the organization of TAG molecules within fat crystals corresponded to the most thermodynamically stable polymorphic form (beta crystals) and to lamellar structures with a thickness of 41.7 Å that correspond to a double chain length organization 2L of the fatty acid chains (fig. 1B). The structural parameters characterized by XRD allowed the

identification of the main TAG molecular species involved in the crystals.

The melting behavior of these TAG crystals has been studied on heating by the combination of XRD with DSC (fig. 2). The XRD patterns recorded as a function of temperature show a progressive decrease in intensity of the peaks recorded both at small and wide angles with no changes in their position (fig. 2A and B). The broad endotherm recorded simultaneously on heating of breast milk corresponded to the progressive melting of the beta 2L (41.7 Å) crystals until their final melting over 43°C (fig. 2C).
The final melting temperature of the beta 2L (41.7 Å) crystals is above the in-body temperature of milk digestion in the gastrointestinal tract of newborns, i.e. 37°C. This result means that at the temperature of milk digestion by infants, breast milk fat globules previously stored in the fridge are partially crystallized, i.e. a mixture of liquid and solid TAG. The impact of the physical state of TAG and particularly the proportion of solid fat on dietary lipid digestion and absorption remains poorly documented. The crystallization of TAG molecules could limit their hydrolysis by the digestive enzymes (bile salt stimulated lipase, gastric lipase, pancreatic lipase), and then affect the bioavailability of high melting point fatty acids such as palmitic acid that is important for breast fed infant nutrition and development. Then, we do recommend warming breast milk at least at 45-50°C before feeding the infants to ensure an optimal breast milk TAG digestibility and absorption.

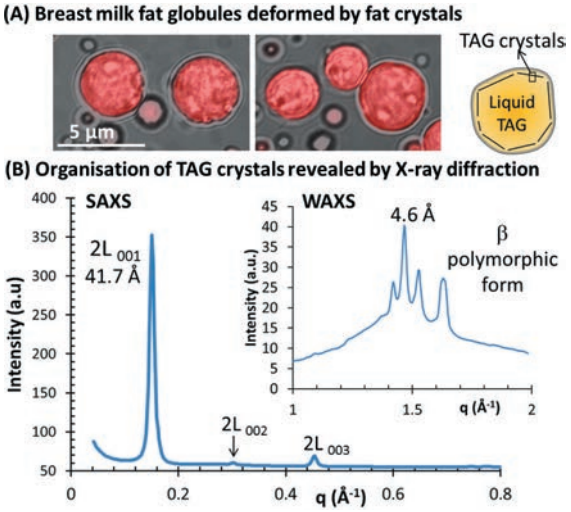

▶ *Figure 1: Fat crystals formed upon storage of breast milk in the fridge. (A) Microscopy images showing the deformation of breast milk fat globules induced by crystals of triacylglycerols (TAG), and schematic representation. (B) Structural analysis of the TAG crystals performed by synchrotron radiation X-ray diffraction at small (SAXS) and wide (WAXS) angles at 4°C.*

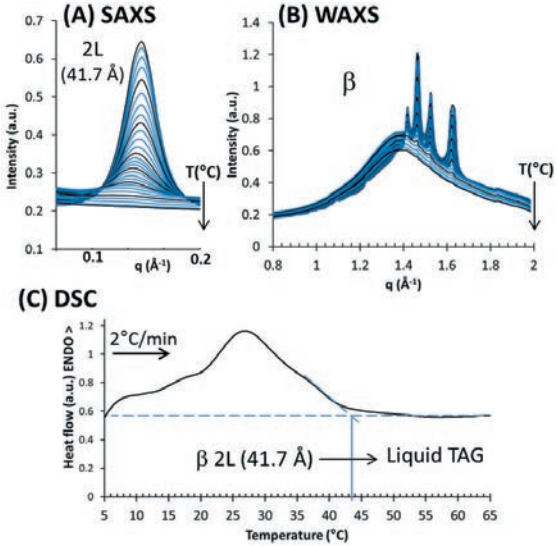

▶ *Figure 2: Melting behavior of the TAG crystals located within breast milk fat globules characterized on heating from 4°C to 60°C at 2°C/min by the coupling of X-ray diffraction at small (SAXS) and wide (WAXS) angles with differential scanning calorimetry (DSC).*

▶ CONCLUSION

This study revealed the formation of a solid TAG phase within fat globules upon storage of breast milk at 4°C [2]. The use of high-flux synchrotron radiation XRD permitted the description of the molecular organization of a complex mixture of TAG within milk fat globules at 4°C and their melting behavior as a function of temperature on heating. The coupling of XRD with DSC recordings permitted us to relate the structural parameters of TAG crystals to the thermal behavior of milk fat globules. The physical state of TAG at the temperature of milk digestion should be further considered for an optimal digestion of milk lipids.

Delivery of vitamins: impact of nanostructures in food emulsions

SCIENTISTS INVOLVED

P. Relkin[1], R. Shukat[1], C. Bourgaux[2]

[1] GENIAL, AgroParisTech, INRA, 91300 Massy, France

[2] NutriNeuro, INRA, Université de Bordeaux, INP Bordeaux, 33000 Bordeaux, France

CORRESPONDENCE

Perla Relkin
perla.relkin@agroparistech.fr

REFERENCES

[1] P. Relkin et al. (2009) J. Therm. Anal. Calorim., 98, 13-18.
[2] P. Relkin et al. (2014) Food Res Int., 63, 9-15.
[3] R. Shukat et al. (2012) J. Therm. Anal. Calorim., 108, 153–161.
[4] P Relkin, et al. (2014) Food Biophys, 9, 389-395.

KEYWORDS

Nanoemulsions, fat crystallinity and polymorphisms, particle size, vitamin.

SCIENTIFIC QUESTION

Light and heat sensitive lipophilic bioactive compounds, such as vitamins and antioxidants, can be protected against oxidation and degradation when incorporated in lipid matrices. It has also been shown that oil droplets in water emulsions may also be used as matrices for the protection of these bioactive compounds, which contributes to the reduction of fat intake in human nutrition. However, immobilisation of the bioactive in lipid droplets seems to depend on their state of crystallization, which is itself dependent on their size (droplet curvature). Thus, size and crystallinity are important factors, which govern the physical stability of the droplets against aggregation and coalescence, and therefore their protection efficiency when exposed to oxidating agents. Edible fats are composed by triacylglycerols (TAG), which form crystals made by longitudinal stacking of molecule layers in lamellar structures and lateral packing of fatty acid chains. The TAG longitudinal organization is comprised between 2 (2L) or 3 (3L) chain-length lamellar structure, leading to repetitive distances in the 40–50 and 55–70 Å ranges, respectively. The lateral packing of fatty acid chains correspond to different subcells used to identify three main polymorphic forms: hexagonal (α-form), orthorhombic perpendicular (β′-form), and triclinic parallel (β-form), ranging between 3.7 and 4.6 Å. The objective of the work was to study the contribution of polymorphisms in solid lipid nanoparticles to be used as bioactive matrix carriers when stored in their moist or dried state conditions, knowing that intensive thermomechanical treatment used for their preparation and long-term storage can be accompanied by chemical degradation of the bioactive compounds.

Thermodynamic and kinetic characteristics (induction temperature or time of crystal growth) of heat-induced transitions in vitamin-loaded hydrogenated palm oil or milk fat droplets were studied using μDSC in scanning or isothermal mode, alone. Combining μDSC and X-ray small- and wide-angle scattering (SAXS and WAXS, respectively) allowed crystals identification in emulsions [1]. The SWING beamline was used on emulsions differing by their compositions and particle size distributions, and which were stored in the liquid state at 4°C or at 20°C after spray drying. They contained 6% whey proteins in the aqueous phase and 20% hydrogenated palm oil of which 25 wt% was replaced or not by α-tocopherol (lipophilic vitamin). The particles size in mother emulsions were managed using high pressure homogenisation at 300 or 1200 bar [2].

MAIN RESULTS

Peaks observed in SAXS and WAXS signals (Fig.1) indicate the presence of 2L longitudinal stacking of triacyglycerol molecules, and lateral packing of fatty acids in α, β′ or β forms, respectively. These peaks were observed in all the emulsions studied whatever their composition and particles size. However as observed previously1, their intensity decreased with decreasing particle size (values in bracket) and with added bioactive lipophilic compounds.

Morever, analysis of the surface under the WAXS signals indicated that the proportions of α, β′ and β lateral packing of fatty acids in lipid droplets were more affected by the presence of vitamin rather than their size. The rate of α−−> β′ and β′ −−> β polymorphic transformations was found to be higher in vitamin-loaded emulsions which presented a lower degree of vitamin protection. This important finding supported the hypothesis following which shelf-life of vitamin-loaded lipid particles is affected by β and β′ , high energy TAG polymorphs capable of expelling the bioactive compound from the core of lipid droplets to their external surface [1, 2, 3].

The lipid organisation was also studied in spray-dried emulsions. SAXS signals were recorded from dried emulsions containing or not vitamin. They all exhibited a Bragg's peak located close to 0.15 $Å^{-1}$, except PET1200. As shown in Fig.2, instead of Bragg's peak in this q range domain, SAXS signal of PET1200 sample presented a shoulder in the q region 4×10^{-2} $Å^{-1}$< q < 1×10^{-1} $Å^{-1}$. In addition, it is seen that the slope of X-ray intensity versus q in the domain lower than 0.02 $Å^{-1}$ is higher for PET300 than PET1200 powder. The SAXS data did not provide enough information to make a claim about the size of scatterers, however for PET300 sample the slope which is of -4 (in correspondence with the Porod-scattering power law that is typically associated in this q region) could indicate the presence of scatterers with a surface fractal dimension of D=2. Conversely, particles in the PET1200 and PET300 samples, which presented different size characteristics and different vitamin ability for long-term protection of vitamin, behave differently in regards to fat crystallisation. After dehydration, PET1200 vitamin loaded emulsions with lower solid fat content and lower energy polymorphs and lower particle size presented a higher degree of long-term protection of vitamin [4].

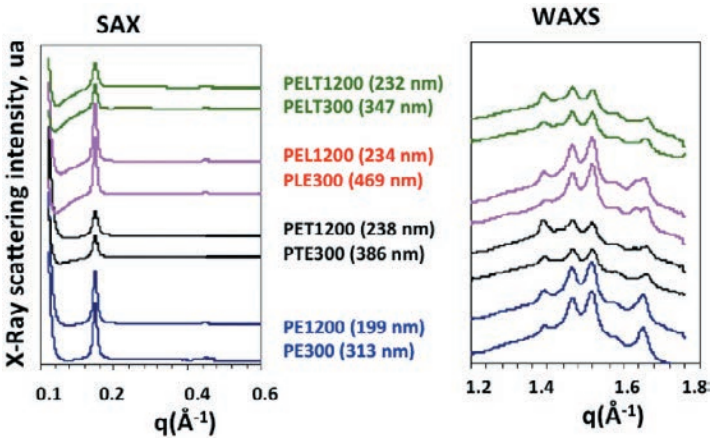

▶ *Figure 1: X-Ray Small (left) and Wide (right) angle scattering curves obtained from nanoemulsions prepared using high homogenization pressure at 300 or 1200 bar. PE and PLE are emulsions stabilized either by protein alone or in presence of lecithin, respectively. PET and PLTE are vitamin-loaded emulsions with α-tocopherol as a model of lipophilic bioactif compound. Numbers in bracket corresponded to their average particle size, in nm [4].*

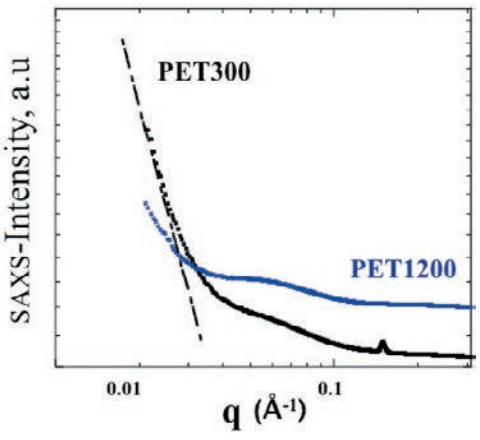

▶ *Figure 2: X-Ray Small angle scattering intensity as a function of scattering vector q, in log-log representation, as observed from spray dried vitamin-loaded emulsions which were produced at 300 bar (ET300) and 1200 bar (ET1200).*

▶ CONCLUSION

Using SWING beamline allowed identification and quantification of crystalline forms in bioactive-loaded nanoemulsions and to demonstrate that low solid/liquid fat content and low energy polymorphs favour lower vitamin degradation upon long-term storage in moist or dried states.

Synchrotron Infrared and Deep UV fluorescent microspectroscopy study of PB1-F2 β-aggregated structures in Influenza A virus-infected cells

SCIENTISTS INVOLVED

C. Chevalier[1], R. Le Goffic[1], F. Jamme[2], O. Leymarie[1], M. Réfrégiers[2], B. Delmas[1]

[1] VIM, INRA, Université Paris-Saclay, 78350 Jouy-en-Josas, France

[2] Synchrotron SOLEIL, 91190 Gif-sur-Yvette, France

CORRESPONDENCE

Christophe Chevalier
christophe.chevalier@inra.fr

REFERENCES

[1] C. Chevalier et al. (2010) J. Biol. Chem. 285, 13233-13243.
[2] A. Miodek et al. (2014) Biosens. Bioelectron. 59C, 6-13.
[3] A. Miodek et al. (2014) Anal Chem. 86, 9098-9105.
[4] J. Vidic et al. (2016) J Biol. Chem. 291, 739-51.
[5] C. Chevalier et al. (2016) J. Biol. Chem. M115.710533 (PMID 26896002).

KEYWORDS

Influenza A virus, Fourier Transform Infra-Red, Amyloid oligomerization, Membrane, fluorescent Imaging, Synchrotron Radiation experiments.

SCIENTIFIC QUESTION

Every year, Influenza A viruses (IAV) are responsible for seasonal epidemics resulting in considerable illnesses, death and significant economic loss. IAV is also a major source of pathogens in animals and causes devastating outbreaks in domestic poultry. PB1-F2 is a small IAV protein dispensable for viral replication but known to enhance virus pathogenicity. To gain insight into the structure/function relationship of PB1-F2, we investigated the structural behavior of recombinant PB1-F2 derived from various origins using biochemical and biophysical approaches, but also in different type of IAV-infected cells (alveolar epithelial and monocytic cells) known to be the major natural target of the virus. We showed that PB1-F2 is an intrinsically disordered protein able to switch from an unstructured state to a β-sheet conformation in a membrane environment [1]. Moreover, PB1-F2 assembles in IAV-infected cells as β-soluble oligomers and fibers to finally aggregate in a cell-type dependent manner [2,3]. In order to decipher the oligomerization process of PB1-F2 and its impact in IAV-infected cells, combined multimodal FT-IR and DUV microspectroscopy were used on the beamlines SMIS and DISCO (fig. 1).

MAIN RESULTS AND PERSPECTIVES

In the present study, we demonstrate the presence of PB1-F2 beta-aggregates in IAV-infected cells at the single cell level using synchrotron radiation. Fourier-transform infrared (FT-IR) and deep UV (DUV) microscopy are non-invasive techniques for monitoring biochemical changes in situ in cells and tissues. Human alveolar epithelial pulmonary cells (A549) and monocytic cells (U937) were infected with a wild-type IAV and its PB1-F2 knock-out mutant and harvested at different times post-infection (fig. 1A). Infrared spectra were recorded in each condition, then compiled and processed to evaluate the change in the component band of the spectra corresponding to the amide I band (secondary structure changes) and the CH_2-CH_3 band (membranes and lipids). The data obtained were analyzed by principal component analysis (PCA). We confirmed the presence of a clear and specific infrared specific β-aggregates signature only in IAV-infected monocytic cells expressing PB1-F2 from 8 hours post-infection (h pi), represented by the presence of a pair of peaks at 1631 and 1693 cm^{-1} (fig. 1D). The comparison of the IR spectra obtained at 8 and 24 h pi highlight the progressive accumulation of β-aggregated structures by a distinct shift in the amide I region of the spectrum. In contrast, 2 peaks at 1653 and 1631 cm^{-1} assigned to α-helical and β-sheet structures respectively were obtained from IR spectra of IAV-infected epithelial cells. Taking advantage of the high frequency of tryptophan residues in the sequence of PB1-F2, we were able to correlate the increase of the auto-fluorescent signal recorded by DUV microscopy with the formation and the accumulation of the β-aggregates in IAV-infected cells (fig. 1F). Furthermore, we also observed that PB1-F2

compromises the integrity of the cellular membranes in a cell-type dependent manner [4], and notably a loss of membrane fluidity in IAV-infected monocytic cells which could be directly linked to the accumulation of β-aggregates in the vicinity of the membrane.

▶ Figure 1: SOLEIL Synchrotron FTIR and DUV set up and experiments. ***(A)*** *A549 or U937 cells were infected with IAV virus expressing (WT) or not PB1-F2 (F2), fixed at 8 and 24h post infection and collected prior to observation by IR or DUV microscopy.* ***(B)*** *The image shows the Continuum XL microscope (Thermo Fisher Scientific) used for FTIR microspectroscopic analysis performed on the SMIS beamline.* ***(C)*** *Transmission Image representing IAV-infected cells observed with the Continuum XL microscope before recording the IR spectra. Each annotated red cross corresponds to the acquisition of one single cell IR spectrum.* ***(D)*** *Score plot and Loading plot of PCA from the amide I band IR spectra. Marked data with the pink triangle correspond to U937 cells infected with WT virus, gray circle to cells infected with F2, and white square to mock-infected cells.* ***(E)*** *The image shows the Telemos full field microscope used to record the Trp fluorescence of IAV-infected cells in the DUV with the DISCO beamline.* ***(F)*** *Comparison of the fluorescence intensity measured in mock, WT, and F2-infected cells. Fluorescence intensity was quantified and normalized to the surface area of the cells. Data are expressed as mean+/- S.E. by an analysis of variance test. ***, p<0.001. Transmission images in bright field microscopy (bottom image) and in DUV fluorescent microscopy (top image) of IAV-infected U937 cells are presented.*

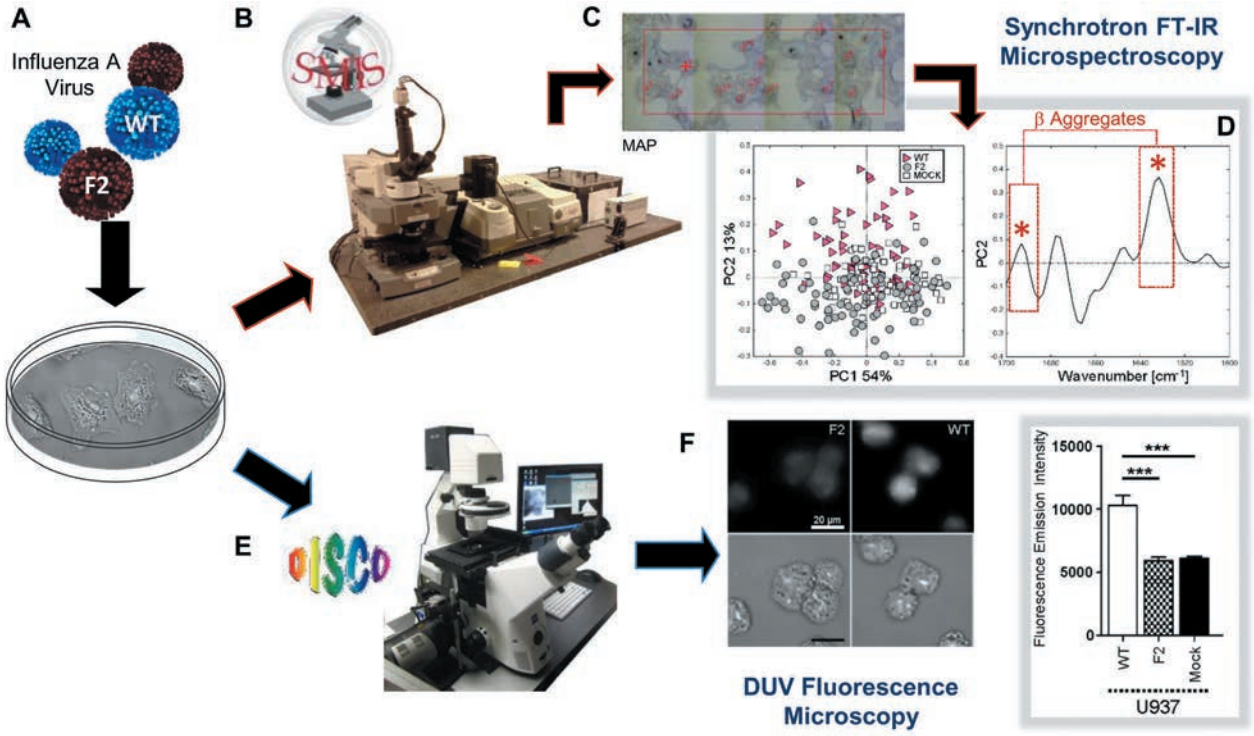

▶ CONCLUSION

To summarize, spectral changes recorded on the SMIS beamline due to the expression of PB1-F2 vary in extent and quality for the different cell types and the IR signature ascribed to β-aggregates can only be observed in monocytic cells. The results obtained on the DISCO beamline are in accordance with the cell-type dependent structural behavior of PB1-F2 during the viral cycle. Moreover, we showed that PB1-F2 expression differentially affects the membranes in monocytic and epithelial cells. Altogether, our results provide new insight into the structural behavior of PB1-F2 and contribute to understanding its role in IAV pathogenesis [5].

SMIS beamline, a powerful tool to detect chemical changes occurring in spinal cord and to assess gene therapy efficacy in an animal model of Pompe disease

▶ SCIENTISTS INVOLVED

L. Dubreil[1,2], J. Hordeaux[1,2,3], J. Deniaud[1,2], C. Sandt[4], F. Jamme[4], M. A. Colle[1,2]

[1] UMR 703 PAnTher: PAnTher, INRA, Oniris, 44300 Nantes, France

[2] LUNAM Université, Oniris, École nationale vétérinaire, agro-alimentaire et de l'alimentation Nantes-Atlantique, 44300 Nantes, France

[3] LUNAM université, Université de Nantes, UFR Sciences et Techniques. 44300 Nantes, France

[4] Synchrotron SOLEIL, 91190 Gif-sur-Yvette, France

▶ CORRESPONDENCE

Laurence Dubreil
laurence.dubreil@oniris-nantes.fr

▶ REFERENCES

[1] P.S. Kishnani et al. (2007) Neurology, 68, 99-109.
[2] N. Raben et al. (2007) Acta Myol., 26, 45-48.
[3] H. Van den Hout et al. (2000) The Lancet, 356, 397-398.
[4] J. Hordeaux et al. (2015) Gene Ther., 22, 316-324.
[5] P. Heraud et al. (2010) Neuroimage, 49, 1180-1189.

▶ KEYWORDS

Glycogenosis type II, Pompe disease, Glycogen, Spinal cord, Neuron, IR micro-spectroscopy, gene therapy.

▶ INTRODUCTION

Glycogen storage disease type II, also known as Pompe disease, is a rare, progressive, and often fatal muscular disease. The underlying pathology is a deficiency of the enzyme acid alpha-glucosidase (GAA) that hydrolyzes lysosomal glycogen. This autosomal recessive neuromuscular disease caused by gene mutation that encodes GAA occurs with a frequency of 1 to 40 000 births in humans. In Pompe disease, the disorder is characterized by lysosomal glycogen accumulation in many tissues with skeletal muscles, heart and the central nervous system (CNS) which results in early onset of organomegaly, hypotonia and cerebral dysfunction [1,2,3].

The purpose of this research project was to administrate a viral vector with the gene encoding GAA (AAV-hGAA) into the cerebrospinal fluid [4] of the 6neo/6neo mouse, a relevant animal model of the Pompe Human Disease and to evaluate the correction of the central nervous system in treated Pompe mice by using complementary approaches (neuromuscular tests, enzymatic measurements, histological analyses and infrared (IR) micro-spectroscopy).

SMIS beamline is a powerful tool to evaluate the efficiency of gene therapy by identification of the glycogen storage, and other chemical modifications in spinal motor neurons and corticospinal white matter tracts, at the cellular

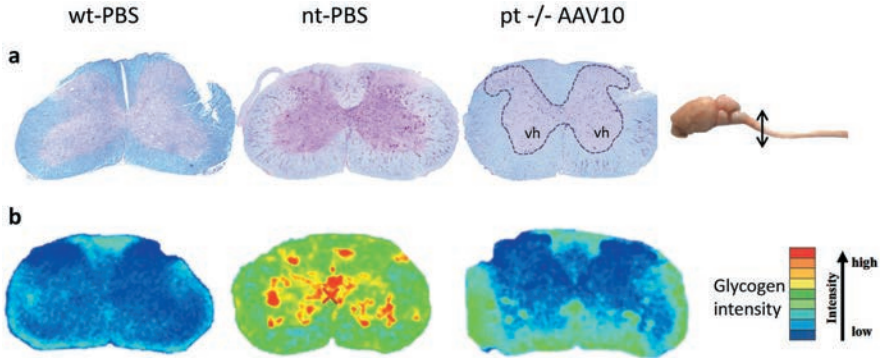

▶ Figure 1: a. representative sections of cross-sectioned cervical spinal cord, paraffin embedding, PAS-luxol fast blue stain. wt is for wild type motor neurons, nt for untreated motor neurons, pt for treated Pompe motor neurons. The glycogen storage appears purple on a blue background, motor neuron of spinal cord are located in ventral horn (vh). b. corresponding chemical imaging obtained from IR mapping acquired on sections after dewaxing and showing the relative concentration of glycogen.

and subcellular level. The main challenges were (i) to probe directly the biochemical changes in nervous tissue without the addition of contrast agent (ii) to map glycogen at a subcellular resolution and (iii) to analyze the myelin structural changes in spinal cord during the course of the disease and after administration of the treatment [5]. The results expected from these experiments would allow us to determine therapeutic window and to consider the validation of the treatment in monkey in order to achieve more precise data for further research on human beings.

▸ MAIN RESULTS

Thanks to the high brilliance of the IR synchrotron beamline of Soleil in the 2.5-100 µm spectral range, glycogen mapping was performed at the subcellular level to evaluate gene therapy efficiency on Pompe mice (Fig. 1).

Principal component analysis (PCA) of IR spectral data from motor neurons show that both treated (blue on Fig. 2) and wild type (black, Fig. 2) mice neurons were merged in the same cluster whereas IR spectra obtained from untreated Pompe mice neurons (red, Fig. 2) were characterized by elevation of the bands assigned to the carbohydrates of glycogen, triplet of peaks at ca 1025, 1080 and 1152 cm^{-1} (Fig. 2).

Furthermore, PCA analysis of spectra data from dorsal corticospinal white matter tracts showed that the intensity of the band at 1640 cm^{-1} was decreased in Pompe mice spinal cord white matter compared to treated and wild type mice (Fig. 3).
Therefore, chemical mapping of the cervical spinal has shown that a single delivery of AAV-hGAA in the cerebrospinal fluid of one-month old 6neo/6neo mice was able to reduce the glycogen storage both in grey and white matter of treated animals giving finally a spectral glycogen profile close to the wild type healthy mice. Additionally, fine mapping of amides function in white matter highlighted a decrease of peak intensity at 1640 cm^{-1} for Pompe mice samples and an increase of this peak intensity in treated as in wild type mice. This specific peak is suspected to be associated with change in B-sheet content or related to the ceramide backbone of sphingolipids of myelin.

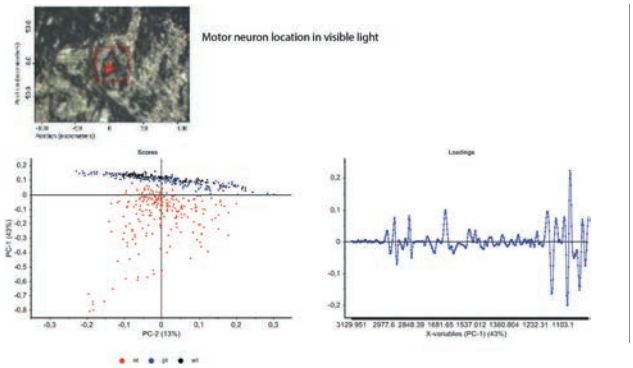

▸ *Figure 2: PCA of the IR spectra collected by mapping motor neurons and corresponding PC-1 loading plot. nt is for untreated motor neurons, pt for treated Pompe motor neurons and wt for wild type motor neurons.*

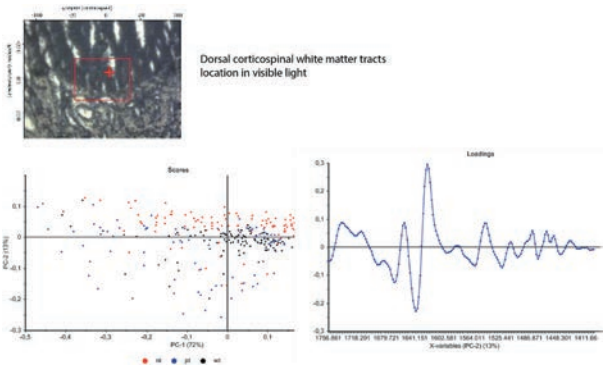

▸ *Figure 3: PCA of the IR spectra collected by mapping spinal cord dorsal white matter and corresponding PC-2 loading plot. nt is for untreated motor neurons, pt for treated Pompe motor neurons and wt for wild type motor neurons.*

▸ CONCLUSION

Synchrotron IR micro-spectroscopic mapping provided a detailed examination of the spinal cord selected regions (motor neuron and corticospinal white matter) and showed distinctly that delivery of AAV-hGAA into cerebrospinal fluid allow the correction of the lysosomal glycogen storage in Pompe mice.

These major results open the possibility to finely monitor the glycogen content using IR micro-spectroscopy on tissue section without addition of contrast agent. Furthermore, these experiments highlighted a new potential biomarker of the disease with a spectral signature at 1640 cm^{-1} which could also be used as a biomarker of the treatment efficacy. Complementary studies will be performed on SMIS and DISCO beamlines to characterize the biochemical modifications of cardiac muscle during the course of Pompe disease, with a subcellular spatial resolution. The comparison of these modification with those obtained for spinal cord are crucial to define an efficient therapy both on CNS and heart, the most affected organ in Pompe disease.

SOLEIL light reveals common allergenic structures involved in wheat allergies

SCIENTISTS INVOLVED

S. Denery-Papini[1], J-C Gaudin[1], Hamza Mameri[1], Chantal Brossard[1], Frank Wien[2], Yann Gohon[3]

[1] BIA, INRA, 44000 Nantes, France

[2] Synchrotron SOLEIL, 91190 Gif-sur-Yvette, France

[3] IJPB, INRA, AgroParisTech, CNRS, Université Paris-Saclay, 78000 Versailles, France

CORRESPONDENCE

Sandra Denery-Papini
sandra.denery@inra.fr

REFERENCES

[1] S. Denery-Papini et al. (2011) Clin. Exp. Allergy, 41, 1478-1492.
[2] H. Mameri et al. (2015) J. Agric. Food Chem, 63, 6546-54.

KEYWORDS

Food allergy, wheat allergens, antibody binding sites, SRCD, 2D structure.

Allergies have been a serious problem in western countries for 50 years. Due to severe symptoms and the absolute necessity of an eviction diet, food allergies have become a public health problem. This project aimed to improve knowledge about food allergies, and in particular wheat allergies for which only limited data existed. Allergies are triggered by specific interactions between antibodies (IgE antibodies) and proteins that are tolerated in normal conditions. The great majority of food allergens are proteins that are particularly resistant to heat and digestive denaturations ; structural characteristics that confer high allergen potential are not yet fully known. The project's objective was to identify the interaction areas between a given protein and IgE antibodies; these areas are called epitopes and results from interactions between particular structures within a protein and the immune system.

Most epitopes are conformational epitopes and comprise several portions of the protein brought together by folding of the protein.

Their identification requires information about 2D and 3D structures of allergens. Identification of epitopes of wheat allergens was intended to improve the understanding of wheat allergies and their diagnosis and prognosis. Epitopes were searched for in two major wheat allergens: alpha-gliadin and Lipid Transfer Protein (LTP).

Conformational epitope identification was carried out by applying several punctual modifications to different areas of the allergens to identify those that could prevent IgE antibody binding, and thus the areas mainly involved in protein/IgE interaction.

IgE antibody binding was measured by ELISA using sera from wheat allergic patients and the extent of structural modifications were evaluated through changes in their secondary structure content determined using synchrotron radiation circular dichroism (SRCD). In order to precisely localize IgE-binding epitopes, many different biochemical modifications were applied to the allergens. Precise structural changes could have been evaluated by crystallization and 3D structure resolution.

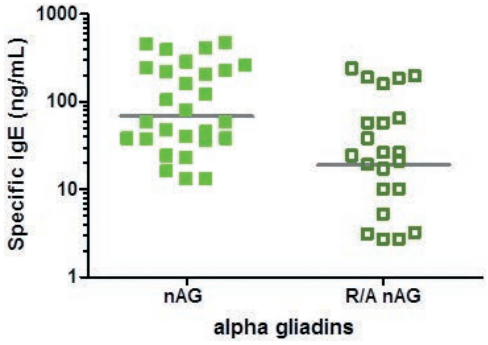

Figure 1: Effect of reduction-alkylation (R/A) of natural (nAG) alpha-gliadin on IgE binding measured by ELISA. Medians, plotted as grey bars, are significantly different.

However, alpha-gliadin is a gluten protein, such proteins being insoluble in saline solution, and for which no crystallization and consequently no 3D structures have been obtained thus far and moreover the evaluation of the impact of multiple modifications using 3D structure resolution would have been too time consuming and expensive. Comparison of 2D structures of the native allergens and of the collection of modified allergens was easily performed using SRCD. SRCD allows a more accurate determination of secondary structure compared to a laboratory dichrograph; this is of particular interest when comparing structures of related molecules.

Among the different biochemical modifications applied to both allergens, reduction of the intra-molecular bonds of the proteins had the most drastic effects on IgE-binding and probably disrupted some of the conformational epitopes. Fig. 1 shows the decrease measured with 28 patient sera for IgE-binding to the reduced/alkylated alpha-gliadin compared to the native protein. Although, for alpha-gliadin, no significant effect of intra-molecular bond reduction was observed on the secondary structures measured by SRCD (Fig 2), reduction may have an indirect but drastic effect on the global folding of the protein. On the contrary, for LTP disruption of two particular intra-molecular bonds abolished the protein interaction with IgE and caused a drastic change in protein secondary structure (Fig 3). Other modifications, except one, carried out on the LTP had only minor impacts on IgE-binding and on the protein structure.

These results indicated that intra-molecular bonds play a major role in the allergen potential of some major wheat allergens and are involved in areas bound by patient IgE antibodies.

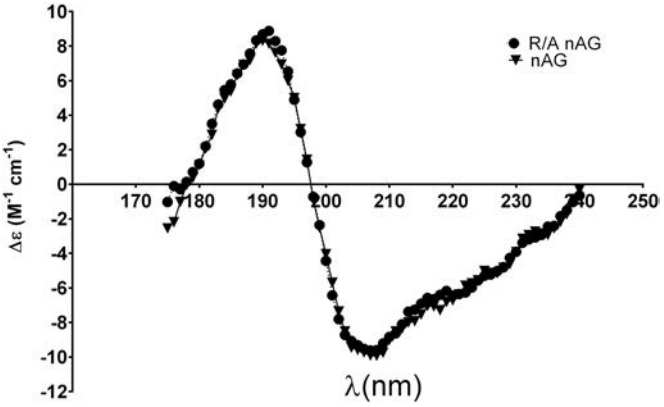

▶ *Figure 2: Effect of reduction-alkylation compared to native proteins on secondary structures of alpha-gliadin (2A). Dot and triangular symbols represent respectively data for reduced/alkylated (R/A nAG) and native (nAG) alpha-gliadins.*

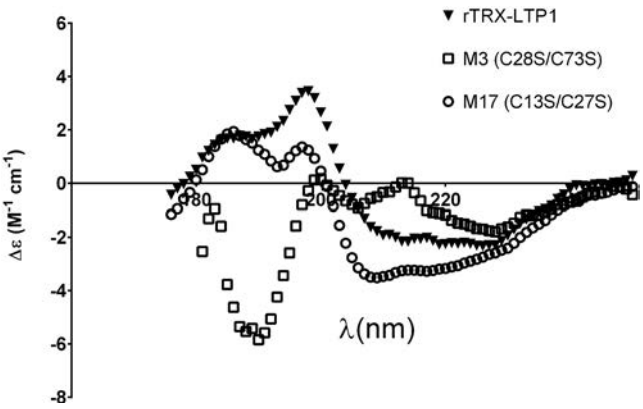

▶ *Figure 3: Effect of mutations of two disulfide bonds of LTP on secondary structures measured by SRCD. Spectra were acquired for LTP modified at the disulfide bonds C28/C73 (M3, square symbols) and C13/C27 (M17, dot symbol) and compared to the spectra of native protein (rTRX-LTP1, triangle symbols).*

▶ CONCLUSION

Although, alpha-gliadins and LTP have very different characteristics, they share some structural features in link with their ability to interact with IgE antibodies occurring in food allergies to wheat. The DISCO beamline at SOLEIL Synchrotron participated in the elucidation of these structures that probably possess an important role in disease initiation or symptom triggering.

Short ragweed pollen allergy in the light of SOLEIL beamlines

SCIENTISTS INVOLVED

R. Groeme[1], S. Airouche[1], D. Kopečný[2], J. Jaekel[1], M. Savko[3], N. Berjont[1], L. Bussieres[1], M. Le Mignon[1], F. Jagic[4], P. Zieglmayer[5], V. Baron-Bodo[1], V. Bordas Le Floch[1], L. Mascarell[1], P. Briozzo[4], P. Moingeon[1]

[1] Stallergenes Greer, 92160 Antony, France

[2] Faculty of Science, 78371 Olomouc, Czech Republic

[3] SOLEIL Synchrotron, 91192 Gif-sur-Yvette, France

[4] IJPB, INRA, AgroParisTech, 78026 Versailles, France

[5] Allergy Center Vienna West, Austria

CORRESPONDENCE

Pierre Briozzo
pierre.briozzo@inra.fr

REFERENCES

[1] J. Bouley et al. (2015) J. Allergy Clin. Immunol., 136, 1055–1064.

[2] R. Groeme et al. (2016) J. Biol. Chem., 291, 13076-13087.

KEYWORDS

Ragweed, allergen, cysteine protease, 3D structure, immunotherapy.

Short ragweed (*Ambrosia artemisiifolia*) pollen is a major cause for hay fever and allergic asthma. It is a serious human health concern in Northern America, from which the plant is originally native, and more recently in several European countries, where it continuously spreads. Ten short ragweed pollen allergens have been registered by the International Union of Immunological Societies. Among them, two enzymes are the major allergens: the pectate lyase Amb a 1 and the cysteine protease Amb a 11. The latter, recently identified [1], displays high sequence identities with allergens belonging to the C1A family of cysteine proteases. Firstly, the major allergens Der p 1 (24% identity) and Der f 1 (26%) from house dust mites, the most prevalent indoor allergens. Secondly, the plant allergens actinidin from Kiwi fruit (37%) and papain (35%) from Papaya.

A thorough understanding of the molecular events leading to allergy is facilitated by the elucidation of the three-dimensional structure of the allergen molecules. Furthermore, these structures pave the way for the rational design of variants with reduced IgE binding, which have possible uses in specific allergy vaccination In order to better understand the biochemical and structural basis for Amb a 11 allergenicity, we produced its recombinant proform (pro-r Amb a 11).

MAIN RESULTS AND PERSPECTIVES

Pro-r Amb a 11 was produced in *Escherichia coli* and refolded. *In vitro* maturation at pH 5.0 induced an autocatalytic processing resulting in the cleavage of both N- and C-terminal propeptides, revealing the enzymatic activity. Secondary structures of pro-rAmb a 11, pro-rAmb a 11 ΔCT lacking the C-term profragment typical of Amb a 11, and of the mature and active rAmb a 11 were assessed by synchrotron radiation circular dichroism (SRCD, DISCO, Fig. 1). Spectra of the various forms of Amb a 11 are similar, irrespective of the presence of the N- and C-terminal propeptides, thus indicating that the overall fold of Amb a 11 does not change significantly following maturation: the estimated α-helical contents were always between 27 and 29% [1]. The secondary structure content of the natural purified proform of Der p 1 (nDer p 1) is significantly different.

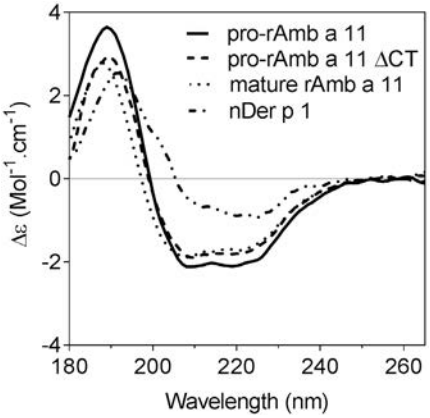

Figure 1: Activation of the recombinant proform of Amb a 11 does not significantly change the secondary structure content. SRCD spectra of pro-rAmb a 11, pro-rAmb a 11 ΔCT, rAmb a 11 and purified Der p 1 from Dermatophagoïdes pteronyssinus.

Pro-rAmb a 11 was purified using immobilized metal affinity allowed by the N-terminal polyhistidine tag, then by size exclusion chromatography. The purified pro-rAmb a 11 crystallized in orthorhombic $P2_12_12_1$ and

trigonal $P3_121$ space groups, leading to 2.70 Å and 2.05 Å resolution structures, respectively (PROXIMA 2A). The enzyme is a dimer in the crystals. Indeed, small-angle X-ray scattering coupled to on-site high-performance liquid chromatography (SWING, not shown) suggests that the concentrated Amb a 11 solution contains a mixture of monomeric and dimeric forms. Overall, both crystal structures show a typical C1A cysteine protease fold (Fig. 2). A specific network of molecular interactions connects the catalytic triad of the enzyme and the N-terminal propeptide. The latter forms a lid that covers the active site, hampering substrate proteolysis.

The allergenicity of Amb a 11 was assayed in a murine sensitization model. When compared with naive animals, mice sensitized to either pro-rAmb a 11 or rAmb a 11 exhibited a clear airway hyperresponsiveness (AHR). In parallel, eosinophils and type 2 innate lymphoid cells (ILC2) increased in bronchoalveolar lavages (BAL). Both AHR and inflammatory cell infiltrates were markedly higher in mice sensitized with the mature rAmb a 11 form. It suggests that the cysteine protease activity critically contributes to a strong allergenic inflammation. This is consistent with documented evidence that activities of Der p 1 and Der f 1 house dust mites cysteine proteases promote airway epithelium disruption, immune cell activation, and inflammation. To confirm the role of the protease activity on Amb a 11 allergenicity, we inhibited Amb a 11 enzymatic activity with the irreversible cysteine protease inhibitor E64. Mice sensitized with E64-inhibited rAmb a 11 exhibited significantly lower AHR, eosinophil and ILC2 infiltrates in BALs (Fig. 3).

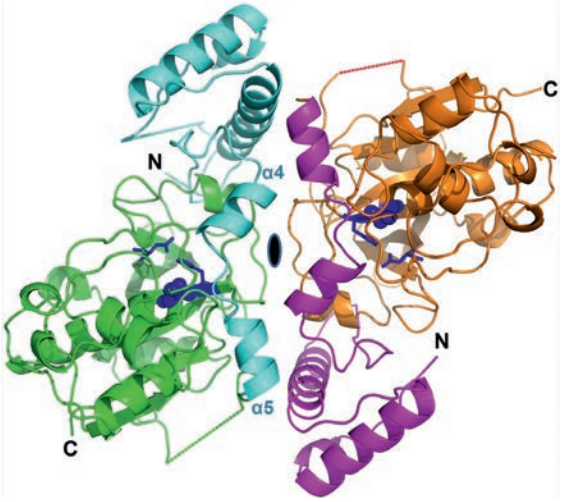

▶ *Figure 2: Overall fold of pro-Amb a 11. High-resolution structure of the dimer viewed along its 2-fold non-crystallographic symmetry axis (black ellipsis). Monomers A (left) and B (right) from the high-resolution structure are green and orange with the N-terminal propeptide cyan and magenta, respectively. Dotted lines indicate segments for which no clear density was observed. The catalytic triad is purple-blue with Cys-155 shown in spheres and His-289 and Asn-310 in sticks. Helices α1 and α5 from the N-terminal propeptide, that hamper access to the active site, are labeled.*

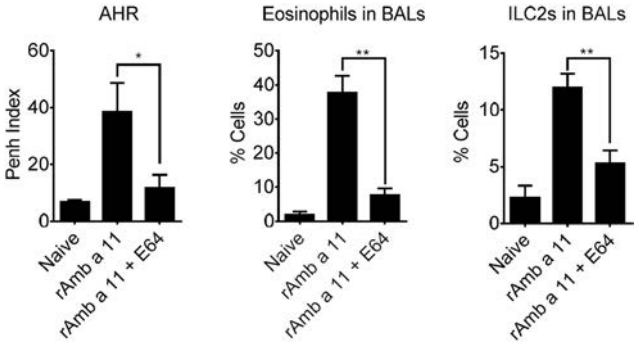

▶ *Figure 3: Impact of the inhibition of protease activity on Amb a 11 allergenicity. Left, AHR was assessed by whole body plethysmography at day 25. Centre and right: percentages of eosinophils and ILC2s were evaluated by flow cytometry. Results are expressed as mean values +/- S.E. (error bars) with n=6 mice per group. Statistical differences between rAmb a 11 and E64-inhibited rAmb a 11 were calculated using the non-parametric Mann-Whitney t test.*, p<0.05;**, p < 0.01.*

▶ CONCLUSION

Three SOLEIL beamlines allowed to better characterize the recombinant Amb a 11 proenzyme solution, and later on to determine its high-resolution crystal structure. Amb a 11 is a key component of the ragweed pollen for allergy diagnosis and immunotherapy purposes, and the properly folded and strongly allergenic rAmb a 11 molecule described here represents a valuable tool in this regard.

Plant Science under climate change

Plant science is an important research field for INRA scientists at SOLEIL. Various beamlines permit the collection of significant results on the transport of minerals and circulation of fluids in living plants, and also on mechanic properties of cell wall.

A speciation study on biologically relevant samples (Grillet *et al.*) led to an important discovery that paves the way for future work on the control of metal loading (Fe) in seeds (LUCIA).

Climate change and global warming affect the environment so it is vital to understand the behaviour of plants, especially crops, faced by multiple stresses associated with climate change. Certain studies require non-invasive observations on whole plants.

The direct and in vivo analyses performed at PSICHE by Badel *et al.* on hydraulic failure in trees is an example of such a study and provided reference results on the behaviour of long vessel plants that are required to close a debate on the way plants withstand water stress.

Combining mechanical testing using an original sensing device and IR micro- spectroscopy (SMIS) established links between cell wall polymer orientation and mechanical properties in very small samples (Barron *et al.*).

Ascorbate is the key to unlocking Fe transport in seeds

SCIENTISTS INVOLVED

L. Grillet[1], L. Ouerdane[2], P. Flis[2], M.T.T. Hoang[1], M.P. Isaure[2], R. Lobinski[2], C. Curie[1], S. Mari[1]

[1] B&PMP, IBIP, CNRS, INRA, Université Montpellier II, ENSAM, 34060 Montpellier, France

[2] LCABIE, IPREM, CNRS, Université de Pau et des Pays de l'Adour, 64063 Pau, France

CORRESPONDENCE

Stéphane Mari
stephane.mari@inra.fr

REFERENCES

[1] L. Grillet et al. (2014) J. Biol. Chem., 289, 2515-2525.
[2] L. Grillet et al. (2014) Front Plant Sci., 4, 535.
[3] C. Goodman (2014) Nat. Chem. Biol., 10, 169.

KEYWORDS

Iron, seed, ascorbate, *Arabidopsis*, *Pisum sativum*, XANES

CONTEXT

As the cofactor of many electron transfer enzymes, iron (Fe) is essential for all living organisms. The characterization of the chemical forms of Fe circulating between tissues is crucial to further understand the processes of transport to its final targets. The objective was to identify the chemical forms of Fe that are delivered to the embryo during seed development. This information is biologically crucial to further decipher, at a molecular level, how the process of Fe loading in seeds is controlled. In this study, the analysis of Fe transport in plants was focused on the process of seed loading, using pea (*Pisum sativum*) and *Arabidopsis thaliana* as biochemical and genetic models, respectively. The embryo sac liquid (ESL, 20 µL per seed), which corresponds to the liquid that feeds the growing embryo, was sampled from pea seeds, immediately frozen in liquid nitrogen and analyzed for Fe speciation. This chemical information was a prerequisite to unravelling the transport process in embryos. Given the reduced size of the samples and their biological origin, we needed a high flux focused beamline equipped with a cryostat in order to obtain X-ray absorption spectroscopic data that could help us to identify the Fe forms that are being transported towards the embryo.

RESULTS

XANES spectra were collected from pea ESL samples and from several standard complexes investigated using the LUCIA beamline (Fig. 1A). The ESL spectra obtained showed features of Fe(III) compounds such as Fe(III)-citrate or Fe(III)-malate. Actually, the best linear combination fits obtained for the ESL XANES spectra, corresponded to a mixture of 79% Fe(III)-citrate and 21% Fe(II)aq (Fig. 1B). The molecular

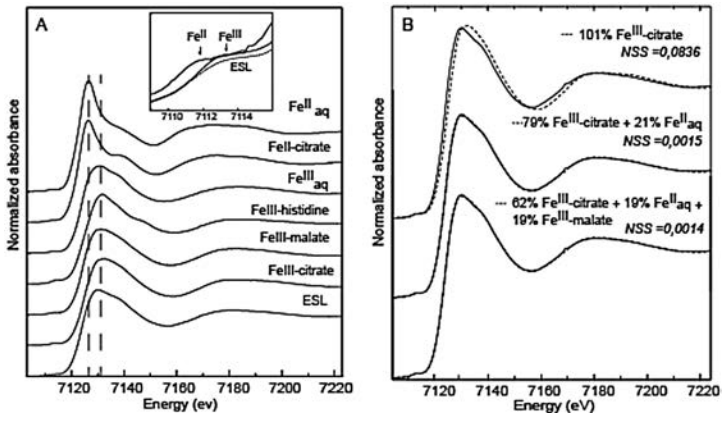

Figure 1: Fe K-edge XANES spectra of ESL and selected Fe model compounds (A) with the pre-edge structures of Fe^{II}_{aq}, Fe^{III}_{aq} and ESL (inset). One-, two-, and three-component fits (dotted lines) of ESL XANES spectrum (plain lines) (B).

identity of the Fe complexes was obtained by an approach based on the coupling of chromatography with mass spectrometry. Four different Fe complexes were identified; the two most abundant corresponded to ferric complexes with citrate and malate (Fig. 1C). Traces amounts of ferrous ions were detected, bound to another important metal chelator, nicotianamine (compound 4, Fig. 2). Taken together, these results confirmed the data obtained by XANES spectroscopy and indicate the major role of citrate and malate in the circulation of Fe in plant seeds.

This result provides significant advances in the understanding of Fe transport. In fact, plant cells are not capable of transporting Fe(III) directly and Fe acquisition requires a reduction step to generate Fe(II) that is the form readily transported across membranes. We thus hypothesized that pea embryos would also express a ferric reduction activity. Indeed, isolated embryos are able to reduce Fe(III) in vitro as shown by a colorimetric assay where the Fe(II) generated produces a pink coloration (Fig. 3 A). Unexpectedly, this ferric reduction activity was not encoded by the expected membrane-bound Ferric Reductase Oxidase (FRO) gene family since none of the known plasma membrane FRO proteins are expressed in embryos. Actually, this reduction activity corresponded to the efflux of a reducing compound that was further identified as ascorbic acid. Such a mechanism, never identified in plants before, represents a new strategy for taking up Fe, positioning ascorbate as a central player in Fe homeostasis [1].

We sought to confirm genetically this mechanism using the model plant *Arabidopsis thaliana* where the biochemical mechanism is conserved. We thus used the ascorbate synthesis defective mutants *vtc2* and *vtc5*, which displayed a decreased ferric reduction activity and a reduced accumulation of Fe in embryos and whole seeds (Fig. 3 B and C respectively).

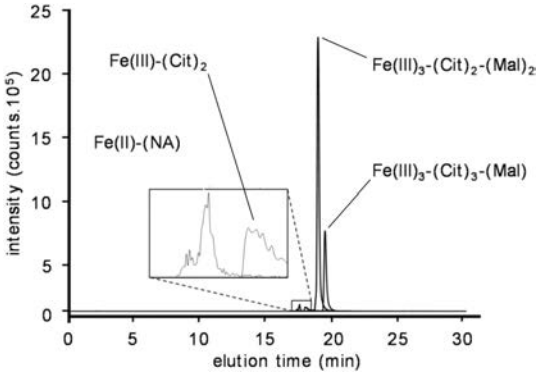

▶ *Figure 2: Result of chromatographic separations and ESI MS analysis evidences Fe (II or III)-malate (mal), -citrate (cit) and – nicotianamine (NA) complexes.*

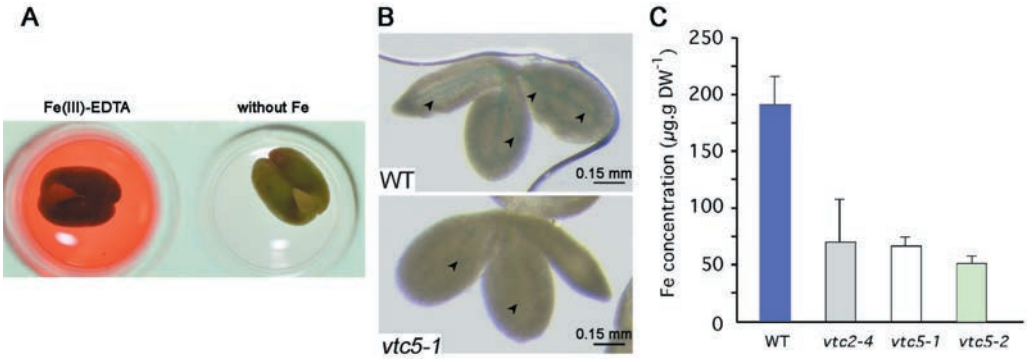

▶ *Figure 3: (A) Isolated pea embryos incubated with 300 µM BPDS and 100 µM Fe(III)-EDTA (left) or without Fe (right). Ascorbate synthesis deficient mutants (vtc2-4, vtc5-1 and vtc5-2) accumulate less Fe in embryos than wild type (WT), as revealed by Fe staining in blue in embryos (B) and in whole seeds (C).*

▶ CONCLUSION

These results illustrate how a speciation study on biologically relevant samples led to an important discovery that paved the way for future work on the control of metal loading in seeds [2, 3].

In vivo monitoring of hydraulic failures in trees

▶ SCIENTISTS INVOLVED

E. Badel[1], R. Burlet[2], G. Charrier[2], B. Choat[3], H. Cochard[1], S. Delzon[2], S. Jansen[4], A. King[5], N. Lenoir[6], N. Martin[7], J. Torres[2]

[1] PIAF, INRA, Univ. Clermont-Auvergne, 63000 Clermont-Ferrand, France

[2] BIOGECO, INRA, Université de Bordeaux, 33400 Talence, France

[3] HIE, Western Sydney University, 2753 NSW, Australia

[4] ISBE, University of Ulm, 89081 Ulm, Germany

[5] Synchrotron SOLEIL, 91190 Gif-sur-Yvette, France

[6] Placamat, CNRS, Université de Bordeaux, France

[7] URFM, INRA, Avignon, France

▶ CORRESPONDENCE

Eric Badel
eric.badel@inra.fr

▶ REFERENCES

[1] H. Cochard et al. (2013) J. Exp. Bot., 64, 4779–4791.
[2] J.M. Torres-Ruiz et al. (2014) Physiol. Plantarum, 152, 465-474.
[3] H. Cochard et al. (2015). Plant Cell Environ., 38, 201-206.
[4] J.M. Torres-Ruiz et al. (2014). Plant Physiol., 167, 40-43.
[5] B. Choat et al. (2016) Plant Physiol., 170, 273-282.

▶ KEYWORDS

Trees, plants, cavitation, embolism, hydraulic, drought resistance, water stress, 3D visualization, X-ray micro-tomography, *in vivo*.

▶ WATER TRANSPORT AND FAILURES IN TREES

The transport of water in trees is driven by the transpiration process that occurs in the stomata at the leaf surface. The vaporisation generates a water/gas meniscus with a nanoscale curvature. This produces a very high level negative pressure difference and a high level pressure gradient along the long hydraulic continuum that transports the water from the roots to the leaves. Thus, in the conducting conduits, the water columns are under negative pressure (under tension); which is very metastable. When plants experience water stress, this physical tension stress can increase until the irreversible failure of the hydraulic column that rapidly losses its conducting functions. The physical phenomenon is initiated by the cavitation event: an air bubble is aspirated from a neighbouring embolized conduit into a conducting conduit through microscopic holes in the double cell wall: the pits. The impacted conduit empties almost instantaneously and becomes non-conducting; the water column is irreversibly broken: this is the gaseous embolism. If the water stress increases, the embolism can propagate from conduits to conduits, and severely decreases the conducting function of water in the organs, and finally may impair the survival of the tree.

▶ X-RAY MICROTOMOGRAPHY OBSERVATIONS

The destructive methods traditionally used for measuring the loss of conductivity as a function of hydraulic tension, have clear limitations, particularly for plants with long conducting vessels. The direct observation by X-ray micro-tomography, that allows visualizing the hydraulic statute of the conduits, is now available as a reference method for embolism

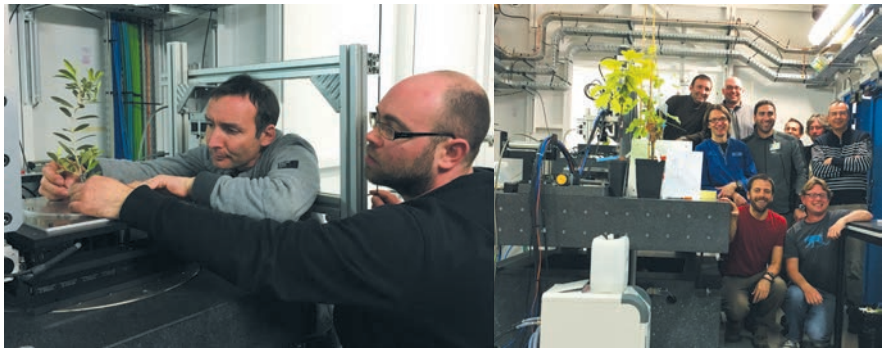

▶ *Figure 1: Setting the trees in the PSICHÉ X-ray beam (left) and the international team including several INRA researchers in the PSICHÉ experimental hutch (right).*

measurements. Many micro-tomographic devices are available in the laboratories (like the Nanotom bought by INRA in Clermont-Ferrand) but synchrotron beamlines offer complementary facilities. The very high intensity and stability of the X-ray beam, the scan speed and the size of the sample holder are some of the crucial parameters that allow carrying out many scans in a short time. The PSICHÉ beamline in SOLEIL offers all these facilities. One of the features of PSICHÉ beamline is to propose a hollow rotary stage with a specific sample holder for installing tall plants, which is particularly suitable for our trees (Fig. 1). In addition, the quality of synchrotron radiation allows obtaining high quality images which significantly facilitate analysis.

▸ FIRST EXPERIMENTS AND RESULTS

An international team, including several INRA researchers (Fig. 1) was built in order to investigate the formation and propagation of embolism in the vascular tissues of living plants. During the first campaign performed in 2015 on the PSICHÉ beamline, several species including *Vitis vinifera*, were scanned in different water stress conditions (variation of water potential, Ψ). During this experimental session, we specially focused on the hydraulic behaviour of stems and petioles. The 3D micro-tomographic images allowed extracting transversal cross sections (Fig. 2) that clearly showed the gradual occurrence of the embolism that spread in the vascular network when the water tension increased. The measurement of the number and size of the embolized vessels provided the required data in order to build "vulnerability curves" that depict the sensitivity of a organ (Fig. 3). Simultaneous observations in different organs of the plants (stem or petioles) allowed sorting them in terms of cavitation sensitivity (Fig. 2 and 3). Moreover, these direct and *in vivo* observations provided reference results about the hydraulic behaviour of long-vesselled plants that are required to close a debate on the way the plants withstand water stress.

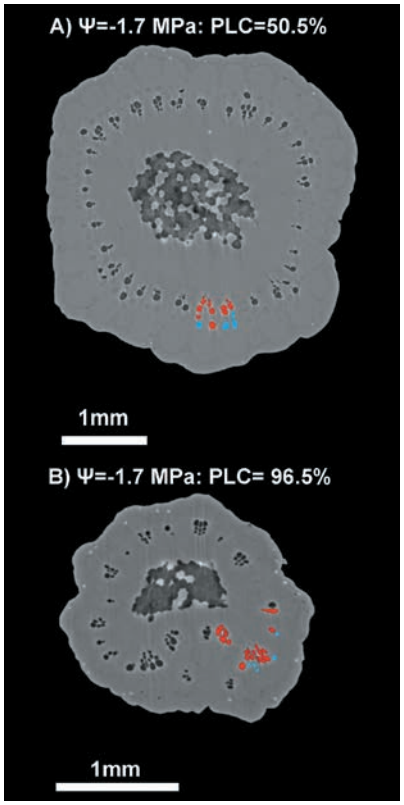

▸ *Figure 2: In vivo observation of the embolism spreading in Vitis vinifera stems (A) and petioles (B). PLC values refer to the percent loss of hydraulic conductivity of the cross section. Black holes correspond to the air-filled vessels, while other vessels are still water conducting. This difference is enlightened in a small region of interest using blue and red colours which represent the water- and air-filled vessels, respectively.*

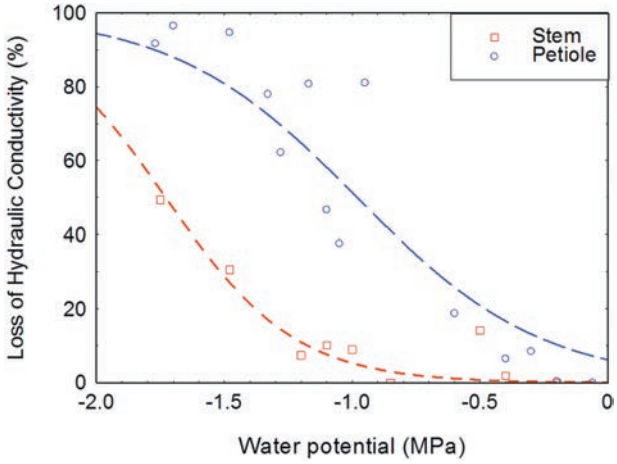

▸ *Figure 3: Percentage loss of theoretical hydraulic conductance depending on water potential in petioles and stem. Computation of the hydraulic conduction is performed using the distribution and the dimensions of the conducting vessels and the classical Hagen-Poiseuille theory. The dimensional characteristics of the vascular system are provided by image analysis on the cross sections slices extracted from the 3D tomographic scans.*

▸ CONCLUSION

These first experiments in the new micro-tomographic facility in the PSICHÉ beamline are very encouraging. The technical settings are essential for experiments with long samples like trees with elongated stems. Many other experiments can now be considered in order to investigate the hydraulic behaviour of plants to understand the cavitation and embolism spreading mechanisms and the interspecific variability we observe in plants when they experience water stress conditions.

Orientation under stress of cell wall polymers of the wheat aleurone cells: coupling mechanical test and infrared microspectroscopy

▶ SCIENTISTS INVOLVED

C. Barron[1], A. Sadoudi[1], F. Mabille[1], M. Martelli[1], F. Jamme[2], S. Lefrançois[2], P. Dumas[2]

[1] IATE, INRA CIRAD Supagro UM, Montpellier, France

[2] Synchrotron SOLEIL, 91190 Gif-sur-Yvette, France

▶ CORRESPONDENCE

Cécile Barron
cecile.barron@inra.fr

▶ KEYWORDS

Molecular orientation, wheat, tensile test, FTIR.

▶ SCIENTIFIC QUESTION

Wheat grain peripheral tissues can be compared to multilayer materials, predominantly composed of plant cell walls. They are made up of several tissues differing in their cellular organization or composition. Their mechanical properties (cohesion and adhesion) are key properties to explain their ability to be dissociated during milling process and were mainly related to plant cell wall structures. Indeed, as a cell frontier, they are forming a continuous network which is at the origin of the mechanical properties of products. From a molecular point of view, these properties (extensibility, rigidity) are related to the cell wall polymers organization, in particular through polysaccharides (arabinoxylans) crosslinking via phenolic bridges. The influence of covalent cross-links was analyzed at the tissue level but the analysis of the macromolecules orientation under stress, at the cell wall scale, would highlight more directly the link between covalent crosslinking and mechanical property.

▶ MAIN RESULTS AND PERSPECTIVES

To simplify the system, this study was carried out on the aleurone layer, accounting for 50% by weight of the wheat grain peripheral tissues. This tissue can be hand-isolated and many data (biochemical, spectroscopic, mechanical) have been already acquired. The wheat aleurone layer is composed of a single layer of cells forming a honeycomb structure. The cell dimensions are about 40 µm in diameter, incompatible with the infrared analysis in transmission, in contrast to plant cell walls which are 4 µm thick. An original method of preparation has been developed to isolate a wall of the aleurone layer, using cold laser ablation (to open cells) and sonication to remove cell contents (Fig. 1). A microtest tensile stage has been adapted to be placed between the lens and the condenser of the SMIS microscope, thanks to a dedicated XYZ stage which has been specifically developed (Fig. 1). Using this original experimental device, tensile/compression mechanical tests at constant displacement rate (from 0.04 µm.s^{-1} to 25 µm.s^{-1}) can be carried out on small biological samples (3 mm gap, total displacement: 10 mm).

▶ *Figure 1: **A)** Experimental device on the SMIS microscope. **B)** Cross section of the aleurone layer placed on the microtensile stage (observation: epifluorescence microscopy under UV light. Blue autofluorescence due to cell wall phenolic compounds).*

The intensity of the synchrotron signal and its natural polarization, has allowed analyzing, throughout the cell, the orientation of the plant cell wall polymers. Two types of uniaxial tensile tests were carried out: (i) discontinuous test with different stop to acquire spectrum at fixed strain value (Fig. 2), (ii) continuous tests with ongoing spectral acquisition throughout the sample deformation (Fig. 3). Thanks to the brilliance of synchrotron radiation, acquiring spectra on a 12x12 µm area with a good signal to noise ratio was achievable with an acquisition time (a few seconds) consistent with the duration of the mechanical test. Prior orientation of cell wall polysaccharides has been highlighted. Moreover, spectral changes were observed in the polysaccharides fingerprint spectral range when the wall is placed under stress during a uniaxial tension test just before failure (Fig. 3). This methodological development will allow analyzing the differences in spectral changes for aleurone cell walls more or less cross-linked (using natural variability or exogenous oxidative treatment).

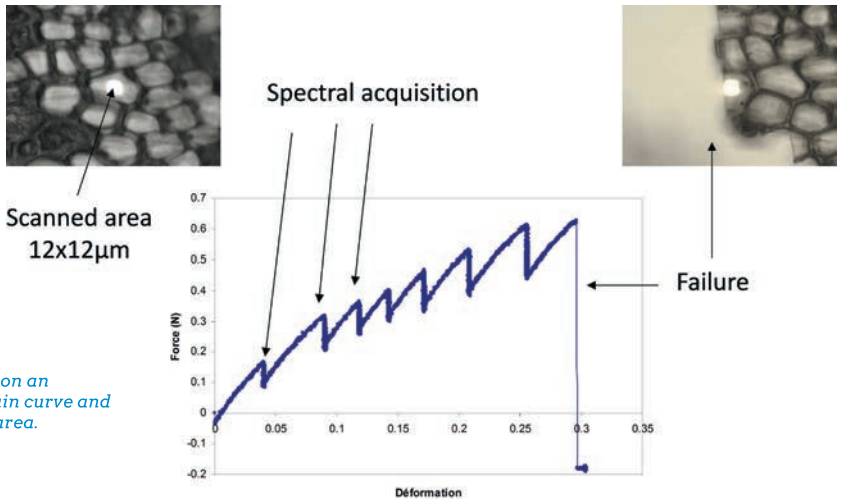

▶ *Figure 2: Discontinuous tensile test carried out on an aleurone sample (ablated+sonicated). Force/strain curve and microscopic observation of spectral acquisition area.*

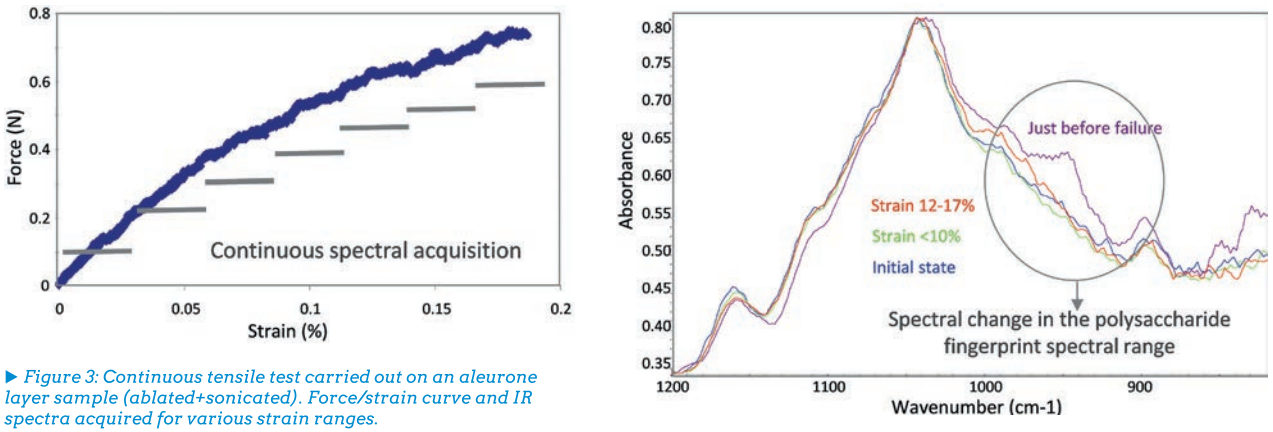

▶ *Figure 3: Continuous tensile test carried out on an aleurone layer sample (ablated+sonicated). Force/strain curve and IR spectra acquired for various strain ranges.*

▶ CONCLUSION

Cell wall polymer orientation was shown in the wheat grain aleurone layer at cell scale thanks to brightness and natural polarization of synchrotron beam by coupling mechanical test and IR spectroscopy on the SMIS beamline. A microtensile stage was adapted to be placed between the lens and the condenser of the SMIS microscope, using a dedicated XYZ stage specifically developed for this study. The analysis of very small sample area is now available all along its deformation and could be of great value for interfaces analyses or biomaterials applications.

Towards bioeconomy

In the context of global warming, mainly due to the use of fossil fuel carbon sources, efforts are required to promote new production pathways for molecules of interest from renewable resources. Innovative and cost-efficient use of biomass for the production of bio-based products and bioenergy require the removal of numerous bottlenecks.

▶ GREEN BIOTECHNOLOGY

In the context of bio-refineries development, the extraction of cellulose from plant by-products could be improved by the use of enzymes. Nevertheless, the presence of lignin remains a constraint. Devaux *et al.* used auto-fluorescence imaging (DISCO, UV microscopy) and IR micro-spectroscopy (SMIS) to localize in a time-dependent manner the changes to maize stem cell walls induced by hydrolytic enzymes.

INRA scientists have extensively explored the structure and physico-chemical properties of various plant polymers since the opening of SOLEIL.

DISCO deep UV light has been used for the direct label-free observation of the mode of action of hydrolytic enzymes on subcellular structure (starch grains) revealing original modes of actions of amylases (Rolland Sabaté *et al.*).

Starch based biodegradable biocompatible biomaterials have promising applications, for example, salivary duct surgery.

Chaunier *et al.* monitored the behavior of starch-based materials upon immersion in specific physiological media (SWING).

▶ WHITE BIOTECHNOLOGY

Original developments were made by Meneghel *et al.* at SMIS beamline for the observation of single living microorganisms 10 to 100 times smaller than eukaryotic cells.

Investigating the biochemical composition of microorganisms at the single-cell level (Fonseca *et al.*, SMIS) is a means for improving understanding of how carbon fluxes are directed towards molecules of biotech interest (lipids, sugars...), and how microbial populations react to stresses. Moreover, statistical approaches developed at SMIS and DISCO beamlines allow the study of population stress-response heterogeneity.

Use of auto-fluorescence or of fluorescent dye allows the performance of cell lipid structure imaging and membrane fluidity measurement in individual living microorganisms (Froissard *et al.*, DISCO).

The successful acquisition of the ATR-FTIR spectra of individual bacteria in a liquid environment with an inverted microscope (SMIS) represents a major breakthrough in analytical biology.

Biomass hydrolysis: a time-lapse localization of enzymes and modifications of maize stem cell walls by autofluorescence imaging and IR microspectroscopy

SCIENTISTS INVOLVED

M.-F. Devaux[1], F. Jamme[2], W. André[2], E. Bonnin[1], B. Bouchet[1], C. Alvarado[1], S. Durand[1], P. Robert[1], F. Guillon[1]

[1] BIA, INRA, 44316 Nantes, France

[2] Synchrotron SOLEIL, 91190 Gif-sur-Yvette, France

CORRESPONDENCE

Marie-Françoise Devaux
marie-francoise.devaux@inra.fr

REFERENCES

[1] S.Y. Ding et al. (2012) Science, 338, 1055-1060.
[2] F. Jamme et al. (2013) Biol. Cell., 105, 277-88.
[3] F. Allouche et al. (2012) Chemometr. Intell. Lab., 117, 200-212.
[4] C. Sandt et al. (2013) J. Biophotonics, 6, 60-72.

KEYWORDS

Time-lapse imaging, enzymatic degradation, enzyme autofluorescence, infrared microfluidic microspectroscopy, cell types, multimodal and multispectral imaging.

The enzymatic conversion of lignocellulosic materials for the production of fine and bulk chemicals in place of petroleum feedstock is a very promising approach due to high enzyme selectivity and mild use conditions. Lignocellulosic material mainly contains cell walls that consist of a network of cellulose micro-fibrils embedded in a matrix of hemicelluloses and encrusted by lignin. The complex architecture of plant cell walls makes them very resistant to degradation and the heterogeneity of composition according to cell type makes it difficult to determine the source of this recalcitrance. Using cellulase enzyme cocktails on maize stem sections, some cell walls are fully degraded while others do not seem to be modified [1]. Techniques able to simultaneously observe enzymes and cell wall degradation for different cell types are required to get a deeper insight into the degradation. Information concerning the specific binding of enzymes to cell walls is searched for, the kinetics of degradation of the different cell types and the potential biochemical modifications of recalcitrant cell walls during the reaction. Time-lapse localization of enzymes and the evolution of the biochemical composition of cell walls is required for this purpose.

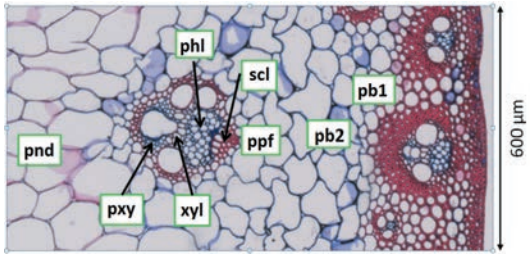

*Figure 1: Maize stem section. FASGA coloration where lignin appear in red. Cell types: **pb1**: parenchyma close to the rind region, **pb2**: parenchyma below the rind, **ppf**: touching bundle parenchyma. **scl**: sclerenchyma, **phl**: phloem, **xyl**: xylem fibers, **pxy**: xylem parenchyma, **pnd**: recalcitrant parenchyma.*

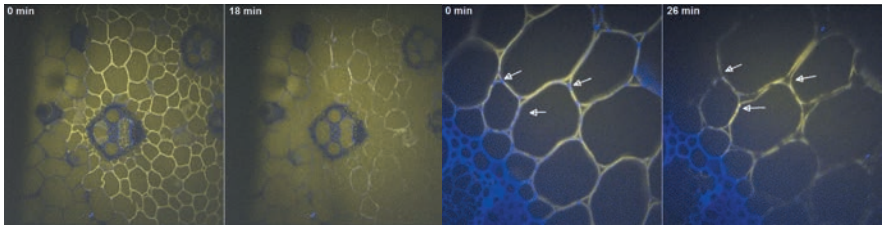

Figure 2: Example of time-lapse images. Left: x10, field of view: 1230 µm, right: x40, field of view 320 µm. Time 0 min was observed about 10 minutes after enzyme deposition. Blue corresponds to cell wall fluorescence alone, yellow to enzyme fluorescence alone and white to both.

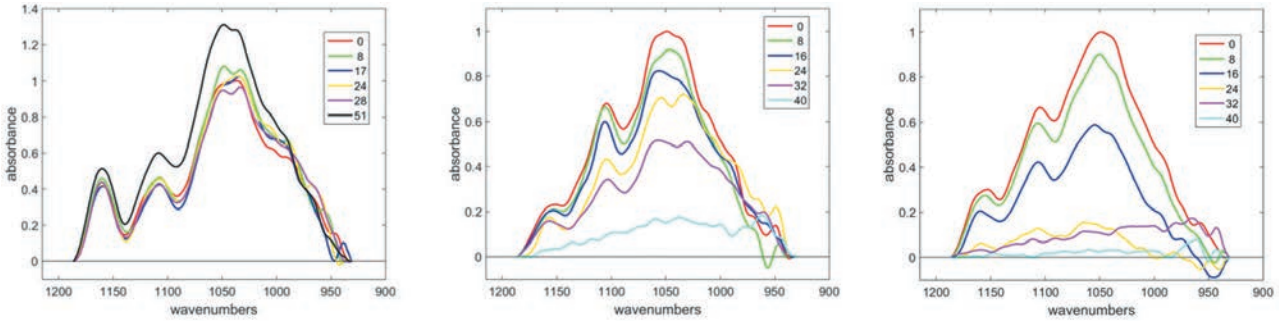

▶ *Figure 3: Example of time-lapse mid infrared spectra in the sugar region 1200-945 cm^{-1}. Left: recalcitrant parenchyma (pnd), middle parenchyma below the rind (pb2), right: parenchyma close to the rind (pb1), numbers from 0 to 51 correspond to time in minutes.*

In the project described here, the enzymatic degradation of maize stems, selected as a model because it is a typical biomass application, was studied.

The enzymatic degradation of different cell types was studied (Fig. 1) using a cellulase preparation from *Trichoderma reesei* (Celluclast 1.5L - Novozyme NS50013). On the DISCO beamline, the autofluorescence of tryptophan at 275 nm allows enzyme imaging without any labelling by collecting light emission between 320 and 350 nm. Using the same excitation, the autofluorescence of phenolic compounds makes cell walls visible beyond 380 nm [2]. Time-lapse multispectral autofluorescence images were therefore acquired to visualize both enzymes and cell walls during degradation. Mid-infrared microspectroscopy was used observe the evolution of polysaccharides in maize stems [3] over time. The synchrotron source provides spatial resolution compatible with the cell and cell wall sizes. We have used the microfluidic device developed by SMIS beamline [4] to record time-lapse infrared spectra during enzymatic reaction. ZnS windows were used to measure the sugar infrared fingerprint between 1200 and 900 cm^{-1}.

For the first time, enzyme autofluorescence was observed on maize sections without any labelling that could modify the affinity of the enzymes towards the sample (Fig. 2). At x10 magnification, contrasts between cell types were evidenced: enzymes were excluded from sclerenchyma and from some parenchyma cells, which were consequently not degraded (pnd). In degraded parenchyma (pb1, pb2, ppf), in phloem and xylem parenchyma, enzymes were concentrated on the cell walls. The degradation speed depended on cell type. It was more rapid in pb1 and ppf than in pb2. At x40 magnification, the enzyme distribution was not homogeneous on parenchyma cell walls (Fig. 2, x40, time 0 min). Dotted blue points reveal a lower enzyme affinity at cell junctions and in some regions of cell walls between two cells. After 10 min, enzymes were also localized in the dotted regions. Time-lapse images showed that degradation resulted first in cell separation before fragmentation (Fig. 2, x40, time 26 min) and then complete degradation of cell walls.

The SMIS beamline microfluidic cell was used to acquire infrared spectra of cell walls in the aqueous reaction medium. The spectra were computed by taking the aqueous medium as background, therefore avoiding deformation due to Mie scattering. Time-lapse spectra were measured during enzymatic reaction for selected cell types. In recalcitrant cell walls (pnd, xyl, scl), the 1510 cm^{-1} band assigned to lignin was observed together with the ester bound at 1250 cm^{-1} and no evolution of the infrared spectra were observed with time (Fig.3 left). In degraded cell walls, degradation was attested by a general decrease of absorbance. The sugar degradation was found more rapid for parenchyma close to the rind compared to the one below (Fig. 3, middle and right). In addition, variations in the original spectra were observed within a given cell type and within single cells. For example in parenchyma below the rind, the proportions of bands at 1040 / 1060-1035 cm^{-1} – assigned to xylan and cellulose – at 1160 cm^{-1} – assigned to phenolic compound - at 985-960 cm^{-1} - assigned to substitutions on the polysaccharide main chains - varied.

▶ CONCLUSION

Time-lapse study using enzyme autofluorescence imaging and microfluidic infrared microspectroscopy at the synchrotron SOLEIL was proven as a highly promising technique for evaluating in situ maize stem cell wall enzymatic degradation. The results obtained using a cellulase cocktail provided new information both on maize stem cell types and on enzyme affinities. The visualization of enzymes without any labelling showed that no enzyme binding was evidenced on recalcitrant cell walls and that on the contrary the enzymes were concentrated on degraded cell walls. An unexpected variability was found in cell wall biochemical composition within a given cell type that could result in the heterogeneous binding of enzymes observed and therefore in variations in polysaccharide degradation. Further studies using pure enzyme instead of cocktails would provide a deeper insight into the mechanism that resulted in degradation and therefore to recalcitrance.

Depict the mode of action of amylolytic enzymes on starch granules

SCIENTISTS INVOLVED

A. Rolland-Sabaté[1], J.-P. Ral[2], F. Jamme[3], M. Réfrégiers[3], A. Buléon[1]

[1] BIA, INRA, 44300 Nantes, France

[2] CSIRO, GPO Box 1600, Canberra ACT 2601, Australia

[3] Synchrotron SOLEIL, 91190 Gif-sur-Yvette, France

CORRESPONDENCE

Agnès Rolland-Sabaté
agnes.sabate@inra.fr

REFERENCES

[1] G. Tawil et al. (2011) Anal. Chem., 83, 989-993.
[2] F. Jamme et al. (2014) Anal. Chem., 86, 5265-5270.
[3] A. Whan et al. (2014) J. Exp. Bot., 65, 5443-5457.

KEYWORDS

Starch, amylolytic mechanisms, amylases, 3D UV imaging.

SCIENTIFIC QUESTION

Starch is a versatile product representing both the major source of carbohydrate in the human diet and over 600 non-food derived applications (Bulking agent, sweeteners, paper or adhesive, etc.). Many biological and industrial processes, such as mammal digestion, plant metabolisms, biofuel production, fermentation or malting rely on the hydrolysis of native starch by amylolytic enzymes. These enzymes, represented mostly by α-amylases, break down the starch macromolecules. This amylolytic process is a heterogeneous phase reaction highly dependent on starch structure. Despite compelling information on kinetic measurements for total digestion of starch suspension, the influence of starch structure on amylolysis by either endogenous or exogenous amylases remains unclear. Following the degradation pathway of single starch granules *in vitro* and therefore visualizing *in situ* the diffusion of amylases would allow a more precise estimation of the amylolytic mechanisms.

The unique high resolution UV imaging setup of the DISCO beamline allowing multi-Z axis acquisition and subsequent 3D image reconstruction provides a great tool to follow single enzyme when acting on non-UV-fluorescent substrate such as starch. Based on tryptophan auto-fluorescence (excitation at 280 nm, emission filter at 350 nm), this unique method is capable of localizing at high resolution (280 nm) amylases on starch without staining or fluorescent probe. This precise amylase GPS allowed us to follow their mode of action and the associated morphological changes of starch granules at different stages of their hydrolysis [1,2].

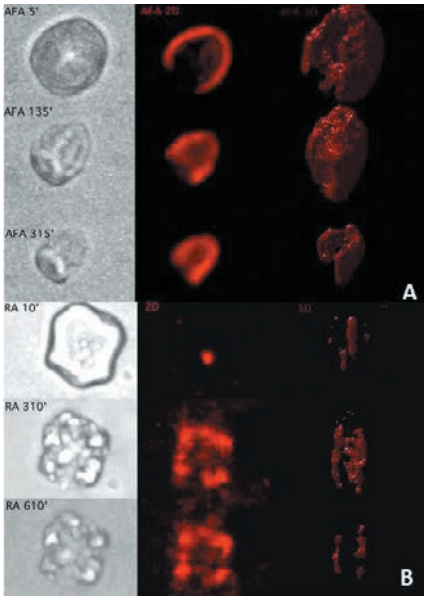

Figure 1: Transmission and corresponding 2D and 3D fluorescence images of the amylase at three different hydrolysis times by AFA (A) and RA (B).

MODE OF ACTION OF AMYLASES

Recently, two new α-amylases from *Anoxybacillus flavothermus* and *Rhizomucor* sp, referred to as AFA and RA, were studied for their ability to hydrolyse concentrated raw maize starch (≤ 31%) and their use in bioethanol production and low temperature glucose syrup production [2]. The UV microscope was used with images

recorded every 500 nm Z steps over 30 μm Z range, at specific steps of hydrolysis. Hydrolysis was directly monitored on series of single starch granules, showing that the process was not synchronous with highly degraded granules present along with intact granules in the same hydrolysis. Fig.1 shows morphological changes and amylase location in single maize starch granules at 3 hydrolysis times by AFA (Fig. 1A) and RA (Fig.1B), respectively. AFA hydrolysis starts from the edges of the granule: the average granule size decreases progressively as hydrolysis progresses, whereas RA hydrolysis starts from the granule core with crack formations (Fig.1B). Hydrolysis progresses to the surface leaving a cavity in the center. This work describes a pioneer 3D mapping of amylase within single starch granules, in real time throughout the hydrolysis and without staining nor sectioning. It shows that the same type of starch granules can be degraded in a very different pathway by amylases from different sources.

▸ EFFECT OF THE ENZYMATIC SOURCES AND BOTANICAL ORIGINS

During the human digestion process, salivary amylases act first on starchy foods followed by pancreatic α-amylases. Each enzyme has a proper mode of action depending on substrate specificity. Using the DISCO imaging system, the action of both purified α-amylases from human saliva (SAL) and porcine pancreas (PPA) was observed on starch granules from different botanical origin. We were able to highlight their different mechanisms. On potato starch, PPA concentrates at the outskirt of the granule hydrolyzing from the outer shell whereas SAL diffuses rapidly inside starch granules using few entry points and fastened hydrolysis (Fig. 2). However PPA hydrolyses more quickly Maize starch granules than SAL suggesting they are more susceptible to hydrolysis than potato ones probably due to a different crystalline structure.

▸ DO ENDOGENOUS AMYLASES HELP THE STARCH AMYLOLYSIS?

For most cereals including wheat, α-amylases are the primary enzymes responsible for starch degradation during grain germination. An innovative grain specific TaAMY3 Over-Expression wheat lines (A3OE) with over 200 fold increase of amylase activity in the mature grain has been developed by the CSIRO Agriculture, Canberra, Australia. Surprisingly, traces of degradation appeared extremely localized and only during grain maturation [3]. By monitoring the fluorescence emission of Trp using synchrotron 3D imaging on starch granules from wheat A3OE lines (showing presence of degradation channels) we were able to confirm the location of the TaAMY3 (Fig. 3A) on the groove surrounding the granule. Moreover, we unraveled the role of endogenous TaAMY3 confirming the enzyme could not fully digest starch granule but instead was capable of drilling extremely localized channels from the surface to the core of the granule. This was the first indication that several α-amylases may act synergistically to fully digest starch granule during germination. To confirm this hypothesis, purified A3OE starch granules were digested by PPA *in vitro*. 3D representation of fluorescence from PPA digested starch granule (Fig.3B) revealed an empty shell-like structure with total absence of background fluorescence in the core indicating complete digestion of the polysaccharide structure. Thus, the localized hydrolysis from TaAMY3 provided entry points for other type of α-amylases and therefore fastened the degradation rate. This experiment opens the way to characterize other isoforms of wheat α-amylase and their mode of action on starch granules.

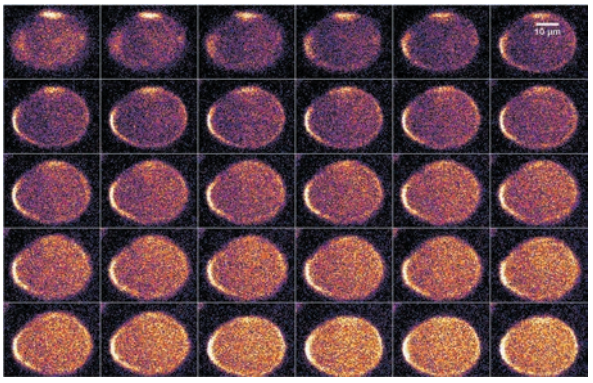

▸ *Figure 2: Wild type Potato starch granules incubated at 40 °C in phosphate buffer with SAL, during 4 h. The pictures have been taken every 8 min.*

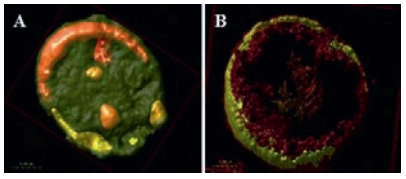

▸ *Figure 3: 3D representation of trp fluorescence on transgenic TaAMY3 overexpressed wheat starch granule. (A) Localization of the TaAMY3 on the external shell, (B) transgenic TaAMY3 overexpressed wheat starch granule after incubation 4 h at 40 °C in phosphate buffer with PPA.*

▸ CONCLUSION

The new setup, specially designed and developed for a 3D representation of the enzyme–substrate interaction during hydrolysis, is particularly effective for improving knowledge and understanding of enzymatic hydrolysis of solid substrates such as starch and lignocellulosic biomass. It could open up the way to new routes in the field of green chemistry and sustainable development, that is, in biotechnology, biorefining or biofuels.

Time resolved study of starch reorganization in starch based biomaterials: effect of immersion in physiological media

SCIENTISTS INVOLVED

L. Chaunier[1], A. Buléon[1], P. Roblin[2,3], M. de Carvalho[1], C. Chevigny[1], D. Lourdin[1]

[1] BIA, INRA Nantes, 44300 Nantes, France

[2] Synchrotron SOLEIL, 91190 Gif-sur-Yvette, France

[3] CEPIA, INRA, 44300 Nantes, France

CORRESPONDENCE

Denis Lourdin
denis.lourdin@inra.fr

REFERENCES

[1] D. Velasquez et al. (2015) Carbohydr. Polym. 124, 180-187.
[2] A. Beilvert et al. (2014) The Laryngoscope, 124, 875–881.

KEYWORDS

Starch, biomaterial, time resolved, physiological media, SAXS, WAXS.

SCIENTIFIC QUESTION

Due to the programmed end of oil sources and environment preservation there is considerable interest in replacing synthetic and nonbiodegradable polymers with biodegradable polymers. In this context numerous bio-sourced polymers are used as eco-friendly alternatives to petrochemicals. Moreover these natural materials such as starch-based materials offer real potentiality for biomedical purposes with an attracted significant interest due to their biocompatibility and biodegradation [1]. For example it could be used for temporary support during the healing of tissue, in the domain of surgery of salivary duct for example (sialendoscopy). Mechanical properties of starch-based materials can be modulated by the addition of a plasticizing agent and shape memory properties can be obtained by controlling their thermo mechanical history. In case of sialendoscopy, the biodegradation is obtained by the action of α-amylase, naturally present in the saliva [2]. The properties of extruded potato starch containing 20% glycerol (PS-G20) during its immersion in a physiological media at 37°C has been studied. After a rapid softening due to water sorption, its modulus stabilizes at about 1-2 MPa during about 30 days, with a limited swelling. In opposite, without plasticizer, starch materials are degraded after a few ten minutes of immersion. The general objective of the project was to improve the knowledge of the different mechanisms involved in the reorganization and/or the crystallization of starch-based materials during their immersion in physiological media and particularly the role of glycerol used as a plasticizer. This knowledge is essential for the design of smart starch based biomaterials as developed in our team. The high signal/noise ratio delivered by the Swing setup allows quantitative measurements even for highly hydrated starch materials. Time-re-

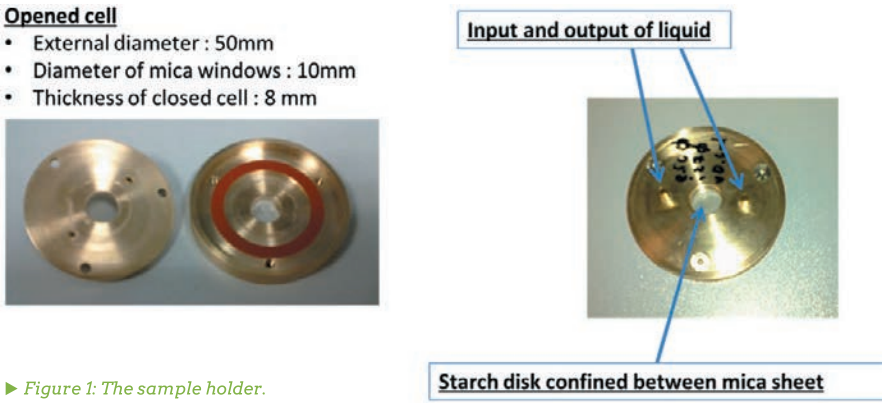

Figure 1: The sample holder.

solved experiments were also performed to assess the kinetics of reorganization from amorphous to crystal induced by diffusion of water within the material. Coupling SAXS and WAXS measurements allowed to describe this organization at different scales.

Starch was extruded as cylinders, with an aspect of solid and transparent thermoplastic polymers. They were cut into 1mm-thick disks with a diameter of about 4 mm. Three different samples were prepared: amorphous potato starch, partially recrystallized potato starch, and potato starch plasticized with 20% of glycerol (also semi-crystalline). In order to study the structure evolution of the sample immersed in the physiological media, a special sample holder, shown in fig. 1, has been especially designed. The disk sample is placed between mica plates in a closed cell allowing circulation of liquid (water or physiological medium, α-amylase at 580 U/L). The sample is pressed against the mica sheet which ensures the tightness and allows a lateral penetration of water only. The changes in the structure induced by water/physiological media intake, were recorded for at least 2h, every 5 minutes during the first hour and then every 15 minutes (Fig. 2). The recording time was a few seconds for each spot, the complete scan all along the diameter of the mica window requiring about 5 minutes. This gives us both the spatial and temporal effect of water intake.

The following conditions were investigated:

	Amorphous starch	Starch+20% glycerol	Semi-crystalline starch
Water	8 hours	4:30 hours	2 hours
α-amylase	2 hours	2 hours	-

▸ MAIN RESULTS AND PERSPECTIVES

The fig. 3 shows characteristic SAXS/WAXS diffractograms recorded from extruded potato starch containing 20% glycerol. At wide angles ($q > 0.3$ Å^{-1}) a progressive increase in B-type crystallinity, the crystalline form characteristic of recrystallized starch in hydrated and cold conditions, is observed. In the middle q range ($0.09 < q < 0.3$ Å^{-1}), no clear change is detected, the slope of the scattering curve remaining constant (around -1.7), which evidences no real change in the interface type with water intake, during the recording time. At smaller angles (around 0.08 Å^{-1}) a soft peak is visible on the dry sample, characteristic of a distance around 90 Å. The corresponding structure is yet unclear. This peak then transforms in simple shouldering upon immersion in water, and progressively shifts towards smaller angles indicating a change in this structure with water uptake and a shift towards higher dimensions. At very small angles, scattering intensity increases with time showing that the size of supramolecular entities observed increases with water absorption in the starch samples.

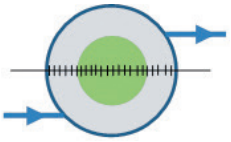

▸ *Figure 2: Starchy sample (green) immersed in circulating aqueous media (blue) and representation of the 21 measurement spots along the 8mm-diameter (total cell diameter is 10mm).*

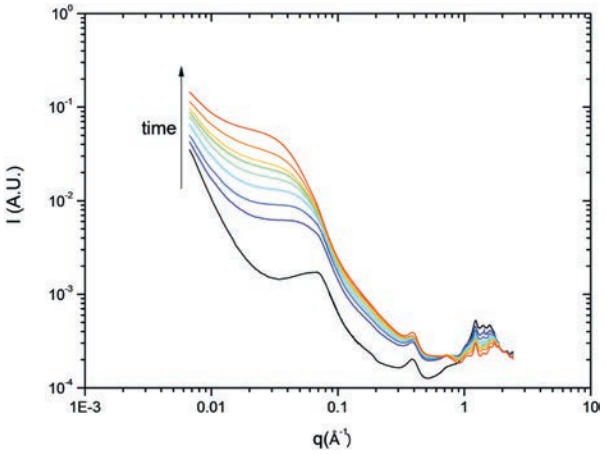

▸ *Figure 3: Scattering curves recorded upon immersion in flowing water (12mL/h). From bottom to top: dry sample (black), starting immersion in water (t=0, dark blue), and the different curves recorded every 6 minutes(blue to orange) up to 42 minutes (red line).*

▸ CONCLUSION

A special device has been set up to observe the structural evolution of starch materials during their ageing in very hydrated conditions including physiological media such as saliva. It has been used for a preliminary study of the degradation of biomaterials designed for the surgery of salivary duct. The processing of a large amount of SAXS and WAXS data is now in progress. The combination of this specific circulating sample holder and the high performances of the SWING beamline could be very efficient for the structural study of biodegradable or biocompatible materials when immersed in specific physiological media or submitted to enzymatic or microbial degradation.

New development on the SMIS beamline for a non invasive analysis of single bacterial cells

SCIENTISTS INVOLVED

J. Meneghel[1,2], F. Fonseca[1], S. Passot[1], S. Lefrançois[2], F. Jamme[2], F. Borondics[2], P. Dumas[2]

[1] GMPA, AgroParisTech, INRA, Université Paris-Saclay, 78850 Thiverval-Grignon, France

[2] Synchrotron SOLEIL, 91190 Gif-sur-Yvette, France

CORRESPONDENCE

Julie Meneghel
julie.meneghel@inra.fr

REFERENCES

J. Meneghel, S. Lefrancois, S. Passot, P. Dumas, F. Fonseca (2016) Journal of Synchrotron Radiation, to be published.

F. Fonseca et al. (2015) 10th SOLEIL Users' Meeting. www.synchrotron-soleil.fr/images/File/soleil/ToutesActualites/Workshops/2015/SUM15/INRA-SOLEIL-2015-Abstract_Book_web.pdf

KEYWORDS

Single bacterial cells, inverted microscope, in situ ATR-FTIR microspectroscopy, heterogeneity.

SCIENTIFIC QUESTION

The interest for non invasive *in situ* analytical techniques stands in the wish to probe matter as closely as possible to reality with minimum perturbation of the specimen, as well as allowing in real time monitoring of the effects of various environmental conditions. Another important requirement is to attain high resolution, thus enabling single cell analysis and heterogeneity assessment of the parameter under investigation. Our project aiming at achieving single bacterial cells analysis in solution by FTIR microspectroscopy fits into these perspectives. In fact, it gives a nonrestrictive chemical picture of the major cellular components (lipids, proteins, etc.). Relating such information to stress tolerance thus helps understanding the underlying cellular damage mechanisms. However, when it comes to water and infrared spectroscopy, OH bonds strongly absorb mid-IR light and exploitation of a great part of the spectrum in hydrated conditions is impossible. Particularly, the examination of the amide I and II region, which reveals protein secondary structures, is infeasible. Consequently, the strategy to overcome this limitation falls into two parts: using a much focused IR beam of a size comparable to a bacterium's (about 1-5 μm^2) while maintaining the photon flux at a high level, and minimizing the quantity of water interacting with the IR beam. For the first point the synchrotron radiation was self-evident. For the second, a new tailor-made equipment was designed by the SMIS beamline staff: an inverted microscope associated with an Attenuated Total Reflectance (ATR) mode FTIR spectrometer and the use of high refractive index (RI) hemispheres, through which the synchrotron light is focused and intense enough to target individual bacteria or small groups of cells (Fig. 1). Besides, in such sampling mode, the IR beam does not get through the specimen as in classical transmission mode, but reflects off of it; this reflection produces an evanescent wave that penetrates shallowly at the sample-hemisphere interface (~1 μm) thus collecting the spectral information only

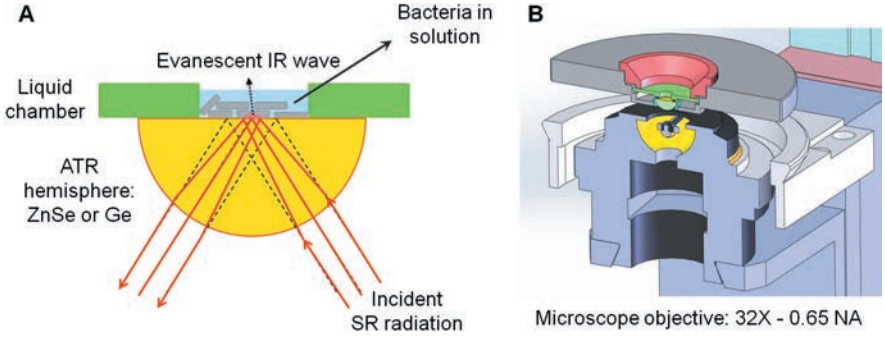

Figure 1: Diagram of the liquid sampling area and ATR principle (A), cross-section view of the inverted microscope (B).

from the first layer of settled down bacteria, and not the surrounding aqueous solution (Fig. 1A). Optical components being adjustable, it is possible to fine-tune the beam size at focus to achieve the desired spatial resolution down to 1 x 1 μm.

▸ MAIN RESULTS AND PERSPECTIVES

If single living eukaryotic cells were successfully investigated under FTIR spectroscopy by using demountable liquid cells or microfluidics that reduce the water layer below 10 μm, nothing has been published yet regarding 10 to 100 fold smaller cells: bacteria. We followed the same approach trying out a microfluidic device and a static liquid chamber in CaF_2 both receiving 2 μm-thick liquid samples. Signal was still extensively absorbed by water; yet, we managed to record FTIR absorbance spectra of good quality arising from 5 to 6 bacteria (Fig. 2) following a time-consuming setting-up of the experimental device, proving that efforts had to be maintained. ATR mode was consequently considered a serious alternative. Preliminary tests performed with the Globar source revealed that the deposition of cells over the ATR crystal is sufficient to obtain absorbance spectra that are not submerged with water features. For this reason the development of the inverted microscope described above was launched. This new device will make possible the visualization of bacterial cells as they settle down and to relate the observed chemical events to a defined group of cells. An additional strength lies in the possibility of moving the hemisphere in X and Y for an accurate selection of the fields-of-view, and of adapting devices such as a temperature controller.

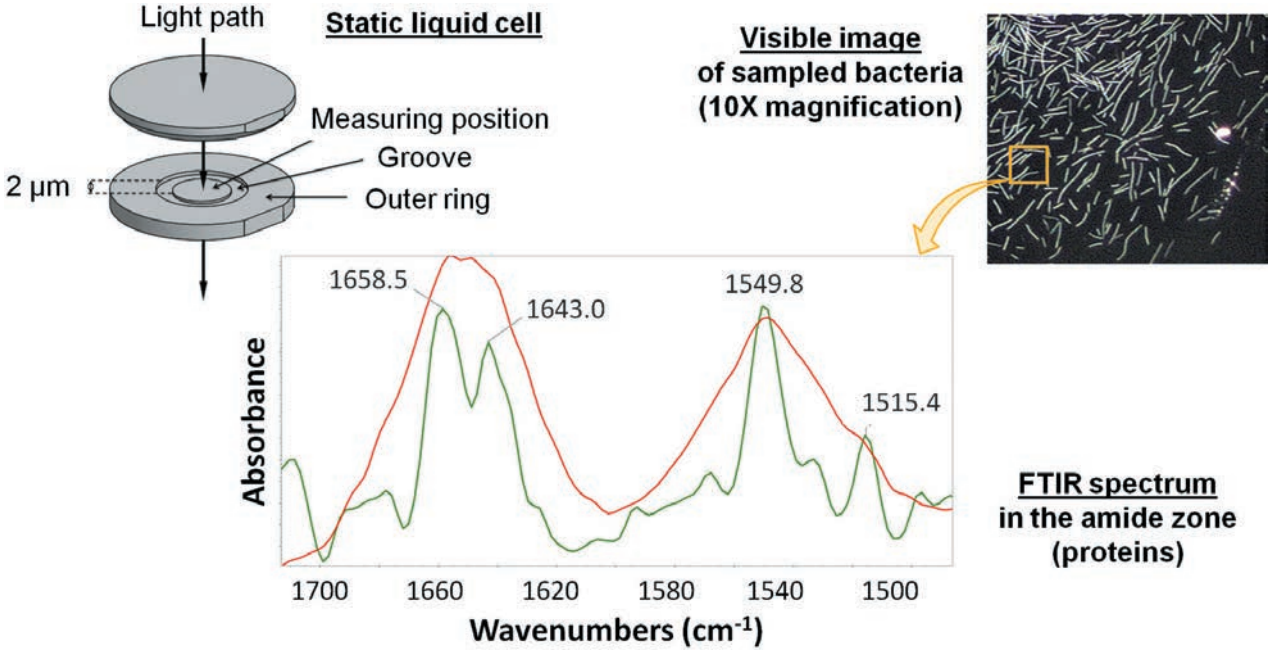

▸ *Figure 2: SR-FTIR microspectroscopy experiment in transmission mode using a static liquid cell. The square (10 x 10 µm²) shows 6 bacteria sampled in solution, the resulting absorbance spectrum (red) and inverted 2nd derivative (green) in the amide I and II region.*

▸ CONCLUSION

Succeeding in recording ATR-FTIR spectra of individual bacteria in a liquid environment with the inverted microscope will represent a major breakthrough in analytical biology, in particular the subsequent mapping of population stress-response heterogeneity. This will allow studying the numerous stress generally encountered by micro-organisms during their production, stabilization or end-using processes. Membrane fluidity of single cells is investigated in parallel by fluorescence anisotropy on the DISCO beamline for a more complete picture of the cellular damage mechanisms. Next step will be to adapt a fluidic device to enable stress response monitoring in real time by modulating environmental conditions.

Biochemical composition of micro-organisms at the single-cell level by synchrotron FTIR microspectroscopy

SCIENTISTS INVOLVED

F. Fonseca[1], M. Froissard[2], M. Mercier-Bonin[3], S. Passot[1], C. Pénicaud[1], C. Saulou[1], F. Jamme[4], P. Dumas[4].

[1] GMPA, AgroParisTech, INRA, Université Paris-Saclay, 78850 Thiverval-Grignon, France

[2] IJPB, AgroParisTech, INRA, CNRS, Université Paris-Saclay, 78000 Versailles, France

[3] Toxalim, INRA, INPT, Université Paul Sabatier, 31027 Toulouse, France

[4] Synchrotron SOLEIL, 91190 Gif-sur-Yvette, France

CORRESPONDENCE

Fernanda Fonseca
fonseca@inra.fr

REFERENCES

[1] C. Saulou et al. (2010) Anal. Bioanal. Chem., 396, 1441–1450.
[2] C. Saulou et al. (2013) Anal. Bioanal. Chem., 405, 2685–2697.
[3] F. Jamme et al. (2013) PLoS ONE, 8, e74421.
[4] C. Pénicaud et al. (2014) PLoS ONE, 9, e111138.
[5] S. Passot et al. (2015) Analyst, 140, 5920-5928.

KEYWORDS

Micro-organisms, biochemical composition, synchrotron-FTIR, single cell, microbial population heterogeneity, cell damage, metabolism.

Micro-organisms (yeast and bacteria) are exposed to different stressful environmental conditions. Sometimes, micro-organisms have to face undesirable stresses during their growth, when they are used in biotechnological processes (fermentation for production of biomass or molecules of interest), for stabilization and final use in food or green chemistry industries or when they are confronted to antimicrobial treatments used for eliminating undesirable micro-organisms. These different kinds of stress, including nutritional deficiency or excess, variations in temperature or in pH, osmotic stress, presence of antimicrobials, induce various physiological cell responses due to modifications in metabolism. However, the biochemical changes and the mechanisms of action involved are still not fully elucidated. Furthermore, the heterogeneity in cell response among the overall microbial population is largely unknown.

A better knowledge of individual cell behavior and the connection between cell biochemistry, biophysics and microbial physiology will make possible to produce homogenous cell populations through reverse engineering. According to the application and for ensuring maximal efficiency of the process under consideration, the homogeneity targeted will concern high lipid content, or high resistance to stabilization processes (freezing) or at the opposite, high sensitivity to antimicrobial treatments.
Fourier transform infrared (FTIR) spectroscopy is a non-invasive technique making possible to monitor biochemical changes in cells and tissues through their mid-IR vibrational modes. This powerful tool gives spectral fingerprints of biological macromolecules such as lipids, proteins, nucleic acids and carbohydrates,

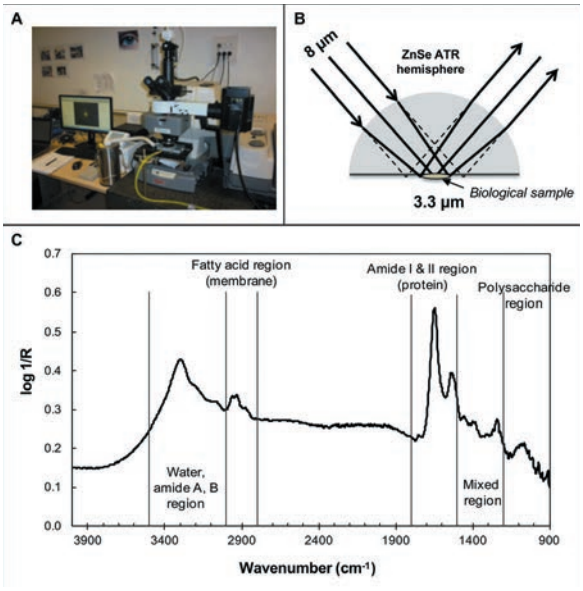

Figure 1: (A) Synchrotron FTIR micro-spectroscopy set up, (B) Schematic representation of the synchrotron light beam crossing the Zinc-Selenide (ZnSe) attenuated total reflectance (ATR) hemispherical element and (C) Representative synchrotron FTIR raw spectra in the 4,000-900 cm^{-1} region of individual microbial cells. Vibrations of characteristic molecular groups are indicated.

and is therefore sensitive to structural and compositional changes in cells. Due to the small size of micro-organisms (in the range of 1-5 µm), only the brilliance of the synchrotron-FTIR (SR-FTIR) beam allows the characterization of their biochemical composition at microbial-cell scale.

Pioneer work [1,2] assessed the changes in cell composition of the yeast *Saccharomyces cerevisiae* and the bacterium *Escherichia coli* after exposure to nano-silver coating or free ionic silver, respectively. By combining the use of SR-FTIR micro-spectroscopy (Fig. 1A) and high refractive zinc-selenide (ZnSe) hemispheres for a better spatial resolution (Fig. 1B), the authors achieved the unique challenge of analyzing biochemical composition at the single-cell level (3-5 µm) for microbial suspensions deposited and dried on the ZnSe hemisphere (Fig. 1C). In *S. cerevisiae*, a transition between active and inactive protein conformations was observed from the amide I peak downshift. Likewise, for *E. coli*, differences in cell composition were detected for proteins, but also for fatty acids as shown through the C–H stretching region. Furthermore, this approach enabled for the first time the assessment of heterogeneity in biochemical composition within cells among a given microbial population.

This innovative approach benefited to Froissard and collaborators, interested in studying the dynamics of lipid storage and cellular carbon fluxes in yeast to better understand metabolism heterogeneity and adaptation to stress induced by lipid over accumulation. Moreover, close collaboration with SMIS beamline scientists allowed the development of data pretreatment for reducing the resonance Mie Scattering, very disturbing for subsequent multivariate statistical analysis such as Principal Component Analysis (PCA) or Partial Least-Square Regression [3].

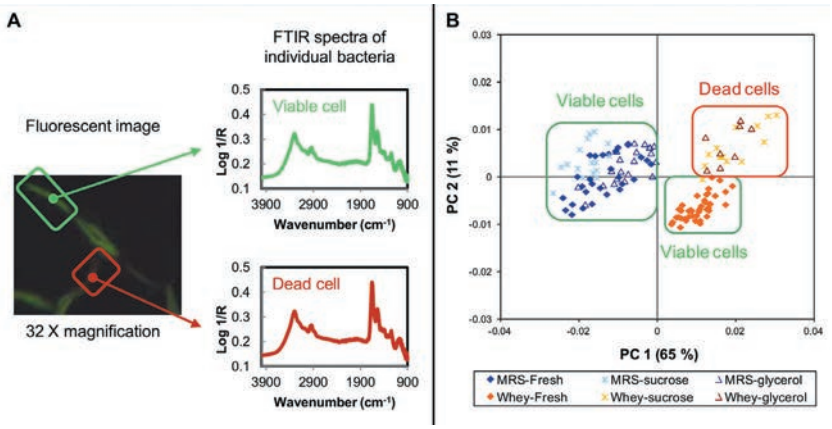

▶ *Figure 2: (A) Simultaneous assessment of physiological state and biochemical composition of single bacterial cell of L. bulgaricus. (B) Principal component analysis (PCA) of FTIR spectra obtained in the lipid region (3,000–2,800 cm^{-1}) after fermentation and after freeze-thawing of L. bulgaricus cells grown either in MRS broth (MRS, blue symbol) or in mild whey medium (whey, orange symbol) and protected by the addition of sucrose or glycerol.*

In order to deeper investigate the mechanisms underlying the cell responses to stress, complementary physiological approaches were developed at cellular level using specific fluorescent probes and analysis by flow cytometry [4]. Recently, an original work [5] reported the first bimodal analysis of bacteria at the single-cell level performed by combining SR-FTIR micro-spectroscopy and fluorescence microscopy at SMIS beamline (Fig. 2A). The simultaneous acquisition of information on the biochemical composition and the physiological state (enzymatic activity and membrane integrity) of *Lactobacillus delbrueckii* ssp. *bulgaricus* cells (*L. bulgaricus*), a bacterium widely used as a starter for manufacturing fermented and healthcare products, following fermentation and freezing allows to assess relevant spectral biomarkers of the cryotolerance of this bacterium. PCA analysis of SR-FTIR spectra indicated that before freezing, freeze-resistant *L. bulgaricus* cells grown in a rich medium (MRS) presented a high content of CH_3 groups from lipid chains, of cell proteins in an α-helix secondary structure and of charged polymers such as teichoic and lipoteichoic acids that constitute the Gram-positive bacterial wall. Physiological damages observed upon freezing with sucrose or glycerol as cryoprotectants, and leading to cell death, were ascribed to biochemical modification of cell membrane phospholipids, in particular to a rigidification of the cytoplasmic membrane following freezing (Fig. 2 B). Moreover, SR-FTIR micro-spectroscopy revealed cell heterogeneity within the cluster of freeze-resistant cells, which was ascribed to the diversity of potential substrates integrated from the growth medium.

▶ CONCLUSION

The multidisciplinary approach undoubtedly achieved major breakthroughs in the understanding of environmental stress impact on microbial populations. In particular, through investigations at the single cell level, the heterogeneity in cell response was highlighted, thus offering new avenues for more subtle physiological characterization, bioprocess optimization and design/combination of challenging tools at the interface between Biology and Physics.

Lipid cell structure imaging and membrane fluidity measurement in single living microorganisms

SCIENTISTS INVOLVED

M. Froissard[1], F. Fonseca[2], Y. Gohon[1], J. Meneghel[2], S. Passot[2], C. Pénicaud[2], F. Jamme[3], M. Réfrégiers[3]

[1] IJPB, AgroParisTech, INRA, CNRS, Université Paris-Saclay, 78000 Versailles, France

[2] GMPA, AgroParisTech, INRA, Université Paris-Saclay, 78850 Thiverval-Grignon, France

[3] Synchrotron SOLEIL, 91190 Gif-sur-Yvette, France

CORRESPONDENCE

Marine Froissard
marine.froissard@inra.fr

REFERENCES

[1] S. Passot et al. (2014) Biomed Spectrosc Imaging, 3, 203-210.
[2] I. Bouchez et al. (2015) Biology Open, 4, 764-75.

KEYWORDS

Membrane fluidity dynamics, anisotropy measurements, microorganisms, cell lipid structures.

The first interaction of cells with their environment is through plasma membrane. It is of great interest for numerous scientific teams to understand how this lipid structure is able to adapt to constraints, such as cold. One of the issues is to know the influence of plasma membrane fluidity and composition on the microorganism resistance to extreme environmental conditions such as freezing procedures or arctic climate.

A PIONEER WORK USING TMA-DPH ON LACTIC ACID BACTERIA

The plasma membrane probes trimethylammonium-diphenylhexatriene (TMA-DPH) and DPH are commonly used to measure fluorescence anisotropy which makes possible the assessment of cell membrane fluidity, but few experimental devices are available to measure membrane fluidity at subcellular level. An original experimental device using fluorescence imaging to obtain membrane fluidity mapping of bacteria following cooling was developed in collaboration with the DISCO beamline.

Cryopreservation of bacteria requires specific cells pre-adaptation as well as a controlled freezing protocol to minimize membrane damage resulting from osmotic cell dehydration. Membrane fluidity has an important role in biophysical events taking place at subzero temperatures by facilitating or not the exchanges between intracellular and extracellular media. The degrees of liberty of TMA-DPH inside the bilayer provide a direct marker of membrane fluidity under DUV excitation. Microscope was modified to carry out fluorescence anisotropy measurement by inserting polarizers into the excitation and emission paths. Fluorescence polarization images of lactic acid bacteria were acquired at controlled temperatures from

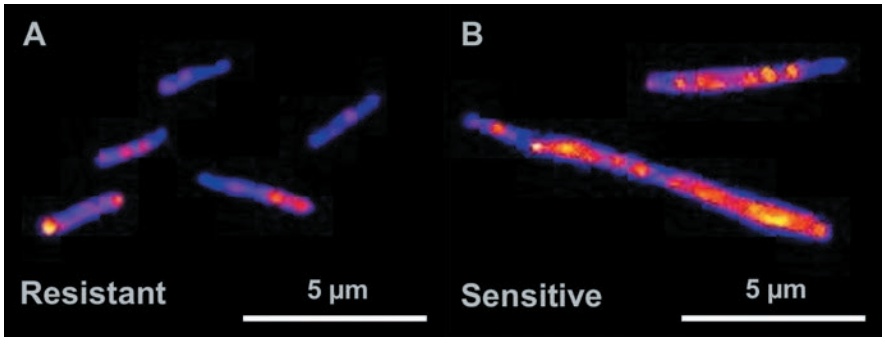

Figure 1: Steady state fluorescence anisotropy images of individual bacteria observed at 4°C using Synchrotron DUV microscopy: freeze-resistant cells grown in MRS broth (A) and freeze-sensitive cells grown in mild whey medium (B). Yellow regions correspond to the highest value of anisotropy and blue regions to the lowest value of anisotropy (adapted from Passot et al. [1]).

0°C to 40°C and anisotropy mapping of cell membrane at the subcellular level was obtained (fig. 1). The higher the anisotropy, the more rigid the membrane is.

Results indicate that the membrane of freeze-sensitive cells rigidifies more extensively at low temperatures than freeze-resistant cells, and that intercellular and intracellular heterogeneities with subdomains concomitantly appear more frequently for freeze-sensitive cells (Fig. 1). The observation of the same feature at high osmolarity during a separate study of the effects of cold and osmotic stresses confirmed the negative impact of osmotic stress during freezing. The results give a glimpse of key levers for commercial production of interesting strains of lactic acid bacteria remained until now underexplored.

▸ NEW QUESTIONS AND TECHNICAL IMPROVEMENT: FROM PROKARYOTE TO EUKARYOTE

Interestingly, lipids and membrane dynamics is a common subject to many DISCO users and it became evident that users can join their expertise for efficient improvement of beamline devices and protocols. INRA scientists decided to combine their efforts through common proposals for measurement of cell plasma membrane fluidity in eukaryotic cells such as yeasts. This approach led to the great upgrade of the end-station (motorization of polarizers, homogenization of light) and establishment of protocols for reliable analysis of membrane fluidity in living eukaryotic cells with intracellular membrane compartments. Contrasted staining with TMA-DPH and DPH in living cells was observed. TMA-DPH stains mainly plasma membranes whereas DPH is rapidly internalized and stains the lipid droplets (Fig. 2). The use of DUV microscopy shows that TMA-DPH is better than DPH for plasma membrane fluidity measurement in eukaryotic living cells. Reinforced by these results we are now exploring the link between cell fatty acid composition (omega 3 content) and membrane fluidity in yeasts of interest for the food and non-food biotechnologies.

▸ ON THE WAY TO MULTIMODAL IMAGING

The INRA consortium is currently working on lipid imaging at SOLEIL to develop more efficient techniques, in particular for imaging native intracellular compartments in living cells. The results on TMA-DPH and DPH fluorescence microscopy will be combined with information obtained using label-free methods based on intrinsic fluorescence or absorbance of molecules upon excitation by DUV. Combining DUV fluorescence and absorption, two emerging techniques, will enable the acquisition of information on both organelle organization and chemical composition. Moreover, by using microfluidics devices, it will be possible to investigate in situ and in real time membrane and intracellular dynamics when cells are exposed to different kinds of environmental stress (osmotic, acid, oxidant, etc).

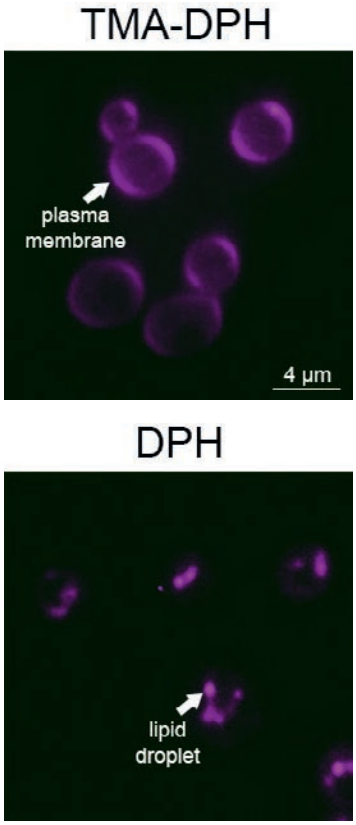

▸ *Figure 2: Saccharomyces cerevisiae cells stained with TMA-DPH (top) or DPH (low). TMA-DPH is mainly associated with plasma membrane and DPH with round intracellular structures corresponding to lipid droplets.*

▸ CONCLUSION

Biophysics of cell lipid structures is a historical research topic. Thanks to the high performance of synchrotron radiation combined with DISCO end-station, INRA and SOLEIL scientists are together developing innovative approaches based on DUV imaging. They gave access to dynamics and heterogeneity of membrane fluidity at the subcellular level. The current challenge is to improve experimental conditions and devices to achieve multimodal, label-free, microfluidics DUV imaging at SOLEIL.

Deciphering the structure of complex assemblies

Many of the products of agriculture (wood, straw, seeds) have very low water content, in comparison with matter from living organisms. They contain numerous molecules that exhibit very high potential for other uses (sugar, lipids, lignins...) that exist in organized forms and very concentrated states (fibers, subcellular protein or lipid bodies...). This makes their study very difficult using classical approaches. Protein nucleic acids assemblies are observed during the whole cell life. Study of these complexes, especially during DNA repair is essential for biology. Double strand breaks are the most genotoxic DNA lesions. McGovern *et al.* dissected the C-terminus region of the bacterial Ku protein, and highlighted its role in the different steps of double strand break repair.

Arabic gum is a polysaccharide widely used as food ingredient. SAXS and synchrotron radiation circular dichroism (SRCD) proved to be the most suitable tools to obtain a model of the folding and 3D structure of gum arabic (Sanchez *et al.*).

Smart activation of ions using UV at DISCO beamline allowed the determination of the very complex structures of natural polysaccharides by tandem mass spectroscopy, such as those determined by Ropartz *et al.*

A similar approach was developed by Canon *et al.* to study proteins in complexes with various ligands (DISCO & DESIRS). SOLEIL light allows structural studies in solid or turbid media.

Astruc *et al.* used the auto-fluorescence spectral signals to characterize the histological cross section of muscle fibers without staining chemicals (DISCO).

SRCD spectra, recorded on organelles, enabled the collection of original sets of data for membrane proteins fold in their natural environment (Gohon *et al.*, DISCO).

Using small angle X-ray scattering (SAXS) at SWING beamline, Roblin *et al.* observed for the first time the structure in solution of two amylosucrases under conditions of polymer synthesis and, simultaneously, of the amylose conformation at the first stages of polymer chain entanglement.

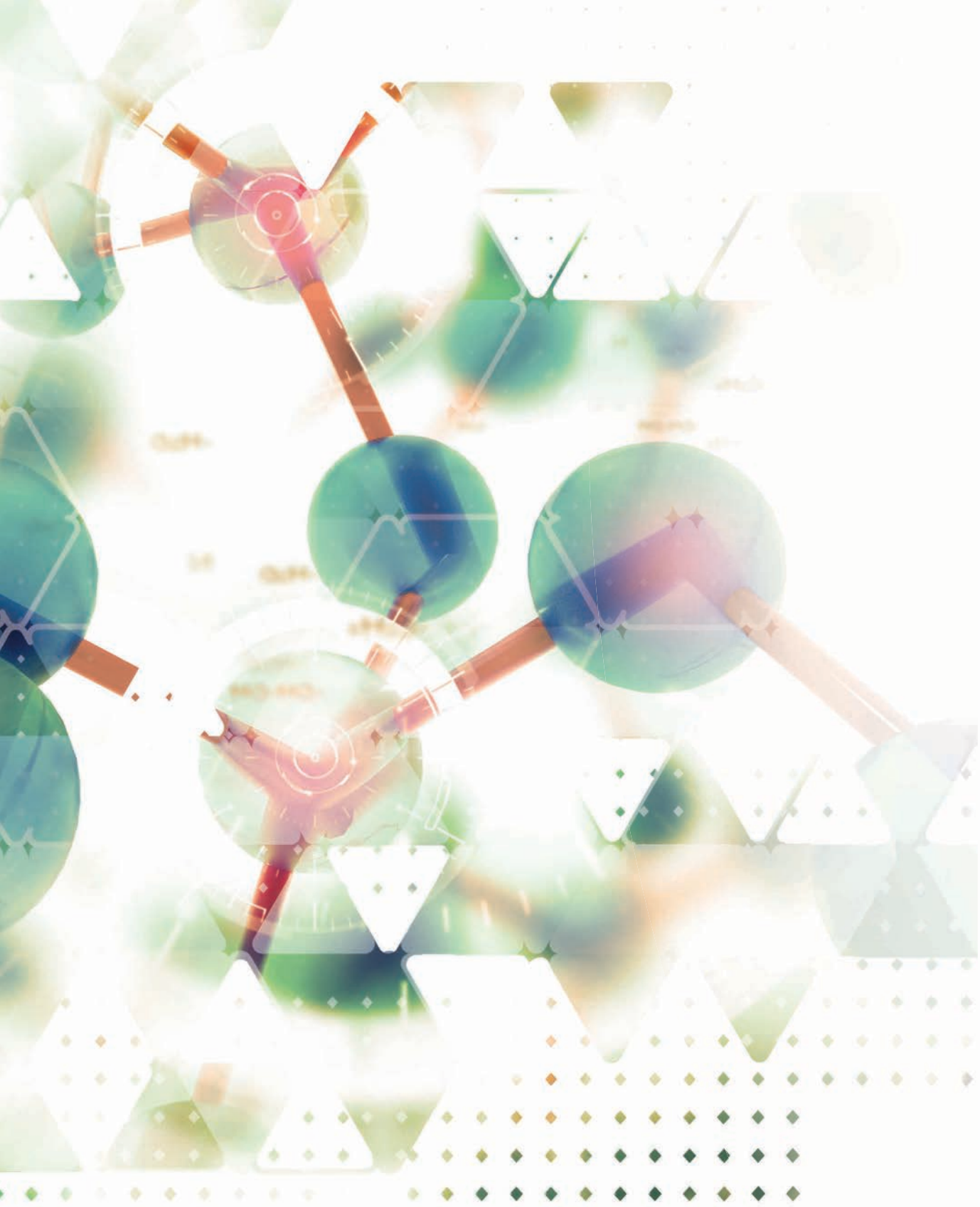

A low resolution study of the *Bacillus subtilis* Ku protein: deciphering the DNA double strand break repair by the bacterial NHEJ pathway

▶ SCIENTISTS INVOLVED

S. McGovern[1], S. Baconnais[2], P. Roblin[3-4], P. Nicolas[5], P. Drevet[6], H. Simonson[1], O. Piétrement[2], J.B. Charbonnier[6], E. Le Cam[2], P. Noirot[1], F. Lecointe[1]

[1] Micalis Institute, INRA, AgroParisTech, Université Paris-Saclay, 78350 Jouy-en-Josas, France

[2] UMR 8126, CNRS, Gustave Roussy Université Paris Sud, Université Paris-Saclay, F-94805 Villejuif, France

[3] SOLEIL Synchrotron, 91190 Gif-sur-Yvette, France

[4] CEPIA, INRA, 4400 Nantes, France

[5] MaIAGE, INRA, Université Paris-Saclay, 78350 Jouy-en-Josas, France

[6] I2BC, iBiTec-S, CEA Saclay, 91191 Gif-sur-Yvette, France

▶ CORRESPONDENCE

François Lecointe
francois.lecointe@inra.fr

▶ REFERENCES

[1] T. Aparicio et al. (2014) DNA Repair (Amst), 19, 169-175.
[2] G.R. Weller et al. (2002) Science, 297, 1686-1689.
[3] S. McGovern et al. (2016) Nucleic Acids Res, 44, 4785-4806.
[4] J.R. Walker et al. (2001) Nature, 412, 607-614.

▶ KEYWORDS

DNA repair, Non Homologous end joining, DNA double strand break, SAXS, Ku, LigD.

The genome of each cell is constantly exposed to a variety of damaging factors. The DNA double strand breaks (DSB) is the most genotoxic DNA lesion and is a well-known causative event in several human diseases [1]. To survive such deleterious damages, cells have evolved two main DSB repair pathways: Homologous Recombination (HR) and Non-Homologous End Joining (NHEJ). Importantly, the NHEJ is essential for some bacteria to survive under genotoxic conditions. Moreover, NHEJ is active in some important human pathogens, such as the causative agent of tuberculosis. Therefore it could be a target of choice for the development of new antibiotics, providing that the molecular mechanism of the NHEJ is understood.

NHEJ is a ligation process requiring two proteins in bacteria: Ku and LigD [2]. A simple mechanistic model has been proposed so far: Ku homodimers bind DNA ends and recruit the ligase LigD to seal the lesion (fig. 1A). To test this model, we characterized the *Bacillus subtilis* Ku protein. We demonstrated that Ku binds to DNA ends and stimulates LigD, as expected, but is also able to thread inward linear DNA molecules after binding. We searched for Ku mutants to evaluate the role of this threading ability on the NHEJ efficiency. Bacterial Ku are composed of three domains (fig. 2A). The Ku core domain (fig. 1B) is conserved and required for DSB binding. The minimal Cter domain is also conserved in bacterial Ku and an extended C-terminal part added to this minimal Cter domain is frequently found in the gene sequences. Roles of the minimal and extended Cter domains remained unknown. We therefore characterized mutant Ku proteins truncated for the extended Cter (KuΔexCter) and for the complete C-terminal region (Ku core, fig. 2A). To ascertain that the different biochemical properties of these mutants compared to the full length protein were due to the different truncations and not to global structural rearrangements of the proteins, we characterized their low resolution structures by Small Angle X-ray Scattering (SAXS).

▶ MAIN RESULTS

Three Ku proteins have been analysed by SAXS: the full length protein Ku and the two C-terminal truncated mutants. They were analyzed by size exclusion chromatography (fig. 2B) with an HPLC coupled to the SWING line to remove aggregates or other contaminants and to obtain a perfect subtraction of the solvent. SAXS data have been obtained for all Ku proteins (fig. 2C). These results, combined with the structural data available for the human Ku homolog, allowed us to propose a structural model for Ku and its derivatives in solution (fig. 1B and 2D). The conclusions of this study [3] were:

- all these proteins are dimers,
- the Ku protein displays a non globular shape with extended arms,
- the C-terminal domain of the homodimeric Ku maps in these extended arms, since these arms decreased or are absent in the truncated Ku mutants, and seems clearly available for interaction with DNA and/or protein in solution,
- the Ku structural model, based on the human Ku 3D structure, fits well with the globular shape of the bacterial Ku core suggesting a conserved core structure. This Ku core structure is not altered in the truncated mutants.

Since the two truncated mutants conserved a shape similar to the wild type Ku protein except the extended arms, we characterized further these mutants and demonstrated that the minimal Cter domain of Ku is required for its interaction with LigD and that the extended Cter domain i) is required for an efficient stimulation of the ligase activity, ii) decreases the ability of Ku to thread inward a DNA molecule and iii) allows the bridging of DNA molecules together [3].

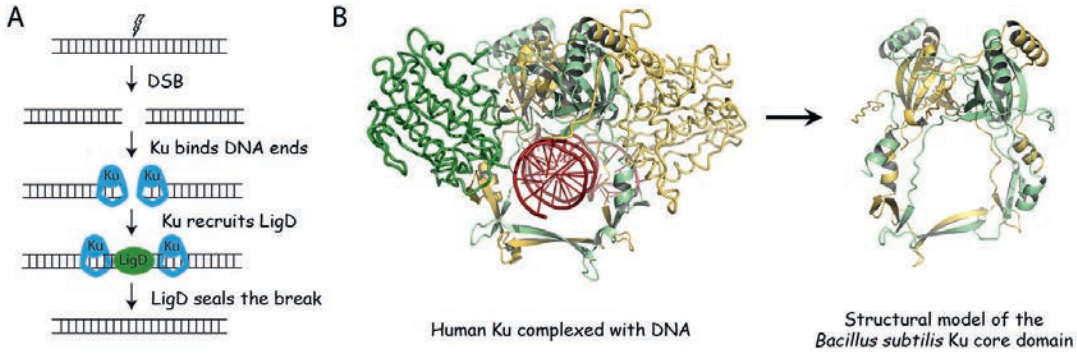

▶ *Figure 1: A. The bacterial NHEJ model. Ku is in blue and LigD in green. DSB stands for DNA double strand break. B. The structural model of the* B. subtilis *Ku core domain. This model was built from the available 3D structure of the human Ku [4] and our experimental SAXS data obtained on the SWING beamline.*

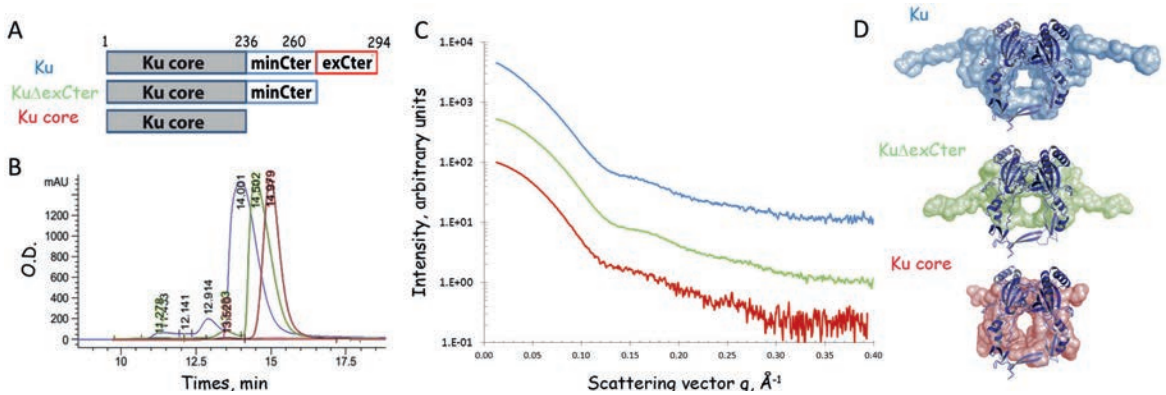

▶ *Figure 2: Low resolution structures of the* B. subtilis *Ku and C-terminal truncated mutants derived from SAXS. A. Proteins used in this study and their domain composition are indicated. minCter and exCter stand for minimal and extended C-terminal domains, respectively. B. Elution patterns of Ku (blue), KuΔexCter (green) and Ku core (red) were obtained after loading on a size exclusion HPLC column coupled to the SWING beamline. C. Experimental scattering curves for Ku and its C-terminal mutants (colors as in B). D. Low resolution shapes of Ku, KuΔexCter and Ku core proteins. Shapes were generated by GASBOR (transparency sphere). The all atom model was calculated with Dadimodo (shown in cartoon) and are superimposed on the GASBOR calculated shapes.*

▶ CONCLUSION

Based on our observations, we propose that Ku binds DSBs via its Ku core domain and recruits LigD to its site of action via its minimal Cter domain. This recruitment would be aided by the high local concentration of Ku at the ends due to its ability to thread and accumulate preferentially at this site thanks to its extended Cter domain. Moreover the ability of this extended C-terminal part to promote bridging of DNA molecules should contribute to increase the efficiency of the ligase activity. Interestingly, the threading of Ku on DNA could also reveal new roles of Ku in the bacterial DNA repair. In conclusion a large set-up of biochemical and biophysical approaches was crucial for the progress of our understanding of the NHEJ molecular mechanism in bacteria. We currently used structural approaches, including the SAXS methodology, focused on the 3D structure and dynamic assembly of a whole NHEJ machinery.

Full of SOLEIL on a plant exudate structure: acacia gum

▶ SCIENTISTS INVOLVED

C. Sanchez[1], M. Nigen[1], A. Lapp[2], P. Roblin[3-4], A. Giuliani[3-4], C. Garnier[5], L. Lavenant-Gourgeon[6], D. Renard[6]

[1] IATE, INRA, Montpellier SupAgro, CIRAD, Université de Montpellier, 34060 Montpellier, France

[2] Laboratoire Léon Brillouin CEA Saclay, 91190 Gif-sur-Yvette, France

[3] Synchrotron SOLEIL, 91190 Gif-sur-Yvette, France

[4] CEPIA, INRA, 44000 Nantes, France

[5] IGDR, CNRS, Université de Rennes 1, 35000 Rennes, France

[6] BIA, INRA, 44300 Nantes, France

▶ CORRESPONDENCE

Denis Renard
denis.renard@inra.fr

▶ REFERENCES

[1] D. Renard et al. (2006) Biomacromolecules, 7, 2637-2649.
[2] C. Sanchez et al. (2008) Biophysical J., 94, 629-639.
[3] D. Renard et al. (2012) Carb. Polym., 90, 322-332.
[4] D. Renard et al. (2013) Carb. Polym., 97, 864-867.
[5] D. Renard et al. (2014) Carb. Polym., 99, 736-747.

▶ KEYWORDS

Acacia gum, arabinogalactan-proteins, glycoproteins, self-ordering, SRCD, SAXS, Small Angle Neutron Scattering, transmission electron microscopy, HPSEC-MALLS.

▶ *Figure 1: Acacia exudate.*

▶ SCIENTIFIC QUESTION

Exudate gums are among the oldest natural gums being used as thickening and stabilizing agents. They are produced by many trees and shrubs as a natural defense mechanism, particularly in semiarid regions of Africa. Acacia gum (or gum Arabic; see fig. 1) is defined by the FAO/WHO Joint Expert Committee for Food Additives (JECFA) as: "a dried exudate obtained from the stems and branches of *Acacia senegal* (L.) Willdenow or *Acacia seyal* (Fam. Leguminosae)". Acacia gum is today widely used for its nutritional, flavoring, and surface properties by the food industry (European specification: E414). The Acacia gum can be defined as a hyper-branched polysaccharide with an amphiphilic and polyelectrolyte behavior due to the presence of a polypeptide backbone covalently linked to the sugar moieties and charged sugar residues. The model of the tertiary structure of Acacia gum often described in literature is described in terms of a wattle-blossom macromolecular assembly by virtue of which few discrete carbohydrate blocks are linked by *O*-serine and *O*-hydroxyproline residues to the polypeptide chain. In reality, *Acacia senegal* gum can't be ascribed to a unique macromolecule. It is in fact a continuum of molecular species differing by their protein to sugar ratio, molecular weight, and charges [1]. Depending on the mode of fractionation of the gum, several molecular species can be identified. Fractionation using hydrophobic interaction chromatography revealed three main molecular fractions classified according to their biochemical composition as an arabinogalactan-peptide (AG-peptide), an arabinogalactan-protein (AGP) and a glycoprotein (GP) molecular fraction. This finding opened the route to the thorough structural investigation of each molecular fraction with the objective to relate the structure-functionality relationship of these macromolecular assemblies. In particular, these macromolecules being too large to be crystallized, small angle scattering (SAXS or SANS) techniques and synchrotron radiation circular dichroism were the most suitable tools to determine low resolution three-dimensional structures and secondary structures of the polypeptide backbone.

▶ MAIN RESULTS

A breakthrough in the field of arabinogalactan-protein-type macromolecules.

It was first clearly identified that the major molecular fraction, AG-peptide, appeared to be a dispersion of two-dimensional structures with a radius of gyration of ~6.5 nm and an inner dense branched structure. AG-peptide appeared in solution with a disk-like morphology with a diameter of ~20 nm and a thickness below 2 nm [2]. In addition, ab initio modelling produced a porous oblate ellipsoid particle

with a central intricated "network". Both transmission electron microscopy and atomic force microscopy confirm the thin disk model and structural dimensions (Fig. 2).

A new vision to understand the structure of arabinogalactan-protein macromolecular assembly.

The two other molecular fractions, AGP and GP, were identified as porous ellipsoids able to evolve in supramolecular architectures and as an assembly of ring-like glycoproteins modules, respectively [3, 4]. A remarkable feature of all particle morphologies was the presence of an outer structure combined to an inner more or less porous network of interspersed chains or interacting structural blocks, as previously found for the AG-peptide molecular fraction. In addition, secondary structures with the presence of polyproline II (PPII) and turns were characteristic of hydroxyproline-rich glycoproteins with arabinosylated and arabinogalactan polysaccharide side chains grafted to the polypeptide backbone.

More recently, by combining enzymatic hydrolyses on AGP molecular fraction, structural studies and theoretical calculations, the AGP macromolecular assembly was seen as a self-similar structure (Fig. 3). AGP would be made of a self-similar assembly of two types of building blocks, the second being a five-fold repetition of the first one, for which palindromic amino acid sequence would ensure a self-ordering of carbohydrate moieties along the polypeptide chains [5]. The cleavage therefore led to hydrolysed building blocks with similar secondary structures and conformations whatever the enzyme used.

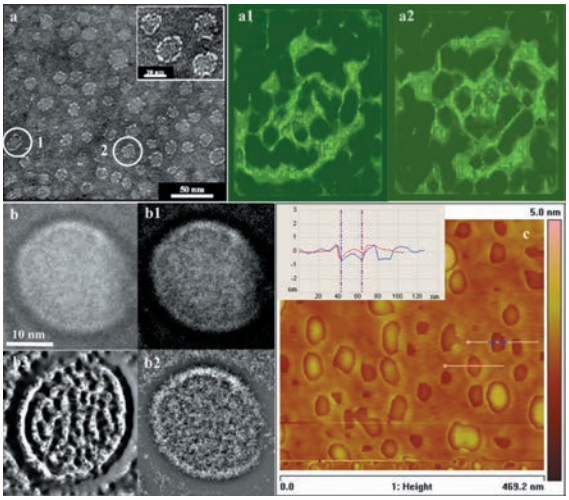

▶ *Figure 2: Thin oblate ellipsoid structure of the arabinogalactan-peptide (AG-peptide) fraction from Acacia Senegal gum.*

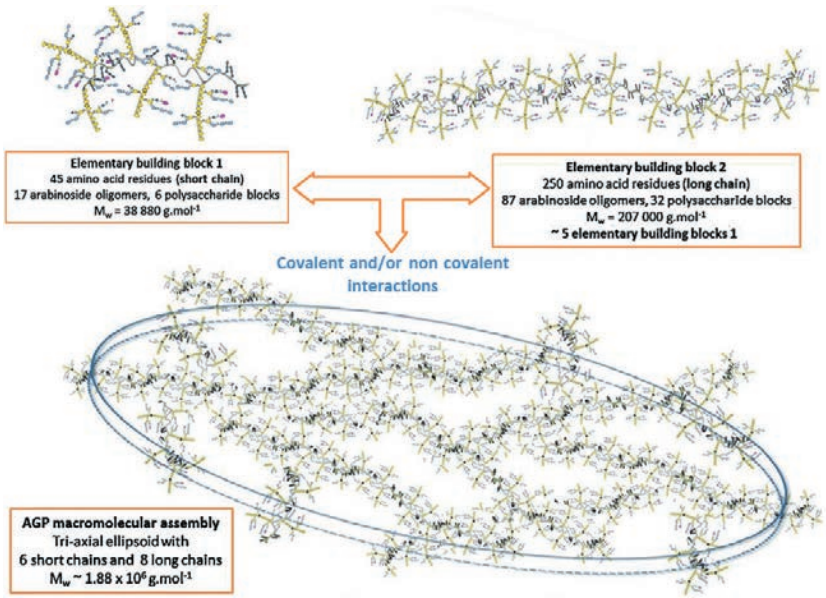

▶ *Figure 3: Self-ordering of elementary building blocks 1 and 2 leading to the arabinogalactan-protein (AGP) macromolecular assembly from Acacia Senegal gum.*

▶ CONCLUSION

The use of various biophysical methods (SRCD and SAXS available at SOLEIL Synchrotron, SANS available at Orphée neutron source) allowed the thorough structural characterization of an important hydrocolloid, Acacia gum and its molecular fractions. Even if a structural consensus is not found today on these hyper-branched amphiphilic charged polysaccharides, a three-dimensional model of this important polysaccharide was recently proposed based on a self-similar assembly of two types of building blocks.

Synchrotron radiation as a way to reveal the structural complexity of carbohydrates using mass spectrometry

SCIENTISTS INVOLVED

D. Ropartz[1], A. Giuliani[2,3], H. Rogniaux[1]

[1] BIA, INRA, 44300 Nantes, France

[2] Synchrotron SOLEIL, 91190 Gif-sur-Yvette, France

[3] CEPIA, INRA, 44000 Nantes, France

CORRESPONDENCE

David Ropartz
david.Ropartz@inra.fr

REFERENCES

[1] D. Ropartz et al. (2014) Anal. Chim. Acta, 807, 84-95.
[2] D. Ropartz et al. (2015) Anal. Chem., 87, 1042-1049.
[3] D. Ropartz et al. (2016) Anal. Chim. Acta, 933, 1-9.

KEYWORDS

Oligosaccharides, Structure, isomers, Vacuum ultra-violet, photon activation, Tandem mass spectrometry.

SCIENTIFIC QUESTIONS

Carbohydrates are involved in many biological functions and represent a vast reservoir of molecules of high functional interest for several industries such as materials, food, pharmacy/medicine and as an alternative to fossil fuels. These functions being tightly connected to their structure, the structural characterization of carbohydrates is of key importance to better understand the properties of these molecules as well as to tailor compounds with enhanced functionalities. However, the complexity and heterogeneity of natural carbohydrates has long challenged the field of analytical chemistry and many of these structures remain unsolved. Tandem mass spectrometry (MS) provides key advantages to address this question. However, in many cases, classical fragmentation by collision-activated dissociation (CAD) fails to reach a comprehensive structural determination, especially when isomers or labile modifications have to be characterized.

Ion activation by photons emerged recently as an alternative activation method in tandem MS. In this study, photons in the vacuum-UV range were used to investigate highly complex mixtures produced by the degradation of natural polysaccharides. The instrument setup consisted of a linear ion trap coupled with a synchrotron beamline in the VUV range (fig. 1). In this energy range, samples have high absorption cross sections, thereby leading to an efficient fragmentation with ions. In addition, the tunability of the synchrotron radiation enabled us to probe photon activation over a wide range (5-24 eV). The originality lies in much higher photon energy than previously reported for the activation and structural characterization of complex carbohydrates.

To our best knowledge, this experimental setup is unique in the world.

MAIN RESULTS AND PERSPECTIVES

Photons at 18 eV were found to provide the most abundant and diverse fragment ions in a single step of activation, upon a dissociative photoionization (DPI) process for both ionization modes and for both types of oligosaccharides investigated herein. Fragments were more evenly distributed over the mass range than in low-energy collision activated dissociation (CAD) and unique fragment distributions were observed, such as systematic series of consecutive ions, including many structurally informative cross-ring fragments. Besides, in contrast to CAD, the main advantage was the absence of both neutral losses and double cleavages, which led to a much easier interpretation of the fragmentation spectra.

Complex mixtures of enzymatic degradation products of polysaccharides were successfully characterized. In particular, some chemical functions (such as methyl-esters [1] and sulfate [2]) which are crucial for the functions and properties of polysaccharides, were unequivocally positioned along the polysaccharide backbones despite their lability.

Also, for the first time, photo-activation in the VUV range was performed following a direct coupling with UPLC (fig. 2) [3]. This demonstrated that VUV-activation can be

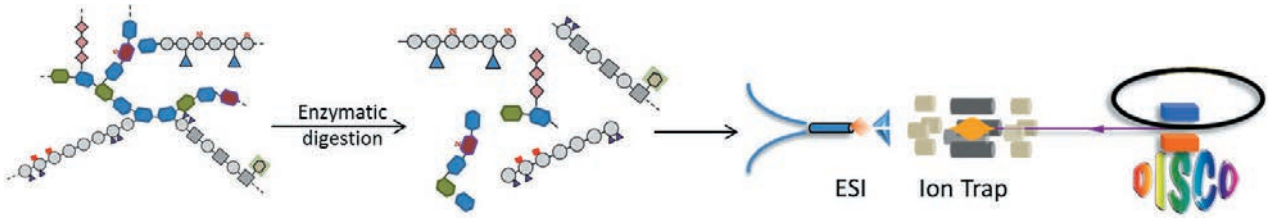

▶ *Figure 1: Experimental scheme implemented for the characterization structural motifs of the polysaccharides by coupling the synchrotron beamline and tandem mass spectrometry.*

performed in a timescale compatible with that of UPLC chromatographic separation. The dynamic range was improved and a tremendous amount of information was yielded, even on minor species. The compatibility of VUV-activation tandem MS with online chromatographic separation should contribute to increase the attractiveness of the DISCO beamline for biologists in other fields of application (e.g. in lipids, metabolites, peptides).

Until now, the polysaccharides structures that we studied on the DISCO beamline were mostly acidic and linear structures. However, many polysaccharides are neutral and exhibit high degrees of branching. Additionally, the structure and the function of neutral polysaccharides present at low concentration in algae are still unknown. Our further developments on the DISCO beamline will thus be to evaluate the VUV-activation method for the structural determination of neutral and branched polysaccharides from plants and algae.

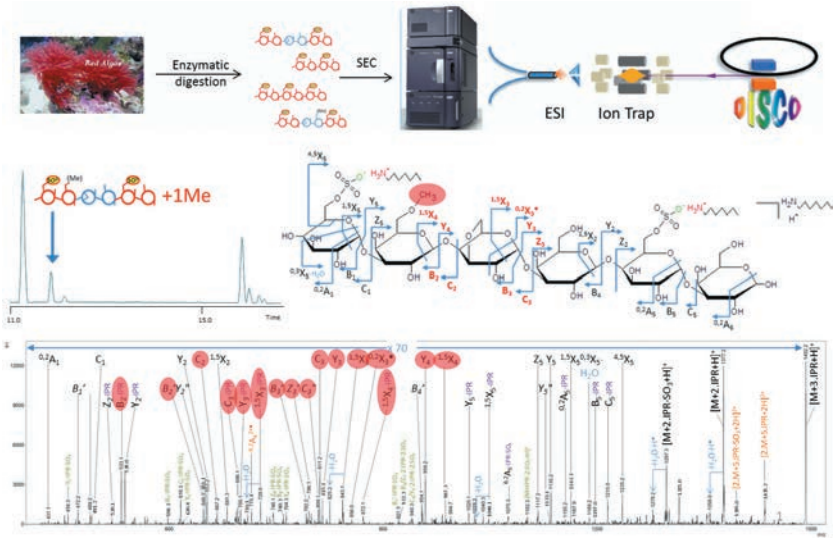

▶ *Figure 2: Example of characterizing an oligosaccharide in a complex mixture, made possible by coupling UPLC-VUVPD.*

▶ CONCLUSION

The structural information provided by VUV photon activation tandem MS led to an unprecedented description of the compounds released upon enzymatic hydrolysis of natural polysaccharides. This included a complete description of their chemical modification patterns and the unambiguous positioning of their sub-units. The comprehensiveness of this description provided key elements that permitted to refine the mode of action and specificity of the enzymes used. Compared to more conventional activation methods in tandem MS, the VUV activation of oligosaccharides led to rich fragmentation spectra with many cross-ring fragments and only minor losses of the labile functions such as sulfate groups. In particular, the method was able to resolve numerous isomers.

Our studies thus provided a demonstration that the activation of ions with highly energetic photons is a valuable method for the determination of unknown structures of extreme complexity by tandem MS, such as those of natural polysaccharides. These studies also proved that the activation happens in timescales compatible with those of UPLC, and can thus be directly coupled to online separation of the compounds, thereby providing a powerful mean to decipher complex mixtures in biology.

Astringency and the interactions between a human salivary proline-rich protein and tannins

▶ SCIENTISTS INVOLVED

F. Canon[1], B. Cabane[2], D. Durand[3], P. Sarni-Manchado[4,5], M. Réfrégiers[6], L. Nahon[6], J. Pérez[6], A. Giuliani[5,6], V. Cheynier[4]

[1] CSGA, CNRA, INRA, UB, 21000 Dijon, France

[2] PMMH, ESPCI, CNRS, Université Paris-Diderot, 75000 Paris, France

[3] I2BC, CNRS, CEA, Université Paris Sud, 91400 Orsay, France

[4] SPO, INRA, 34000 Montpellier, France

[5] CEPIA, INRA, 44000 Nantes, France

[6] Synchrotron SOLEIL, 91190 Gif-sur-Yvette, France

▶ CORRESPONDENCE

Francis Canon
francis.canon@inra.fr

▶ REFERENCES

F. Canon et al. (2013) Angewandte Chemie 52, 8377-8381.
F. Canon et al. (2013) Langmuir 29, 1926-1937.
F. Canon et al. (2015) Tetrahedron 71, 3039-3044.

▶ KEYWORDS

Structure-Function, Intrinsically disordered proteins, Salivary Proline-rich proteins, Tannins, Binding site, Non-covalent complexes.

▶ SCIENTIFIC QUESTIONS

Astringency is a sensory attribute due to tannins that is described as a drying-out, roughening, and puckery sensation felt in the mouth. Despite its importance regarding food acceptability, the molecular phenomena driving this perception are still unclear. Interactions occurring in mouth between tannins and salivary proline-rich proteins (PRPs) could play a major role in astringency as these proteins have a high affinity for tannins and are particularly abundant in the saliva of mammals consuming tannin-rich diet. PRPs are intrinsically disordered proteins (IDPs) which are characterized by the lack of a well-defined secondary and tertiary structure and by numerous repeated sequences. As a consequence, the study of such proteins using classical techniques of structural biology such as NMR or X-ray crystallography is extremely challenging. In this work, we have studied the interactions of a model tannin, epigallocatechin gallate (EgCG), with a recombinant human salivary basic PRP, IB5. The present work aims at characterizing the structure of IB5 in solution, the non-covalent interaction between IB5 and EgCG (stoichiometry, EgCG distribution...) the IB5•EgCG aggregates and the binding site of tannins on IB5.

To address these different points, we used a multi-technique approach based on mass spectrometry (MS) and small-angle X-ray scattering (SAXS) and developed a new technique coupling MS and synchrotron radiation.

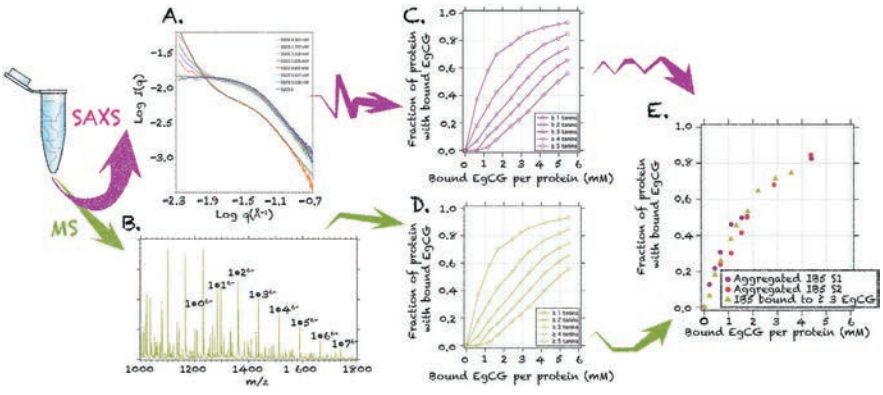

▶ *Figure 1: A. SAXS spectra from samples with the same protein concentration but different tannin concentrations. B. Positive ESI-MS spectrum of IB5 EgCG mixture. C. Fraction of proteins that are aggregated, calculated from SAXS for two different experiments S1 & S2. D. Fraction of proteins that have bound a given number of tannin molecules, from mass spectrometry. E. Comparison between aggregated protein fraction and fraction of proteins having bound at least 3 EgCG.*

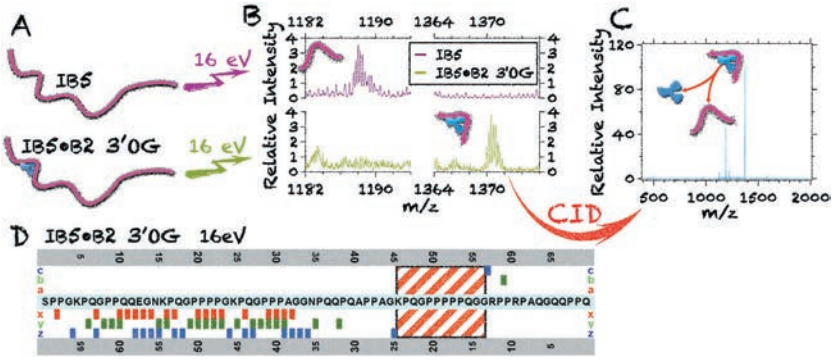

▶ Figure 2: Localization of the B2 3'OG binding site on IB5. The objects $IB5^{7+}$ and $IB5{\bullet}B2\ 3'OG^{7+}$ were selected and irradiated with 16 eV photons (A). Comparison between the MS/MS 16 eV VUV spectra identified specific fragments in the $IB5{\bullet}B2\ 3'OG^{7+}$ fragmentation spectrum in which the m/z ratio had a mass difference corresponding to that of $B2\ 3'OG^{7+}$, and fragments from the fragmentation spectrum of $IB5^{7+}$ (B). CID activation of identified fragments confirmed the presence of the ligand (C). The map of B2 3'OG-carrying fragments identified the 'KPQGPPPPPQGG' sequence as a B2 3'OG binding site on IB5 (D).

▶ MAIN RESULTS AND PERSPECTIVES

IB5 structure

SAXS is one of the most powerful methods for assessing protein dimensions and shape. The scattered intensity is sensitive to the size of the protein in solution but also to the conformational properties of the polypeptide chain. SAXS experiments have confirmed the intrinsically disordered nature of IB5 and revealed that IB5 has an unusual extended conformation compared to other IDPs. This conformation provides a large surface for the binding of tannins and therefore seems to be adapted to the presumed function of PRP.

IB5•*n*EgCG noncovalent complexes

Electrospray ionization (ESI) is a soft ionization technique allowing transfer of intact non-covalent complexes to the gas phase and MS separates ions as a function of their mass-to-charge ratio. MS experiments revealed IB5•*n*EgCG complex stoichiometries from 1•1 to 1•14 in solutions with low ionic strength. However, as tannins have the ability to stack on each other, the higher stoichiometries may not reflect the number of binding sites. Tandem MS experiments (MS/MS) allow to select, activate and then dissociate a specific ion, via different techniques of activation. Among them, collision induced dissociation (CID) induces the dissociation of the most fragile bonds (i.e. non-covalent interactions). Comparison of the energy required to dissociate IB5•*n*EgCG suggests that there are 8 binding sites on IB5. Titration of IB5 by EgCG studied by ESI-MS has revealed that the distribution of EgCG on the binding sites follows a Poisson distribution, suggesting that the binding sites are equivalent and independent. It has also allowed determination of the dissociation constant of EgCG-IB5 interaction, which is around 700 µm.

IB5•EgCG aggregation

At higher ionic strength, SAXS experiments revealed that the binding of EgCG on IB5 lead to the formation of large aggregates. The comparison of SAXS and MS data indicates that the population of aggregates grows with the population of IB5•EgCG complexes having bound at least three EgCG per protein. Therefore, at least 3 tannins per proteins are required to connect IB5•EgCG complexes and form aggregates. The threshold for the formation of these aggregates is in a concentration range that matches the physiological ranges. This suggests that the aggregation of salivary proteins by tannins in the mouth could have a physiological function.

Tannin binding site on IB5

Recently, synchrotron radiation (SR) has been introduced as a new activation technique for MS/MS. In this work, we have probed the potential of VUV-SR to provide structural information on IB5 and IB5•tannin complexes. Fragmentation of the protein at 16 eV induces a rich pattern of fragments, giving a better sequence coverage than other techniques of MS/MS. Activation of IB5•tannin complexes at 16 eV generates fragments of the protein bound to tannins. Indeed, this technique can cleave the peptidic chain while preserving the non-covalent interactions. Analysis of the fragments bound to tannins revealed that these fragments share a common segment of the sequence: KPQGPPPPPQGG. This segment is composed of a cluster of five prolines, which very likely adopts a PPI or a PPII helix conformation in solution. This provides an initial contact point, surrounded by clusters of glycine and alanine residues, which are flexible hinges allowing structural rearrangements and the establishment of additional hydrogen bonds. Investigations on complexes between IB5 and three different tannins (EgCG, B2 3'OG and B2) indicate that the same binding site is involved.

▶ CONCLUSION

We have developed an approach based on SAXS, MS, and synchrotron radiation. These complementary techniques have yielded crucial information on PRP-tannin interactions. Such approach appears to be promising in particular for the study of intrinsically disordered proteins and their non-covalent complexes.

Autofluorescence varies with the muscle fiber type and postmortem time

SCIENTISTS INVOLVED

T. Astruc[1], A. Vénien[1], C. Chagnot[1,2], M. Desvaux[2], Matthieu Réfrégiers[3], F. Jamme[3]

[1] QuaPA, INRA, 63122 Saint-Genès-Champanelle, France

[2] MIC, INRA, 63122 Saint-Genès-Champanelle, France

[3] Synchrotron SOLEIL, 91190 Gif-sur-Yvette, France

CORRESPONDENCE

Thierry Astruc
thierry.astruc@inra.fr

REFERENCES

[1] C. Chagnot et al. (2015) Analyst, 140, 4189–4196.
[2] C. Chagnot et al. (2015) J. Agric. Food Chem., 63, 4782-4789.

KEYWORDS

Rat muscle fibers, UV spectroscopy, histology, fiber types, postmortem, meat

CONTEXT

Skeletal muscle contains about 75% water, 19% protein, 0.5–8%, lipid and 1% glycogen, and is composed of myofibers, connective tissue, intramuscular adipocytes, vascular and nervous tissues. Myofibers, representing 75–90% of the muscle volume, show a heterogeneous population differing in structural, contractile, metabolic and physiological properties. They are generally divided into four types : I, IIA, IIX and IIB. Type I and IIA have an oxidative metabolism, with H_2O and CO_2 as final products, while type IIX and IIB use a glycolytic metabolism, where pyruvate is anaerobically fermented into lactic acid. Myofibers are also characterized by their speed of contraction, ranked I < IIA < IIX < IIB. The underlying molecular basis of this typology is the polymorphism of the myosin heavy chains (MyHC). Four adult MyHC isoforms have been identified in skeletal muscles: types I, IIa, IIx and IIb. These four isoforms allow the characterization not only of the four main pure muscle fiber, but also hybrid fiber types containing several myosin isoforms, such as type I-IIA, type IIA-IIX or type IIX-IIB fibers. These hybrid fibers point out the change from one pure type into another, driven by a change in age, physical activity levels, or exposure to prolonged stress. Many differences in gene expression can be observed when comparing different fiber types, suggesting numerous differences in protein composition depending on the fiber type.
After slaughter, muscle undergoes significant metabolic, physical, structural and biochemical changes determining the quality of meat and meat products. After bleeding, muscle cells deprived of oxygen and nutrients will try to survive by degrading their glycogen through anaerobic glycolysis. After this first phase of postmortem changes, additional biochemical changes and significant ultrastructural alterations are observed, related to the improvement of meat quality, especially tenderness. The speed of these postmortem changes (also called meat maturation) is dependent on the metabolic and contractile types of the muscles considered. Degradation of myofibrillar structure is faster in white than in red fibers.

SCIENTIFIC QUESTIONS

Our main objective was to investigate if the intracellular composition that varies depending on the fiber type and postmortem changes is able to change the optical properties of endogenous fluorophores naturally contained in biological cells. The study was performed by using the synchrotron deep UV (DUV) fluorescence microscope developed on the DISCO beamline providing fine-tuneable excitation from 180 to 600 nm, and full-spectrum acquisition from each point scanned. This unique equipment was the only one adapted to explore the respective autofluorescence response of each muscle fiber types, and to investigate their changes in fluorescence characteristics at 24 h postmortem.

MAIN RESULTS

Rat soleus and extensor digitorum longus (EDL) muscle fibers, previously identified on their cell types by immunohistofluorescence, were analyzed by synchrotron fluorescence microspectroscopy on stain-free serial muscle cross sections [1]. Muscle fibers excited at 275

nm showed emission fluorescence peaks at 332 nm and 410 nm with shoulders at 302 nm (fig. 1) but the highest differences in fluorescence emission intensity among fiber types are observed at 302, 325, 346 and 410 nm. The 410/325 ratio decreased significantly with contractile and metabolic features in EDL muscle, ranked I>IIA>IIX>IIB fibers ($p<0.01$; fig. 2). Compared to type I fibers, the 346/302 ratio of IIA fibers decreased significantly in both EDL and soleus muscles ($p < 0.01$).

The spectral muscle fiber autofluorescence response showed discrimination depending on postmortem time (t0 versus t24h) on both muscles at 346 nm and 302 nm, and to a lesser extent at 410 nm and 325 nm [2]. Taken individually, all fiber types were discriminated, but with variable accuracy, type IIA showing better separation of t0 / t24h than other fiber types.

Differences in intracellular composition related to fiber type or postmortem stage modify the fluorescence characteristics of tyrosine (302 nm) and tryptophan (332 nm) making up the muscle proteins. The discriminant fluorescence around 410 nm may be due to the NADH autofluorescence change, but further investigations are needed to confirm this hypothesis.

▸ PERSPECTIVES

In previous experiments, muscle fibers were characterized by localized spectroscopy. Our outlook is now to identify the types of muscle fibers with fluorescence imaging on free label histological sections by exploiting the identified wavelengths that reveal differences in emission fluorescence depending on metabolic and contractile type. Another perspective is to investigate the fluorescence changes along postmortem ageing of bovine meat in order to quickly identify the level of meat maturation.

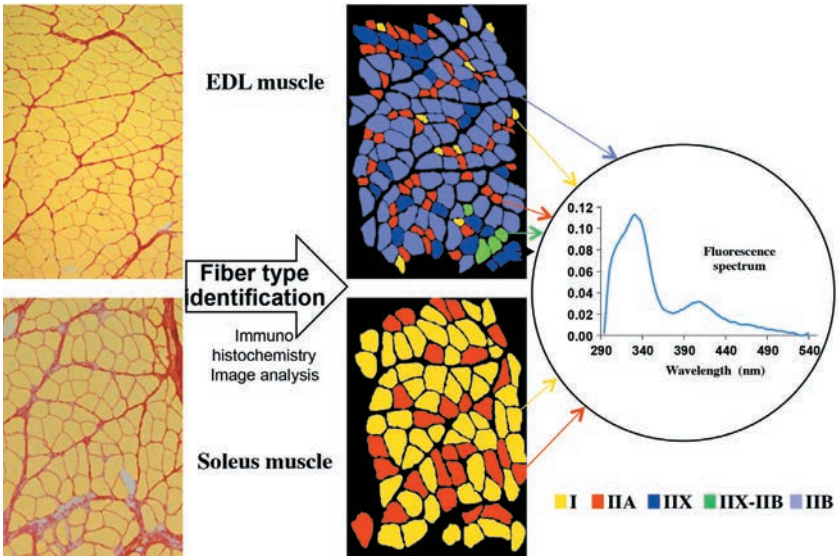

▸ *Figure 1: Fiber types identification and UV spectra acquisition*
Transverse section of rat EDL and soleus muscles. Muscle cells were identified on their fiber type by immunohistochemistry and spectra were acquired in the fibers. The UV spectra show peaks at 332 nm and 410 nm with shoulders at 302 nm.

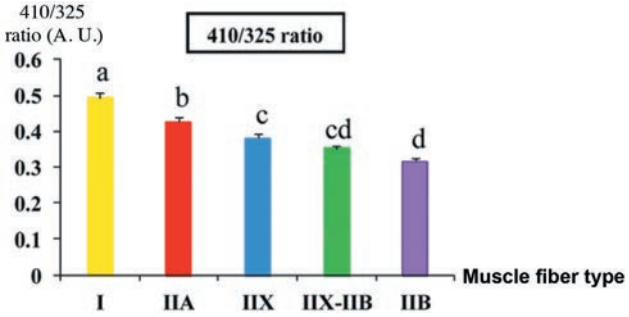

▸ *Figure 2: Fluorescence intensity changes regarding fiber types and postmortem time.*
EDL muscle fluorescence intensity ratio at 410 and 325 nm according to the muscle fiber type. Different letters indicate a significant difference for $p < 0.05$.

▸ CONCLUSION

This study highlights the usefulness of autofluorescence spectral signals to characterize muscle fiber type and postmortem changes on histological cross section of skeletal muscle with no staining chemicals.

SOLEIL sheds the light on lipid bodies protein structure

SCIENTISTS INVOLVED

Y. Gohon[1], J.D. Vindigni[1], M. Froissard[1], A. Giuliani[2-3], F. Wien[2], C. Tribet[4], P. Briozzo[1], T. Chardot[1]

[1] IJPB, INRA, AgroParisTech, CNRS, Université Paris-Saclay, 78000 Versailles, France

[2] Synchrotron SOLEIL, 91190 Gif-sur-Yvette, France

[3] CEPIA, INRA, 44000 Nantes, France

[4] Département de Chimie, École Normale Supérieure-PSL Research University, 75000 Paris, France

CORRESPONDENCE

Yann Gohon
yann.gohon@inra.fr

REFERENCES

[1] C. Deruyffelaere et al. (2015) Plant Cell Physiol. 56, 1374-1387.
[2] Z. Purkrtova et al. (2008) C.R. Biol. 331, 746-754.
[3] M. Réfrégiers et al. (2012) J. Synchrotron Radiat. 19, 831-835.
[4] Y. Gohon et al. (2011) Biochim. Biophys. Acta 1808, 706-716.
[5] J. D. Vindigni et al. (2013) Biochim. Biophys. Acta 1828, 1881-1888.

KEYWORDS

Lipid bodies, oleosome, Synchrotron Radiation Circular Dichroism, Small Angle X ray Scattering, low soluble proteins, protein interaction, lipid design, Arabidopsis thaliana, Saccharomyces cerevisiae.

SCIENTIFIC QUESTION

Most of the organisms studied to date accumulate storage lipids in specialized structures called oil bodies (OB). These intracellular inclusions have a diameter close to the µm, and their organization is unique among organelles. They consist in a core of neutral lipids (triglycerides, sterol esters) surrounded by a monolayer of phospholipids (PLs) in which various proteins are found. While oil bodies have been considered during almost a century as inert balls of fats, they recently earned the status of real organelles, with they own dynamics and original structure. The major questions on OB from various organisms (from crop to humans) are how lipids are accumulated, stabilized and at last mobilized. The nature of the proteins associated with OB, their structure, and their insertion in a unique monolayer are still opened questions. Oleosins are the most abundant proteins of seed OBs. They belong to a multigenic family, with a unique triblock structure (a hydrophobic core flanked with two amphiphilic regions). The N and C terminal regions of oleosins show considerable variation in term of size and sequence. Their hydrophobic segment, the longest known to date, is inserted in a PL monolayer specific of the organelle. Although Oleosins role in organelle stabilization and in the lipids mobilization during the germination [1] is known, data about their secondary structure are scarce and contradictory [2].

The secondary structure of surfactant or organic solvent solubilized oleosins has been investigated by different authors using Fourrier-Transformed Infra-Red microscopy (FT-IR) and Circular Dichroïsm (CD). Oleosins in purified OBs where also studied by FT-IR [2]. All these studies, in very different environments, gave contradictory results on oleosins secondary structure (either maintly α-helical or β-strand folded).

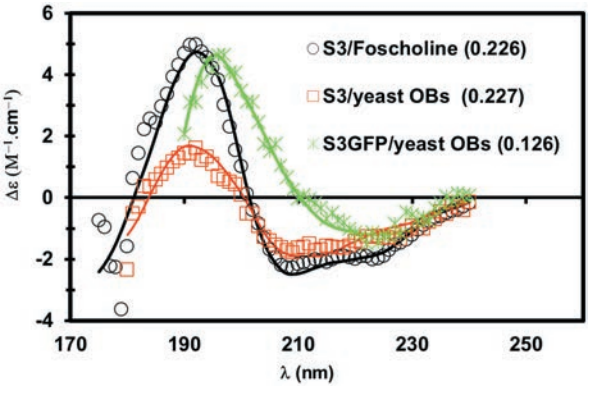

▶ *Figure 1: CD Spectra of oleosin.*

Approaches aimed at maintaining unique oleosin isoforms soluble, used amphiphilic polymers (Amphipols), conventional detergents, or eukaryotic expression system targeting unique oleosins isoforms to OBs with diameter suitable for spectroscopic methods. Synchrotron Radiation CD (SR-CD) at DISCO beamline permits to record spectra on samples very diluted, or diffusing UV light, and at low UV wavelength (180 nm), thus permitting a fine characterization of the β content of proteins [3]. SAXS at SWING beamline also allowed characterizing the protein amphipol assemblies.

▸ MAIN RESULTS AND PERSPECTIVES

Fold of oleosin solubilized by various surfactants

Different oleosins isoforms were maintained soluble in aqueous solution, using various detergents or original amphiphilic polymers, amphipols. Oleosins, insoluble in water based buffers, were maintained soluble (10 min at 200 000 xg) either by anionic detergents or amphipols. Neutral detergents were ineffective. Comparing hydrodynamic radius (obtained by dynamic light scattering) to radius of gyration (obtained by Small Angle X-Ray Scattering, SWING beamline) permitted the characterization of the sphericity of various Apols wrapping around oleosins. Size and dispersity of the complexes were sufficiently low to permit SR-CD measurements. SR-CD spectra were successfully recorded for all complexes. Analysis of these data proved that in all media, oleosins were folded. When maintained soluble with amphipols the oleosins possess more beta and less alpha secondary structures than in the SDS detergent (a denaturing molecule). These are the first reported structural results on lipid bodies proteins maintained in solution with amphipols, a promising alternative to notoriously denaturing detergents.

Fold of oleosin in an oil body environment

To study the fold of integral membrane proteins inserted in a cellular OB environment, the major *Arabidopsis thaliana* seed oleosin (S3), was targeted to *Saccharomyces cerevisiae* OBs. The diameter of purified yeast OBs harboring S3 or S3 fused with the Green Fluorescent Protein (GFP) was smaller and more homogeneous than plant OBs. Comparison of the secondary structure of S3 and S3–GFP was used to validate the structure of folded S3. SR-CD measurements indicated that S3 and S3–GFP in yeast OBs contain mainly beta secondary structures. While yeast OBs are chemically different to *A. thaliana* seed OBs, this approach allowed the secondary structure of S3 oleosin in OB particles to be determined for the first time. These results were consistent with the high beta content of the hydrophobic central domain of oleosins observed in amphipols polymers and in foscholine is an analogue of phospholipids, thus validating both approaches.

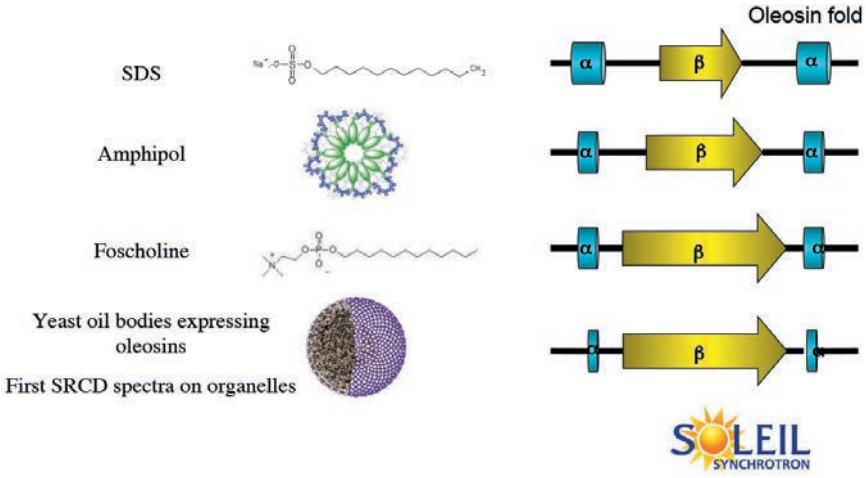

▸ *Figure 2: Model of the fold of oleosins in various environments. In blue, the hydrophilic extremities; in yellow, the hydrophobic central part. At the bottom, the folding models proposed with beta-sheets in the form of arrows and alpha helixes in the form of cylinders.*

▸ CONCLUSION

The use of various biophysical methods (Synchrotron Radiation Circular Dichroism, Xray scattering, available at SOLEIL Synchrotron) permitted to characterize oleosin fold in both environments: surfactants or native-like yeast OBs. These approaches lead to a secondary structure model for oleosins in which the central hydrophobic region adopts an original beta fold among eukaryotic proteins [4, 5] (Fig. 2).

Polysaccharide skeleton under X-rays

SCIENTISTS INVOLVED

P. Roblin[1,2], D. Guieysse[3], J. Perez[1], F. Guerin[3], M. Axelos[4], A. Buleon[4], G. Potocki-Veronese[3]

[1] Synchrotron SOLEIL, 91190 Gif-sur-Yvette, France

[2] CEPIA, INRA, 44300 Nantes, France

[3] LISBP, Université de Toulouse, CNRS, INRA, INSA, Toulouse, France

[4] BIA, INRA, 44300 Nantes, France

CORRESPONDENCE

Gabrielle Potocki-Veronese
veronese@insa-toulouse.fr

REFERENCES

[1] G. Potocki-Veronese et al. (2005) Biomacromolecules, 6, 1000-1001.
[2] S. Emond et al. (2008). FEMS Microbiol Lett., 285, 25-32.
[3] P. Roblin et al. (2013) Biomacromolecules, 14, 232-239.
[4] L. K. Skov et al. (2001) J. Biol. Chem., 276, 25273-25278.
[5] F. Guérin et al. (2012) J. Biol. Chem., 287, 6642−6654 ; S. Emond et al. (2008). FEMS Microbiol Lett., 285, 25-32.

KEYWORDS

Enzymes, amylose, SAXS, conformation.

SCIENTIFIC QUESTION

Due to their carbon-neutrality and renewability, biosourced polymers are seen as attractive alternatives to polymers issued from fossil carbon for a wide range of food and non food applications. If a wide range of polymers is available in Nature (proteins and polysaccharides like cellulose, starch, alginates...), microbial and enzymatic synthesis routes are more and more used for producing new polymers (PLA, PHA are the best examples), for optimizing their properties or for designing copolymers or hybrid systems. The understanding of both synthesis mechanisms and relationships between structure and physico-chemical properties is necessary for controlling the polymer production routes and their functionalities. In the field of polysaccharide synthesis, bacterial glucansucrases are highly attractive tools, since they catalyze the synthesis of α-glucans like dextrans, amylose or alternan, directly from sucrose, a cheap agroresource. Among them, amylosucrases are the only known enzymes that catalyze *in vitro* synthesis of amylose from sucrose and without any primer. Amylose is a linear polymer consisting of α(1,4)-linked glucosyl residues [1] and is also one of the two polysaccharides which constitute starch, the major energy storage form in higher plants such as cereals, legumes, and tubers. Amylosucrases thus constitute an efficient alternative to mimic *in vitro* amylose polymerization during starch biosynthesis or processing (starch gels). Recombinant amylosucrases, *from Neisseria polysaccharea* (*Np*AS) and *Deinococus geothermalis* (*Dg*AS), have been widely studied [1,2] for amylose synthesis at various temperatures. The reaction starts by sucrose hydrolysis. The released glucose is then used as first acceptor to produce by successive transfers malto-oligosaccharides and amylose chains which precipitate once the critical concentration and chain length are reached. The average chain length, polydispersity, morphology, crystallinity, and crystal size can simply be modulated by varying initial sucrose concentration. In order to get knowledge on chain self-association during amylose synthesis, small Angle X-ray Scattering (SWING beamline) was used to study the structure in solution of *Np*AS and *Dg*AS under conditions of polymer synthesis and, simultaneously, the conformation of amylose and the first stages of its entanglement/crystallization [3].

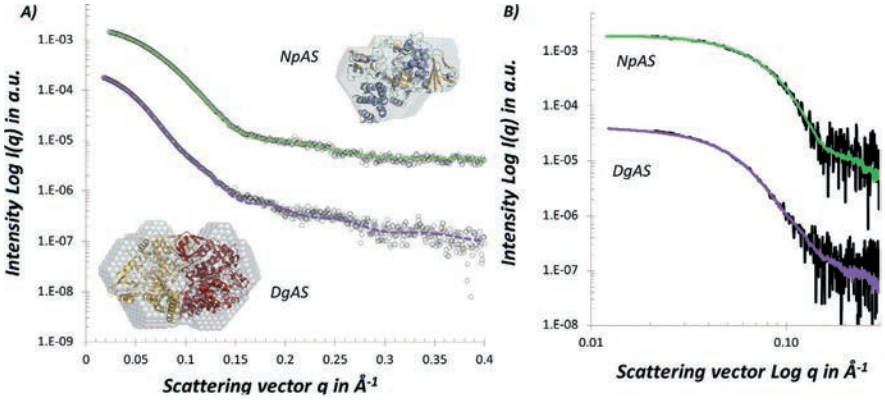

*Figure 1: **A)** Comparison of experimental SAXS curves from Np*AS *and Dg*AS *in solution (black curves) and their theorical SAXS curves (green: Np*AS*; purple: Dg*AS*) calculated from the corresponding crystallographic structures. The shape modeled starting SAXS data of both enzymes are superimposed to the crystallographic structures. **B)** Comparison of experimental SAXS curves of pure enzymes measured by coupling SAXS to HPLC (colored curves; green: Np*AS*; purple: Dg*AS*) with SAXS curve contribution of both enzymes extracted from reactional media analysis.*

▸ STRUCTURE IN SOLUTION OF GLUCANSUCRASES DURING SYNTHESIS

The SAXS curves recorded for *Np*AS in solution at 30°C and *Dg*AS at 50°C were identical to those calculated from their respective tertiary and quaternary structures obtained by X-ray crystallography [4,5] (Fig. 1A). Moreover, SAXS curves recorded for both enzymes with and without substrate (ie sucrose) were strictly superimposed (Fig.1B), showing that their conformation in solution does not vary during catalysis. It demonstrates that, at the SAXS resolution, the crystallographic structure is conserved during catalysis.

▸ CONFORMATION AND ENTANGLEMENT OF AMYLOSE CHAINS

The SAXS curves of amylose were extracted at different times of synthesis, by subtracting the respective signal contribution of enzymes, sucrose and oligosaccharides present in the reaction medium. For *Np*AS (Fig. 2), signal intensity progressively increases until 8 h of synthesis. After 8 h, the curve shape changes, intensity at small angles strongly increasing due to polymer aggregation. The intensity decrease observed at 22 h is due to precipitation and subsequent decrease of polysaccharide concentration in solution. Signal intensity at times lower than 8 h perfectly reflects the polymer concentration experimentally measured at the same reaction time. Polymer SAXS curves were fitted with scattering curves calculated from a mixture of cylindrical and wormlike objects (Fig. 2). The average contour length L of the fitted wormlike objects ranges from 134 Å at 2.6 h to 216 Å at 4.6 h, corresponding to a degree of polymerization (DP) of 27 and 43, respectively. These DP values are very close to those experimentally determined by size exclusion chromatography. From 2.6 to 4.6 h, the height of the fitted cylinder increases from 112 to 150 Å, and the average diameter from 10.6 to 15.8 Å, probably due to the beginning of aggregation between cylinders. The average width determined for the wormlike and the cylinder objects corresponds exactly to the width of a single amylose chain and of a double helix, respectively (Fig. 2). Amylose chains are well-known to form double helices in crystalline structures and in gels, while wormlike structures have already been observed by cryo-transmission electron microscopy of diluted suspensions of amylose. Wormlike structures are also used to describe the conformation in solution of polysaccharides with low DP, chain length being not sufficient to allow them wrapping into random coils before their entanglement when concentration increases. For *Dg*AS, synthesis kinetic was slower, and the relative amount of cylinders was much lower. The length of the fitted wormlike structures progressively increased to reach a maximum average value around 185 Å, corresponding to DP 37, which is close to that found by Emond and coworkers [2]. Moreover, no formation of clusters of double helices was evidenced. This lack of self-association of individual double helices into clusters is probably related to the higher temperature used for amylose synthesis with *Dg*AS. At 50°C, amylose is indeed more soluble than at 30°C, which prevents further chain entanglement and precipitation.

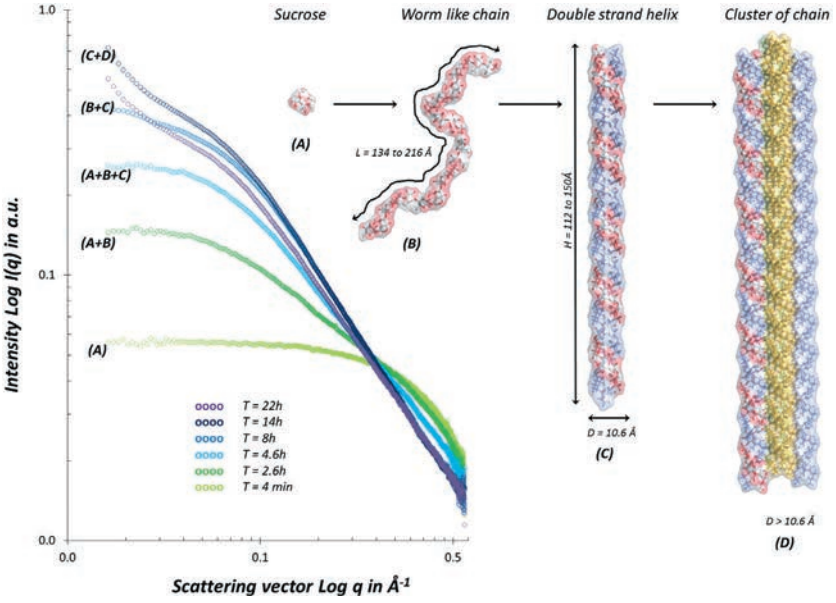

▸ *Figure 2: SAXS curves of amylose synthesized by* Np*AS at different reaction times. Model of amylose chains in wormlike structure, double helix and packing of double helices leading to crystallization.*

▸ CONCLUSION

SAXS analysis allowed us to show that the overall structure of the targeted glycoside-polymerases is conserved when these enzymes are complexed with their substrates and products. Such an experiment is unique, as SAXS analysis of protein conformation is usually performed using inert substrate analogs or with inactive enzyme mutants. The conformation of amylose was simultaneously studied during its synthesis. The formation of isolated double helices, once the wormlike chains have appropriate size, and the subsequent aggregation of double helices before precipitation and crystallization experimentally confirm that junction zones are formed as double helical fragments during amylose gelation. This highly generic approach paves the way to the acquisition of key knowledge to establish the relationships between molecular structure, supramolecular organization and properties of polymers of biological and biotechnological interest.

Focus on the beamlines and setups primarily used by INRA scientists

This section presents the three beamlines where the staff includes an INRA engineer during 2016:

- DISCO beamline covers the energy range from visible light to vacuum ultraviolet (VUV, 1000 – 60 nm). It is devoted to imaging and bio-spectroscopy applied to biochemistry, chemistry and cell biology.
- NANOSCOPIUM beamline is a multimodal, multi-length-scale beamline dedicated to scanning X-ray micro- and nanoprobe experiments (30 nm - 1 µm spatial resolution range) in the 5-20 keV energy range. X-ray fluorescence (XRF), X-ray absorption spectroscopy (XAS) and phase-contrast imaging techniques can provide simultaneous information on elemental distribution and speciation, and on the sample morphology, both in 2D and 3D.
- SWING beamline is a small angle X-ray scattering (SAXS) beamline. It provides information on the structure of matter at scales ranging from nanometers to micrometers. Many issues related to soft matter, to the conformation of macromolecules in solution and to composite materials are addressed. Wide varieties of samples are studied - solutions, gels, amorphous solids, crystallized solids – in all of their corresponding environments. Recent developments of original sampling devices made on this beamline are also presented.

Although not specifically introduced in this document, SMIS is another beamline whose equipment and characteristics are of particular interest for INRA users. It is dedicated to microscopic analysis in the infrared range of a variety of samples, ranging from polymer films and multilayers, minerals and other geological materials, biological and biomedical samples, to archaeology. A combination of experimental setups allows analysis under various temperature and pressure conditions. Finally, nanoscale IR absorption spectroscopy has recently been implemented at SMIS.

The DISCO beamline: a multipurpose beamline dedicated to biology and chemistry

SCIENTISTS INVOLVED

A. Giuliani[1,2], F. Jamme[1], F. Wien[1], and M. Refregiers[1]

[1] Synchrotron SOLEIL, 91190 Gif-sur-Yvette, France

[2] CEPIA, INRA, 44000 Nantes, France

CORRESPONDENCE

Matthieu Réfrégiers & Alexandre Giuliani
matthieu.refregiers@synchrotron-soleil.fr
alexandre.giuliani@synchrotron-soleil.fr

REFERENCES

[1] A. Giuliani et al. (2009) J. Synchrotron Radiat. 16, 835–841.
[2] M. Réfrégiers et al. (2012) J. Synchrotron Radiat.19, 831–835.
[3] A. Giuliani et al. (2011) J. Synchrotron Radiat. 18, 546–549.
[4] A. Giuliani et al. (2012) Nucl. Instruments and Methods B, 279, 114–117.
[5] A. R. Milosavljević et al. (2012) J. Synchrotron Radiat. 19, 174–178.

KEYWORDS

Imaging, spectroscopy, conformation, SRCD, fluorescence, mass spectrometry.

The DISCO beamline possesses three experimental stations using the visible, ultraviolet and vacuum-ultraviolet part of the electromagnetic spectrum. In addition to the imaging endstation (described in a separate article), the beamline also has a circular dichroism spectrometer and a general-purpose irradiation station. The latter may be coupled to mass spectrometers for ionization or to perform tandem mass spectrometry.

DISCO is a bending magnet based beamline using the visible and ultraviolet (UV) range of the spectrum [1]. This feature makes DISCO intermediate between the low and high-energy beamlines.
DISCO is a bending magnet based beamline. In order to maximize the photon flux in the 1 to 20 eV range, a large part of the beam is used similarly to the infrared beamlines. Owing to the large horizontal divergence of the source, a mirror system has been installed in the front-end, very close to the bending magnet. The power emitted by the source is distributed along the vertical axis, the most energetic radiations are found very close to the orbit. Hence, it is possible to remove the high energy content of the emission by positioning a cold finger in the orbit plane. This protects the first mirror and creates two beams separated by the shadow of the absorber.

Fig. 1a presents the optical layout of the beamline and fig. 1b a sketch of the different experimental stations. Downstream of the first mirrors (M1 and M2), a pair of mirrors (M3 and M4) deflect the beam horizontally toward a mirror (M51), which reflects one quarter of the light towards the imaging station (CX3 in fig. 1). The remainder of the beam reaches a monochromator, used for both CX1 and CX2 stations (fig. 1). Station CX1 is dedicated to synchrotron radiation circular dichroism (SRCD) whereas CX2 is an atmospheric pressure irradiation branch referred to as APEX. Hence, DISCO possesses three branches, two of which are operated simultaneously.

IMAGING STATION

The equipment available at the imaging station is described in greater details in the article entitled "DUV Imaging branch at DISCO beamline: DUV autofluorescence microscopy for cell biology and tissue" (page 80).

SYNCHROTRON RADIATION CIRCULAR DICHROISM (SRCD)

A normal incidence grating of the monochromator delivers monochromatic radiation in the 600 – 125 nm wavelength range, with a resolving power between 300 and 120, with

photon fluxes in the range of 2.10^{10} photons/s [2]. Downstream of the monochromator, the beam is selected by a system of adjustable slits and is polarized by the combination of a linear polarizer and photoelastic modulator. A photomultiplier detects the light passing through the sample. The sample holder system is mounted on exchangeable drawers which allow quick changing of the configuration. The chamber is fitted with several ports to install other detection system or activation capabilities. The sample holder receives calcium fluoride or quartz cells with optical path lengths ranging from 2µm to several mm. Sample loading can be automated thanks to coupling with an autosampler. Moreover, the cells can be continuously rotated for linear dichroism studies for example. The chamber and the drawers are presented in fig. 2.

▸ THE APEX BRANCH

The Atmospheric Experiment (APEX) branch has been designed to deliver UV radiation in the 4 to 20 eV range at atmospheric pressure [3]. For this, a differential pumping system has been designed. A curtain gas, usually a rare gas transparent in the wavelength range of interest, is introduced in front of the orifice of the differential pumping system. This branch is open to users and is coupled to various user chambers. The VUV radiation of the APEX branch has been used to perform photoionization prior to mass spectrometry [4] analysis and also for ion activation in tandem mass spectrometry [5].

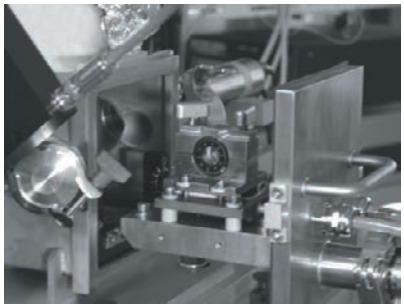

▸ *Figure 2: Picture of the experimental chamber of the SRCD station.*

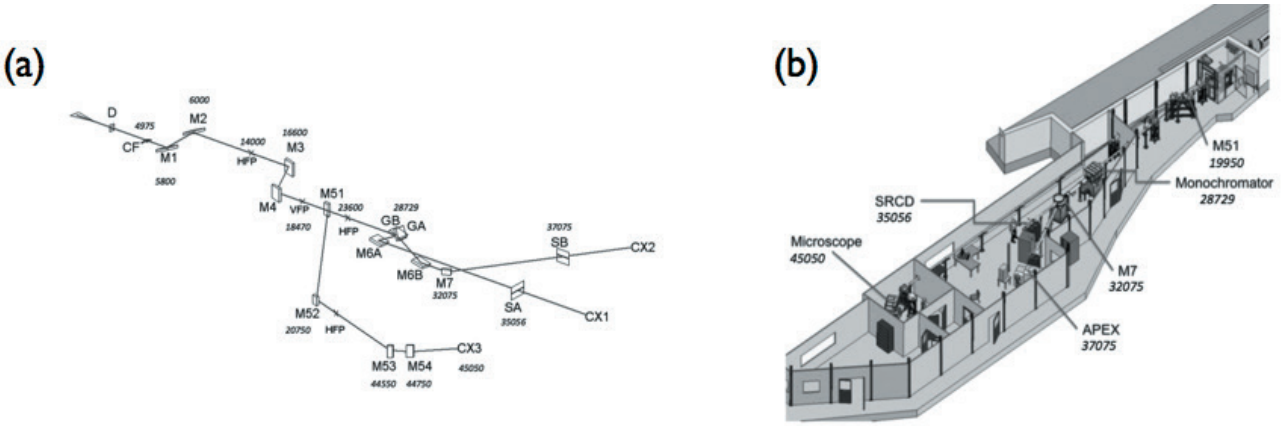

▸ *Figure 1: a) Sketch of the optical path of the DISCO beamline showing the optical elements and their distance to the source. b) Installation drawing of the beamline.*

▸ CONCLUSION

DISCO is a polyvalent beamline dedicated mainly to biology and chemistry. It covers a wide range of wavelength ranging from the visible to vacuum-ultraviolet making it suitable for absorption spectroscopy, linear and circular dichroism, fluorescence and photoionization.

DUV Imaging branch at DISCO beamline: DUV autofluorescence microscopy for cell biology and tissue

▶ SCIENTISTS INVOLVED

M. Refregiers[1], F. Wien[1], A. Giuliani[1,2] and F. Jamme[1]

[1] Synchrotron SOLEIL, 91190 Gif-sur-Yvette, France

[2] CEPIA, INRA, 44000 Nantes, France

▶ CORRESPONDENCE

Matthieu Réfrégiers & Frédéric Jamme
matthieu.refregiers@synchrotron-soleil.fr
frederic.jamme@synchrotron-soleil.fr

▶ REFERENCES

[1] A. Giuliani et al. (2009) J. Synchrotron Radiat., 16, 835-41.
[2] F. Jamme et al. (2010) Microsc. Microanal., 16, 507-514.
[3] G. Tawil (2011) Anal. Chem., 83, 989–993.
[4] E. Batard et al. (2011) PLoS ONE, 6, e19440.
[5] F. Jamme et al. (2013) Biol. Cell., 105, 277–288.

▶ KEYWORDS

Microscopy, imaging, autofluorescence, label-free.

The DISCO beamline is open to users since September 2009. The imaging branch uses the deep ultraviolet range to probe the intrinsic fluorescence biomolecules without the need of specifics external probes.

The UV autofluorescence of cells and tissues has long been evaluated for its diagnosis potential. However, because sources and microscopes that allow obtaining reliable information in the deep UV (DUV, 200–350nm) are difficult to obtain and couple, most medical diagnoses are concentrated on the autofluorescence spectroscopy and microscopy of endogenous probes. Synchrotron radiation is a broadband light that can be monochromatised in almost any energy range. The DISCO beamline at the synchrotron SOLEIL optimises the vacuum UV (VUV) to the visible range of the spectrum [1]. The energies accessible on two microscopes at atmospheric pressure are defined by quartz cut-off, from 200 nm to longer wavelengths (600nm) [2;3]. For biological relevance, we specifically focus on the range 200–350nm that is very rarely used for microscopic purposes, especially under 250 nm.

▶ DUV FLUORESCENCE MICROSCOPY

Kohler developed DUV microscopy in 1904 as a bright field transmission technique. This was implemented for one main reason: to improve the spatial resolution of cellular imaging. It passed through the century allowing seeing the un- seen, namely nucleic acids in cells, and to observe colour differences in tumours

under UV excitation for cancer diagnosis. Thanks to developments in detectors, it became a quantitative method to observe protein and DNA contrast at 280 and 260 nm. However, because of the differences of optical density in deep UV transmission images, scattering errors are difficult to avoid and interpreting DUV images is challenging. Although most biomolecules do present a contrast in DUV transmission microscopy, few of them will re-emit fluorescence. This autofluorescence is very important in the sense that it permits better discrimination of molecules. Moreover, following auto-fluorescence opens label-free studies of molecules of interest without any external probes or radiolabelling that could impair activity of the molecule of interest [3;4]. Although many studies were conducted in DUV fluorescence spectroscopy as a diagnosis tool, mainly for cancer, very few were conducted on DUV fluorescence microscopy or microspectrofluorimetry on biopsies and tissues. The majority were performed using an excitation wavelength longer than 350 nm, mostly due to the lack of laser lines below this value, despite very promising sensibility and sensitivity using DUV excitation.

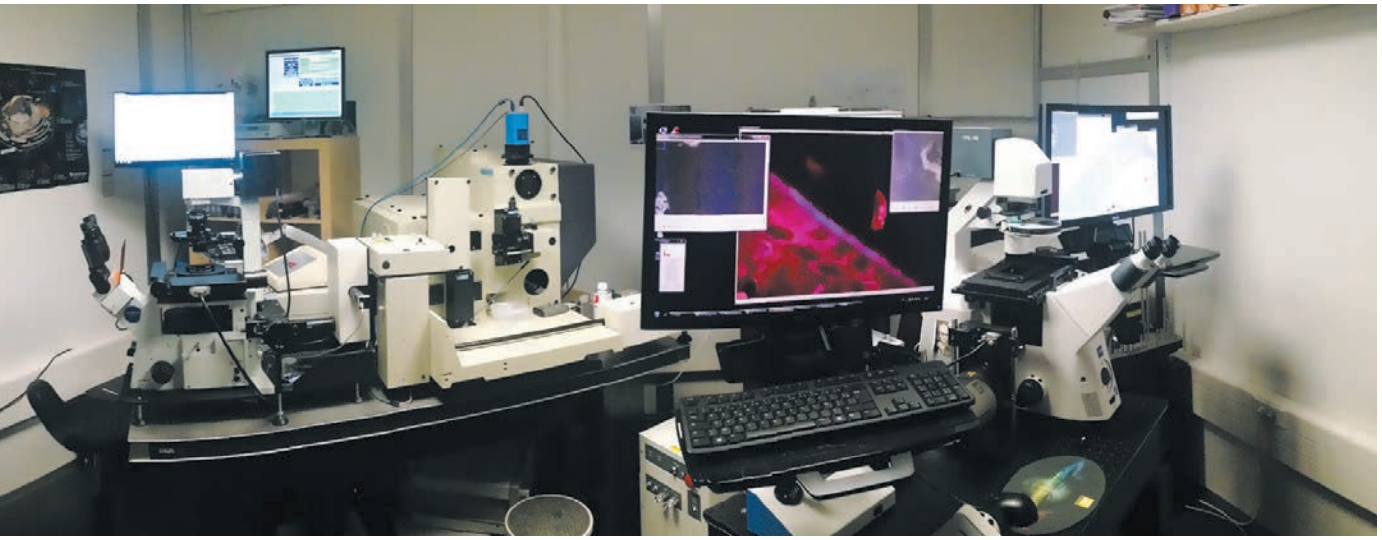

▶ *Figure 1: The DUV fluorescence microscopy branch on DISCO beamline.*

▶ CONCLUSION

Many endogenous fluorophores have an absorption/excitability maximum in DUV below 350 nm, especially tryptophan. Signal attributed to tryptophan typically exhibits fluorescence intensities orders of magnitude greater than those from other endogenous fluorophores. And although its fluorescence can serve as an additional marker for monitoring cellular status, due to lack of DUV fluorescence microscopy, this fluorophore is often ignored.To fulfil this need, we have developed a synchrotron-coupled DUV microspectrofluorimeter which is operational since 2010 [5] (Fig.1).

Hierarchical length-scale scanning imaging at the Nanoscopium beamline to study simultaneously the elemental and morphological variation of the sample

▶ SCIENTISTS INVOLVED

A. Somogyi[1], K. Medjoubi[1], G. Baranton[1], V. Le Roux[1], M. Ribbens[1]

▶ INRA CORRESPONDENT

C. Rivard[1]

[1] Synchrotron SOLEIL, 91190 Gif-sur-Yvette, France

▶ CORRESPONDENCE

Andrea Somogyi
somogyi@synchrotron-soleil.fr

▶ REFERENCES

[1] A. Somogyi et al. (2015) J. Synchrotron Rad., 22, 1118–1129.
[2] K. Medjoubi et al. (2013) J. Synchrotron Rad., 20, 293–299.
[3] N. Leclercq et al. (2015) Proceedings of ICALEPCS, Melbourne, Australia, WEPGF056.

▶ KEYWORDS

Scanning multi-technique X-ray imaging, nano-imaging, XRF, phase contrast, multi-length scale studies.

▶ CHARACTERISTICS OF THE BEAMLINE

The Nanoscopium 155 m long beamline is situated in the L13 source straight section of Synchrotron SOLEIL. It is dedicated to scanning multi-technique hard X-ray nano-imaging in the 5–20 keV energy range [1]. Scanning X-Ray Fluorescence (XRF) spectrometry offers the possibility of simultaneous detection of most of the elements of the periodic table having atomic number greater than that of Al. The beamline will also offer the study of the chemical speciation of elements with Z>22 (Ti). By introducing a dedicated detector into the transmitted beam different transmission modalities, such as absorption-, differential phase- and scattering contrasts can be measured, which provide information about the sample morphology (electron density variation). These techniques can be applied simultaneously (fig. 1).

The schematic beamline layout is shown in fig. 2. The undulator, the front-end (FE) and the pre-focusing mirrors (M1, M2) are located in lead-shielded hutches in the synchrotron building, while the monochromators, the secondary source defining aperture (SS) and the two experimental hutches are situated in a dedicated building extension. All hutches are thermally isolated and are equipped with +/- 0.1°C temperature control. The consecutive, complementary chromatic (focusing by Fresnel Zone Plate, FZP) and achromatic (focusing by Kirckpatrick-Baez, KB mirror-pair) multi-technique nano-imaging experimental stations are situated in the two experimental hutches (EH1 and EH2). These ensure optimizing the experimental conditions in the function of the energy bandwidth, demanded flux, nano-beam size, coherence characteristics and the required energy tunability of the actual experiment.

The main scientific fields foreseen at the beamline are biology, life sciences, geo-biology, and environmental sciences. The study of the spatial distribution of transition metals in animal or plant tissues and cells or the investigation of the elemental composition, uptake, and sequestration mechanisms in soils, plants or other environmental samples are some of the representative examples of research possibilities at Nanoscopium.

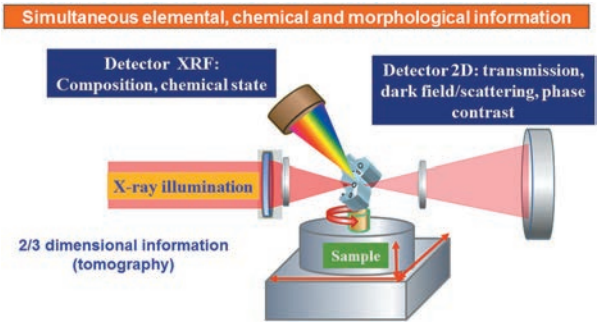

▶ *Figure 1: Scheme of scanning multi-technique imaging.*

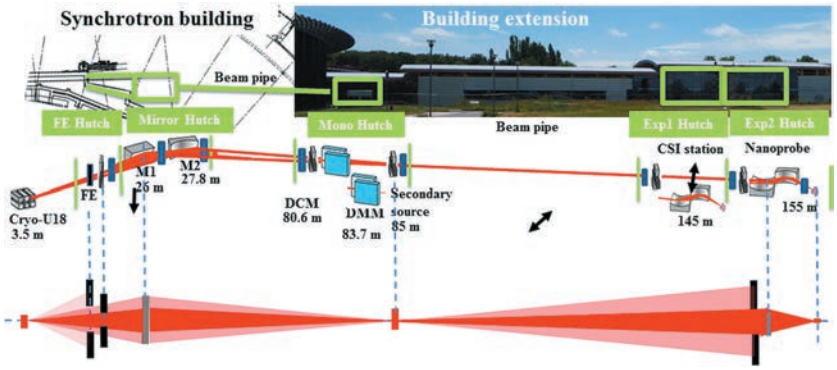

▶ *Figure 2: General layout of the Nanoscopium beamline.*

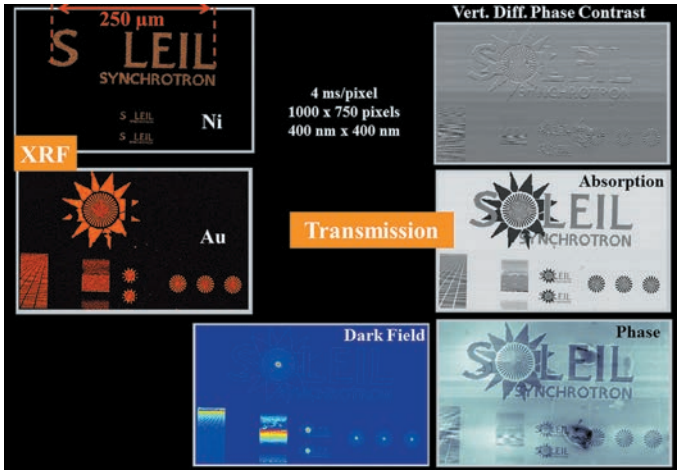

▶ *Figure 3: Scanning multi-technic imaging of a standard structure. See details in the text.*

▶ FIRST RESULTS

The Nanoscopium scanning hard X-ray nanoprobe beamline is in early user-operation phase while continuing commissioning. The measured beamline performance shows good agreement with the main design goals. The recently available highest spatial resolution in 2D imaging experiments is 200 x 200 nm^2. The high intensity of such focused nano-beams makes it possible to obtain, high (sub-) part-per-million (sub-ppm) analytical sensitivity in adapted measurement conditions. Moreover, the beamline is especially well suited for hierarchical length-scale studies of highly heterogeneous samples providing morphological, elemental and chemical information at multiple length scales with adapted (0.2-1 μm) spatial resolution. One of the most important requirements for such experiments is the possibility of fast scanning with down to ms dwell times, which is implemented at the beamline by the Flyscan software and hardware architecture [2, 3]. The proof of principle fast scanning experiments showed the possibility of high resolution 2D imaging of some hundred μm^2 sample areas in some tens of minutes. In fig. 3 the possibilities offered by multi-technique Flyscan is demonstrated through the measurement of a standard sample containing Ni and Au structures. Scanning XRF provides element specific information about the spatial distribution of Ni and Au. The higher sensitivity of phase contrast imaging in the hard X-ray range to light elements compared to absorption contrast imaging is clearly visible from the detailed information on cracks and light element irregularities, which can only be seen in the phase contrast maps (vertical differential phase contrast and reconstructed phase). The highly scattering structures show edges and structures, which are denser (containing structures smaller) than the beam-size. All these modalities have been obtained simultaneous with 400 x 400 nm^2 pixel size and 4 ms per pixel measurement time with the Flyscan architecture of SOLEIL.

▶ FURTHER DEVELOPMENTS AND PERSPECTIVES

The beamline aims to offer scanning tomography measurements in the near future, providing information about the elemental composition and sample morphology within virtual sample slices within intact unstrained and uncut samples. As a next step we intend to push down the spatial resolution of these scanning techniques to the sub-100 nm range with 50 x 50 x 50 nm^3 as the ultimate resolution goal. The installation of a multilayer monochromator will make high flux experiments (without the possibility of chemical speciation) possible. The figure of merit of speed, spatial resolution and appropriate contrast also depends on the analyzed sample type and the detectors used, which will be studied in detail during the next phase of the commissioning. The development of user oriented software for the treatment of multi-technique imaging and tomography data is in progress and is a crucial requirement for the success of the beamline.

Acknowledgement

We acknowledge the help and expertise of the Support Groups of SOLEIL, without which the Nanoscopium beamline project could have been possible.

SWING beamline: Characterize biological and soft matter at nanometer scale

▶ SCIENTISTS INVOLVED

P. Roblin[1,2], A. Thureau[1], T. Bizien[1], Y. Liatimi[1], J. Pérez[1]

[1] Synchrotron SOLEIL, 91190 Gif-sur-Yvette, France

[2] CEPIA, INRA, 44300 Nantes, France

▶ CORRESPONDENCE

Pierre Roblin & Javier Pérez
roblin@chimie.ups-tlse.fr
javier.perez@synchrotron-soleil.fr

▶ REFERENCES

G. David & J. Perez (2009) Applied cryst., 42, 892-900.
T. Bizien et al. (2016) Protein Pept. Lett., 23, 217-231.

▶ KEYWORDS

SAXS, WAXS, structural biology, colloids, nanostructures.

The SWING beamline is open to users since 2007. Small Angle Scattering from high-energy radiation (X-rays) is collected to characterize structures at the nanometer scale. Dedicated optical devices located upstream the sample environment provide a focused and very intense monochromatic X-ray beam. In the experimental hutch, a mobile platform can receive a wide range of sample environments. Scientific domains addressed on the SWING beamline range from biology and organic chemistry to inorganic solid materials.

▶ SAXS

Small Angle X-rays Scattering (SAXS) is a powerful technique that directly provides structural information at scales typically ranging from 1 nm to 1 µm. In biology, SAXS is mainly used to model the shape of macromolecules in solution. Their behavior can be studied in conditions close to their physiological environment and structural variations caused by an application of external constrain or association with partners can be evaluated. During the last years, SAXS methodology has undergone significant improvements both on the experimental and data processing sides.

▶ SWING Beamline

The SWING beamline light source is a U20 undulator which produces a very intense and very slightly divergent multi-wavelength X-ray beam. The beam is then intercepted by a fixed-exit double crystal monochromator which can select a single energy between 5 and 17 keV.
Several optical elements as a Kirckpatrick Baez type double-focusing mirror and three sets of slits are used to focus or collimate the beam,

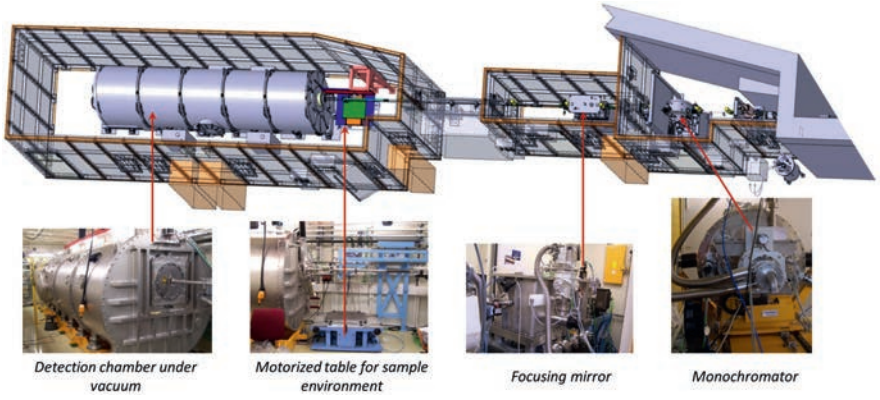

▶ *Figure 1: The SWING beamline: optics hutch (right) and experimental hutch (left), with a focus on 4 pieces of equipment.*

redefine the beam size and eliminate beam tails. The beam size on the sample can be tuned from 25 µm to 200 µm vertically and from 150 to 400 µm horizontally. In the experimental hutch, a XYZ motorized table can support different types of sample environments (in-vacuum flow-through capillary cell, multi-sample holder, high-pressure cell, stopped flow device, in-situ rheometer in Couette geometry, Linkam hot stage...). The signal scattered by the sample is recorded on an Aviex CCD type detector with a sensitive area of 17 cm x 17 cm, positioned in a large cylindrical chamber under primary vacuum to minimize air absorption and parasitic scattering. The sample-to-detector distance is adjustable from 0.5 m to 6 m in order to cover different q ranges from $2.5x10^{-4}$ $Å^{-1}$ to 3 $Å^{-1}$, with $q = 4\pi / \lambda \sin \theta$, 2θ being the scattering angle and λ being the X-ray wavelength, typically around 1 Å.

▸ DEDICATED SAMPLE ENVIRONMENTS

For the analysis of macromolecules such as proteins or other type of biopolymers, the SWING beamline is equipped with a HPLC online associated to a flow-through cell. The purification step with a size exclusion column increases the quality of the measurement, removing aggregates and ensuring a perfect buffer subtraction.

Robotic devices have recently been developed to increase the data throughput. Thanks to the new pipetting robot (cf article p. 86), inhomogeneous samples such as precipitates or viscous solutions can be handled. This robot is permanently associated to the HPLC set-up and used in parallel when direct injection is required instead of chromatographic separation.

Another device, dedicated to the automated cleaning of capillaries, has been also installed on the beamline to remove matter adsorbed on the inner surface of the capillary wall after each measurement to ensure the best possible reproducibility of the experiences. This cleaning device (cf article p. 86) is composed of two syringes adjustable in volume and speed and connected to a selector. The cleaning process consists in the fast injection of a detergent solution, followed by a cleansing step using distilled water. This device could also be easily put to good use to perform mixing reactions, associated either to continuous or stopped flow into the SAXS capillary. The reaction kinetics could then be investigated with a time resolution of the order of a second.

Another sample environment was developed to characterize the evolution of the product or the modification of the substrate for reactions developing over several minutes or hours. This micro-reactor (fig. 2) is composed of a glass cuvette of 7 ml equipped with a magnetic mixer to ensure the homogeneity of the solution and a thermostated chamber to maintain a constant temperature during the kinetics. The device can be used in continuous flow mode if associated to a peristaltic pump connected to the capillary, thereby forming a closed flow path at constant volume. In batch mode, a vertical capillary is connected to the sample by direct immersion and the other extremity to a pump. The pump then regularly aspirates an aliquot of the reaction solution in the measurement window and sends it back. This configuration is adapted as well to very viscous solutions or fragmented solids (such as yogurt).

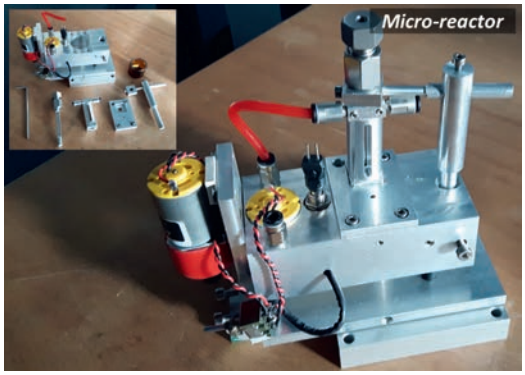

▸ *Figure 2: The micro-reactor sample environment.*

Efforts have also been undertaken to make several types of more classic sample holders easily exchangeable directly by the users. A large variety of samples (liquids, gels or solids) can be measured on the beamline, and different types of capillary supports in horizontal or vertical orientation for static (liquids or powders) or continuous flow measurements (liquids) are proposed, as well as a gel sample holder where the sample is deposited within a spacer in Teflon® and covered with Kapton® foils. A new version of the latter is available, with an access by the top. This configuration allows easy manual injection of reactive solutions to follow the effect of their diffusion inside the gel, by scanning the gel across the X-ray beam.

▸ CONCLUSION

Dedicated to SAXS but opened to any scientific field, SWING offers a variety of sample environments to adapt to different needs. The online HPLC-SAXS was the first worldwide such set-up and is permanently improved in terms of automation. Injection robots, mixers, cleaners, micro-reactors have been developed after thorough discussions with the users, and especially those from INRA, whose requirements are most of the time original and motivating.

Development of new autosampler for direct injection of inhomogeneous sample through cell measurement

▶ SCIENTISTS INVOLVED

P. Roblin[1,2]

[1] Synchrotron SOLEIL, 91190 Gif-sur-Yvette, France

[2] CEPIA, INRA, 44300 Nantes, France

▶ CORRESPONDENCE

Pierre Roblin
roblin@chimie.ups-tlse.fr

▶ REFERENCES

One INRA-SOLEIL patent was deposited to protect the new principle of pipetting and transfer of inhomogeneous solution.

▶ KEYWORDS

Autosampler pipetting robot, compactness, polyvalent, non-homogenous solutions.

▶ SCIENTIFIC QUESTION

This project aims to develop a new autosampler, compact and robust, offering a wide range of applications, able to aspirate and dispense current liquid sample used in biology and chemistry (homogeneous and diluted samples). It will also be compatible with non-homogenous solutions with untypical physical and chemical properties (very concentrated solution, viscous, partially precipitate or crystalline…). The second objective is to have a polyvalent pipetting robot which can be used on different synchrotron beamlines performing experiments with liquids As shown in fig. 1, the pipetting robot has three motorized axes to position precisely the needle above the vial which contains the sample, stored in a thermo-regulated sample holder. The sample pipetting is performed with a first syringe connected to the needle. The vacuum generated by the syringe pipettes the sample, and the speed of the syringe can be adjusted with the viscosity of the sample.

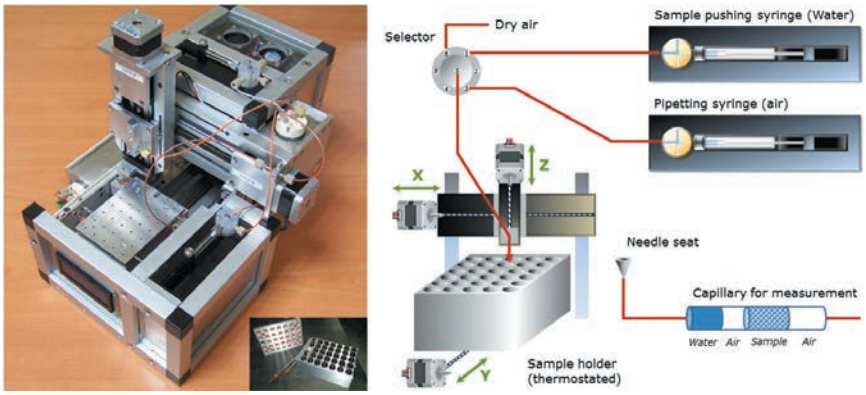

▶ *Figure 1: Principle of operation of the pipetting autosampler.*

The internal volume of the needle and the volume of the following loop measure 60µl and allows to pipette 50µl of sample. In the second step, the 3 motorized axis moves the needle to a seat and the selector's valve connects the needle to a syringe filled with water, which pushes the sample through the capillary. To avoid dilution by water, a small air bubble (5µl) separates the sample from the water. After measurement, the capillary is cleaned with a detergent solution and rinsed with pure water. For the next measurement, the entire circuit is dried with compressed air.

▶ MAIN RESULTS AND PERSPECTIVES

The fig. 2A shows a typical setup for a Small Angles X-rays Scattering (SWING beamline SOLEIL) comprising the pipetting robot, the measurement cell and the cleaning robot. When the sample is pushing through the capillary, the incident beam crosses (perpendicularly) the capillary and a scattering spectrum is recorded on a detector plate. The second fig. 2B shows scattering curves obtained with different concentration of a solution of Bovine Serum Albumin. These curves illustrate the capacity of the pipetting robot to work with highly concentrated sample (> 250 g/L), and the perfect superimposition of a set of curves for a given concentration (magnified blue area) brings out the very good reproducibility of the measurement.
The fig. 2C illustrates the possibility of the robot to manipulate very viscous solutions. To evaluate the ability of the robot to pipette and to transfer the solution into a measurement cell (like a quartz capillary), we use a diode positioned at the center of the X-ray beam to measure the transmitted intensity, allowing us to monitor the spread of the sample through the capillary. We can have a control on the separation of the sample to the water or air and evaluate the real injected volume. Here we tested the limits of the robot by using different type of viscous solution, such as concentrated BSA (1g/l to 500g/l), glycerol (1,5,10,25 and 50%)

and PEG 10K (1,5,10 and 20%).
The pipetting robot can be used also in other sample environment. The compact design and the command with RS232 protocol let us to transfer easily to another beamline or instrument equipped a flow cell. The fig. 3 illustrate this versatility, where the robot is also used on DISCO beamline to perform circular dichroism with synchrotron light (here Aquaspec flow cell, 6µm of flowpath – Brucker). With the same cell, the pipetting robot can be connected to a commercial infrared spectroscopy instrument (Tensor 27 – Brucker). The pipetting robot can be combined with a measurement cell (capillary) and a fraction collector to perform irradiation experiments on sample (METROLOGY beamline SOLEIL).

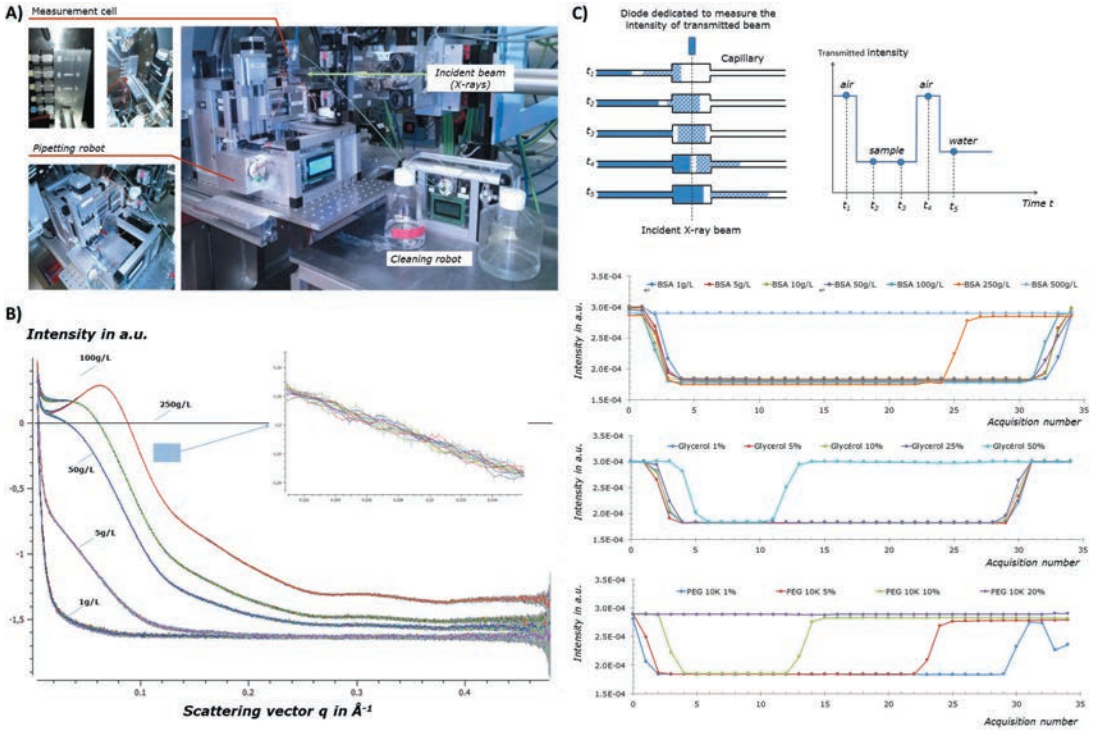

▶ *Figure 2: A) The pipetting robot installed on SWING beamline to perform SAXS experiments. B) SAXS curves obtained with a set of BSA concentrations. For each concentration, 20 injections and measurements were performed and superimposed. C) Evaluation of the ability of the robot to manipulate viscous solution. The transmitted X-ray beam through the capillary is measured with a diode. For each solution and concentration, an intensity profile is plotted to follow the progression of the sample through the capillary.*

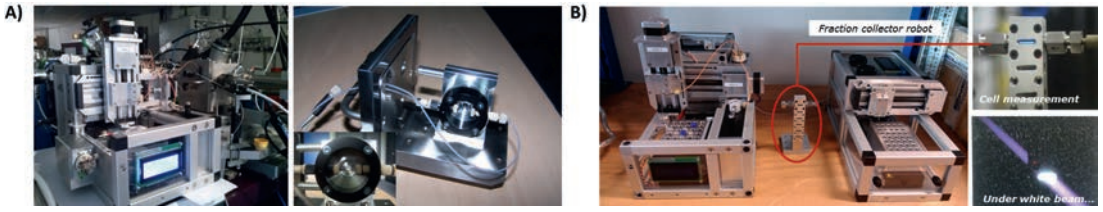

▶ *Figure 3: A) The pipetting robot installed on DISCO beamline to perform SRCD measurements. The measurement cell here is the Aquaspec flow cell with 6 µm of flow path, from Brucker. B) The robot combined to a capillary cell and a fraction collector to perform irradiation experiments. The 2 last images show the fluorescence of the capillary during white beam exposure.*

▶ CONCLUSION

The results obtained with different types of solutions show the pipetting robot can work with inhomogeneous solution thanks to the principle of pipetting and injecting process combining air and water. The diameter of the tubbing allows working with precipitate or crystalline solutions without the risk of clogging the circuit. The compact dimensions, the facility to program a sequence of injection or other type of liquid manipulation (mixing, preparation of a set of dilution, phase extraction...) offer a wide range of applications. The recent results performed on the different beamlines SWING, DISCO and METROLOGY show the possibility to have a common sample environment for different and complementary methods to characterize liquid samples.

PROSPECTS

The overall organization of INRA at SOLEIL and the involvement of the INRA engineers and scientists permitted the attainment of a high success rate in SOLEIL calls for projects. Users benefited from critical reviews of their proposals by a scientific committee of INRA users, from preliminary experiments, from new methodologies such as original sampling robot coupled to HPLC (SWING, DISCO), inverted microscope (SMIS), deep UV microscopy (DISCO), training in data treatment (SWING, DISCO), presentations of the instrument in various INRA centers. They also accessed ten beamlines in addition to the three where INRA engineers act as beamline scientists. Not all the possibilities of the instrument have yet been explored. Indeed mapping the structure of very complex assemblies at different length scales and with different radiation wavelengths used to highlight underlying structural organisation, working on living matter and environmental materials, and increasing spatial resolution will be our main challenges.
It will be very important in the future to continue to provide support to INRA scientists from existing communities (soft matter, structural biology, biotechnology, plant and animal biology, food science...), and to favor the emergence of users from new communities (environmental science, agronomy...). Including INRA scientists in the discussion about the evolution of the different beamlines and experimental setups will help improving the use of SOLEIL in the frame of scientific themes of common interest.

▸ USING THE POSSIBILITIES OF SOLEIL TO MAP THE STRUCTURE OF VERY COMPLEX ASSEMBLIES

Understanding the structure of objects of extreme complexity (polysaccharides, proteins associated with other proteins, sugars, lipids or nucleic acids, under the form of solutions, gels, powders, food matrices) is a challenge, and harnessing complementary information from different approaches will be the key to progress. For example smart activation of ions using UV at DISCO and DESIRS will be valuable for mapping region of protein associated with sugars. Similarly, generation of hydroxyl radicals at METROLOGY will permit finger printing on proteins difficult or impossible to crystallize and hence study at atomic resolution (membrane proteins, protein nucleic acid complexes....). Indeed, to facilitate structural approaches to such difficult targets, SOLEIL plans to offer an advanced Cryo Electron Microscopy (operated like a beamline facility with fully supported access), not only as part of an integrative approach to structural biology, but also for high-resolution tomography of tissues and cells.

▸ TOWARD HIGHER SPATIAL RESOLUTION IN IMAGING TECHNIQUES, FOR LIVING ORGANISMS

Recently developed beamlines such as HERMES or NANOSCOPIUM open new possibilities in terms of cell and tissue characterization. X-ray absorption and phase contrast in the water window (between the carbon and the oxygen K edges) at HERMES provides the opportunity to image whole cells in hydrated state with a resolution of about 40 nm, intermediate between light and electron microscopy resolution. NANOSCOPIUM, a scanning X-ray “nanoscope” working at higher energy (5-20 keV), offers the possibility to map metals in cells and tissues at the sub-cellular level. In addition to imaging, X-ray fluorescence and spectroscopic techniques provide elemental mapping, coupled with determination of chemical state of the element.
Food, nutrition, agriculture and the environmental science will benefit from these new beamlines through various subjects such as structural organization of sub-cellular compartments in cells, location of high value molecules, determination of the status of metals in relation with diseases or migration of nanoparticles through living organisms. Coupled to IR / UV imaging and spectroscopic techniques, these high spatial resolution X-ray imaging tools will provide, to INRA teams, a full panel complementary to the modalities available in their own platforms.

Editorial committee:
Alain Buléon, Thierry Chardot,
Alexandre Giuliani, Isabelle Quinkal,
Camille Rivard and Pierre Roblin.

Design graphique idées fraîches

Copyrights: SOLEIL

Photo credits: SOLEIL, iStock, Fotolia,
Alamy, Francis Canon, Vincent
Moncorgé

Printing: Imprimerie Rochelaise

Communication Unit
SOLEIL Synchrotron
L'Orme des Merisiers Saint-Aubin
BP 48 - 91192 Gif-sur-Yvette Cedex
France
webcom@synchrotron-soleil.fr

www.synchrotron-soleil.fr

INRA
147 rue de l'Université
75338 Paris Cedex 07 - France
Tel: +33(0)1 42 75 90 00
www.inra.fr

SOLEIL Synchrotron
L'Orme des Merisiers Saint-Aubin - BP 48
91192 Gif-sur-Yvette Cedex - France
www.synchrotron-soleil.fr